Vietnamese-German University

COPYRIGHT WARNING

RUHR-UNIVERSITÄT BOCHUM

Vietnamese-German University

MechEng
Mechanical Engineering

DESIGN, MANUFACTURE AND TESTING OF MAGNETO - RHEOLOGICAL BRAKE FOR ELECTRIC SCOOTER

TOPIC

BACHELOR THESIS

Vietnamese-German University

BINH DUONG 2023

Submitted by: Le Hoang Viet Anh

RUB Student ID: 19218798

VGU Student ID: 14648

Supervisor: Prof. Nguyen Quoc Hung

Co-supervisor: Bsc. Do Qui Duyen

DESIGN, MANUAFACTURE AND TESTING OF MAGNETO-RHEOLOGICAL BRAKE FOR ELECTRIC SCOOTER

Le Hoang Viet Anh
Mechanical Engineering
Binh Duong, February, 2023

Affirmation

Le Hoang Viet, Anh

Matriculation Number: 19218798 (RUB Student ID) – 14648 (VGU Student ID)

Title of Thesis:

DESIGN, MANUFACTURE AND TESTING OF MAGNETO-RHEOLOGICAL BRAKE FOR ELECTRIC SCOOTER

I hereby declare in lieu of oath that I have produced the aforementioned thesis independently and without using any other means except the aids listed. Any thoughts directly or indirectly taken from somebody else's sources are made discernible as such. To date, the thesis has not been submitted to any other board of examiners in the same or a similar format and has not been published yet.

Binh Duong, February 08, 2023

Le Hoang Viet Anh

Abstract

The safety in vehicle transportation field is always the most important demand, especially when it comes to the brake of the vehicle. So far, there are many researches have proved that magneto-rheological brake could overcome limitations of traditional brake such as slow respond to driver's command, the shoes of brake are easily wearing after a period of time. Moreover, some critical components include disc surface, fluid pipes, brake pads of traditional brake are vulnerable to damage from external source. An application of magneto-rheological in car has been conducted to replaced traditional brake system by several studies. Inspiring from that, this thesis project introduces the usage of magneto-rheological brake in two-wheel vehicle which is electric scooter specifically.

This paper presents the work in designing a magneto-rheological brake for application in the electric scooter. The work of this thesis consists of main stages in product designing process: requirements determination, calculation, draft design, optimal design by Ansys software, detail design and detail calculation. CAD modeling and simulation are also carried out to ensure the working ability of the design. Technical drawings of all parts of the brake are also exported for manufacturing. Moreover, the conceptual experiment model of the brake is designed to test the actual braking ability. However, due to the limitation of time, only prototype of the brake is fabricated. This product will be kept for further testing and improving before totally using in electric scooter.

Acknowledgement

I would like to express my gratitude towards my supervisor Prof. Nguyen Quoc Hung for providing value guidances and assistances during the process of this thesis. Secondly, I also have a special thanks to my Co–supervisor Bsc. Do Qui Duyen for useful advices and consultations whenever difficulties occur in the thesis process. Last but not least, I really appreciate the support of Mr. Le Hai Zy Zy, he helped me a lot in learning the Ansys software when I started from zero which is a very important point for my thesis. Without any above supports, my thesis would never be completed in the best way.

Throughout this project period, I have learnt many practical knowledge in designing product as well as manufacturing. This is the wonderful preparations for my future career after graduating from Vietnamese–German University.

Table of content

List of figures

List of tables

Abbreviations

MR = Magneto-rheological

MRF = MR fluid = Magneto-rheological fluid

MRB = MR brake = Magneto-rheological brake

CAD = Computer-Aided Design

Chapter 1: Introduction

1.1. Motivation and Objectives of the research

1.1.1. Overview of MR fluid and its application

MRF are suspensions of particles that can be magnetized, and when a magnetic field is applied, they show quick, significant, and reversible changes in their rheological properties. Therefore, MRF is applied in various fields at present such as clutches, valves, dampers, brakes and robotics, especially, application of MRF device in the automotive industry in order to replace traditional mechanical systems. In the scope of this thesis, MR brake systems is mainly discussed.

1.1.2. Trend in electric scooter

Electric scooters are two or three-wheeled vehicles powered by electricity. This power is stored in a rechargeable battery, which drives the functioning of electric motors. The electric energy is expected to be totally replaced fossil fuel for vehicle in the future due to the concerns over greenhouse gas and carbon emissions. This leads to the dramatically increasing of electric vehicle market and electric scooter is not the exception. The electric scooter market is predicted to reach USD 15.22 billion in 2021 to USD 31.04 billion by 2028 at a CAGR of 10.7% during the 2021-2028 period in Asia Pacific (Fortune Business Insights, 2022) [1]

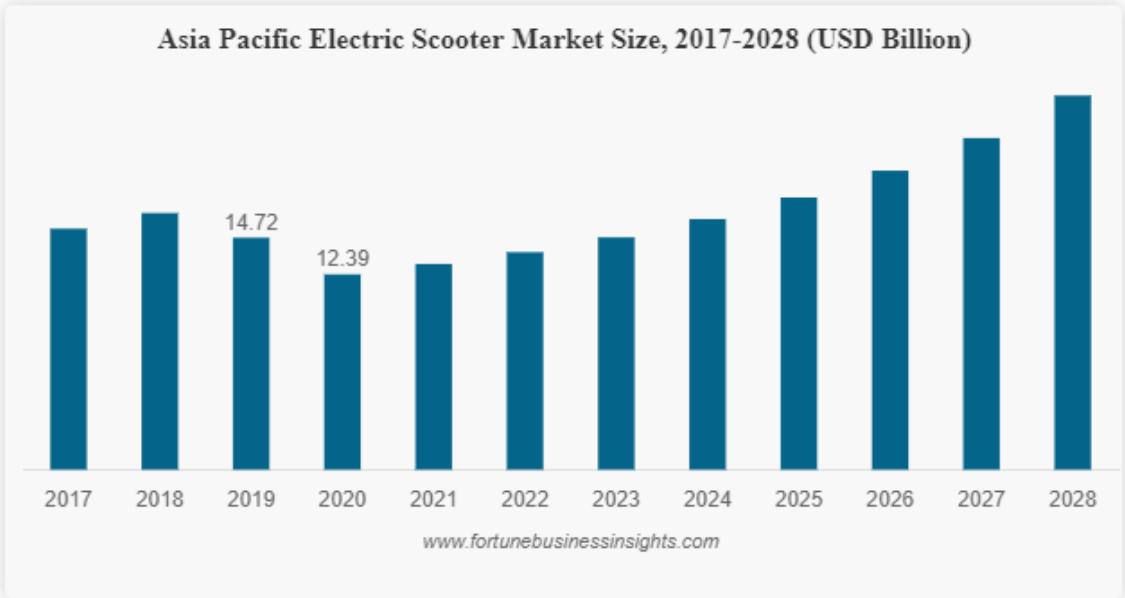

Figure 1.1: Asia Pacific Electric Scooter Market Size, 2017-2018

[1]

1.1.3. Potential of application of MR brake in electric scooter

With the properties that rheological characteristics change rapidly and can be controlled easily in presence of an applied magnetic field of MRB, currently, there are several studies of MR brake for road vehicle applications. Some representative examples could be Park et al. [2] and Karakoket al. [3] have assessed MRBs for typical medium sized car and the research of optimal design MR brake for medium sized car by Q H Nguyen and S B Choi [4]. However, there was no research of MR brakes for electric scooter application.

Since the tendency of using electric scooter is expected to be rising in the future, new brake system such as MR brake has a huge opportunity to be developed in the electric scooter industry. MR brake was proven to increase the life span and reliability of brakes, also, MR brake is harder to occur the slipping situation when performing than traditional braking.

Consequently, the objective of present work is to design and make a prototype of the MR brake for electric scooter. The data after testing the prototype will be recorded to be used in the future plan.

1.2. Scope of the research

The thesis is focused on designing and manufacturing MR brake based on **Bingham plastic model** only. The final product is the MR brake prototype which will be attached on electric scooter and successfully operating later. The main activities of this project consist of:

- Determining the most suitable MR brake for electric scooter by using Ansys software simulation
- Calculating all necessary parameters of choosing MRB
- Exporting the CAD drawing of components of MRB
- Designing experiment model for the MRB
- Machining and assembling of the prototype MRB

1.3. Outline

- Chapter 1: Introduction

Presenting the motivation to choose thesis's topic. Introducing the research content as well as the limitation of the project.

- Chapter 2: Background study

Giving the necessary theorical knowledge which is used in the thesis.

- Chapter 3: Design of MR brake for electric scooter

Presenting an overview of choosing electric scooter configuration as well as procedure of designing the MR brake. Optimalization of the design is also considered in this section.

- Chapter 4: Detailed design of prototype MR brake

Presenting a final MR brake model, detailed parameters of all MR brake's components and the assembly procedure. All design parts are demonstrated by the detailed drawing and assembly drawing. Calculation of mechanical properties of the MRB is also executed in this section.

- Chapter 5: Conceptual design of experiment

Designing of testing model for the MRB of electric scooter to see if the brake could achieve necessary torque.

- Chapter 6: Fabrication of the MRB

Presenting the manufacturing process of the MR brake. All parts of the brake are assembled into complete MRB prototype in this section

- Chapter 7: Conclusion and future works

Discussing the quality of the final MRB prototype and proposing methods for improving the prototype. Moreover, the plan of upcoming tasks for implement of MRB on electric scooter is also presented in this part.

Chapter 2: Background study

2.1. Introduction to magneto-rheological fluid

A magneto-rheological fluid (MR fluid, or MRF) is a type of smart fluid, usually a type of oil whose yield stress increases considerably in the presence of externally applied magnetic field. These fluids are composed of soft, spherical, magnetic particles whose diameters range from 3 to 10 μm dispersed in organic liquid. Typically, the magnetic particles comprise between 20 to 40 percent of the fluid's volume.

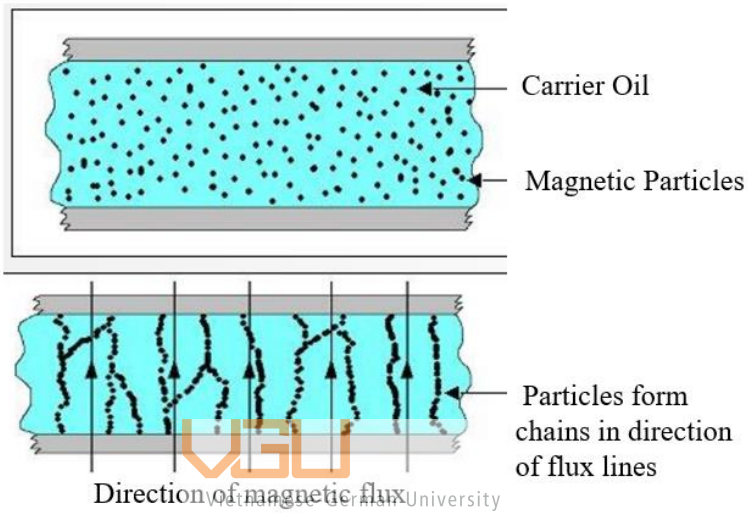

Figure 2.1: MRF schematization of with and without magnetic field presence

The ferrous particles that are scattered throughout the fluid create magnetic dipoles when exposed to a magnetic field. These magnetic dipoles arrange themselves in accordance with the flux lines. This process is reversible and the response time is in order of milliseconds.

2.2. Rheological property of MRF

2.2.1. Field independent Bingham plastic model

Yield stress of MRF: In the presence of magnetic field, MRF becomes quasi-solid which can be assumed properties comparable to solid. This tolerates shear stress up until a point of yield (the shear stress above which shearing occur). This yield stress strongly depends on the strength of the applied magnetic field, but will reach a maximum point after which increases in magnetic flux density have no further effect, as the fluid is then magnetically saturated. The behavior of a MR fluid can thus be

considered similar to a **Bingham plastic model** which is also the method to determine the properties of MRF throughout this thesis.

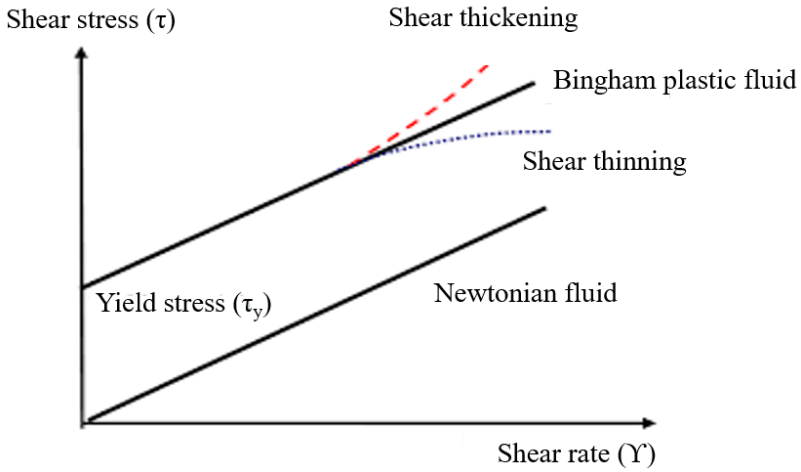

Figure 2.2: Yield stress of MRF compare to Newtonian fluid by Bingham model

(Quoc-Hung Nguyen & Seung-Bok Choi, 2012) [4]

Thus, our model of MRF behavior in shear mode according to **Bingham plastic model** [5]:

$$T = T_y(H) * sgn(\gamma) + \eta * \Upsilon \quad (1)$$

Where: T = shear stress; T_y (H): yield stress at magnetic intensity rate (= H);

Ƞ = Newtonian viscosity; ϒ = shear rate

2.2.2. Field dependent Bingham plastic model

The rheological characteristics of the MRF in the field-dependent Bingham model are estimated by the following equation and are dependent on the applied magnetic field. [5]:

$$Y = Y_\infty + (Y_0 - Y_\infty)\,(2e^{-B\alpha_{sy}} - e^{-B\alpha_{sy}}) \quad (2)$$

Where: Y_0 and Y_∞ are the rheological properties of MRF at zero magnetic field and saturated magnetic field respectively. B is the applied-magnetic flux density, α is the corresponding saturation moment index of the rheological properties.

Chapter 3: Design of MR brake for electric scooter

3.1. Introduction to prototype electric scooter

The electric scooter model which is chosen for this thesis is XMEN PLUS. The model uses Bosch electrical motor for power resource.

Figure 3.1: XMEN PLUS Electric Scooter model

Some necessary technical parameters of the electric scooter for designing MR brake (3):

- Electric motor: 60V – 1200W
- Diameter of front and back wheel: D = 425 mm = 0.425 m
- Maximum speed: v_{max} = 50 km/h
- Mass: M = 95 kg
- Maximum load: 80 kg

(thegioixechaydien, 2019) [6]

Figure 3.2: Back wheel and motor's parameter

3.2. Types of MRB

There are 3 main types of MR Brake that could be chosen for the electric scooter which are Disc, Drum and Hybrid brake. Each types have their own advantages and disadvantages.

3.3.1. Disc MRB Type

Disc MRB consists of brake rotors (thin disc) which are attached directly to the wheel, stationary housing and MR fluid. The MRF is sealed by seal and bearing in the small gap between discs and stationary housing. In normal condition the MRF acts like lubrication, when magnetic field is applied, MRF becomes quasi-solid material. The physical contact which comes from quasi-solid MRF, the disc and the housing creates friction to stop the wheel. This is the braking mechanism for all types of MR brake. In the case of disc MRB type, only the MRF on two side left and right are affected by the magnetic field.

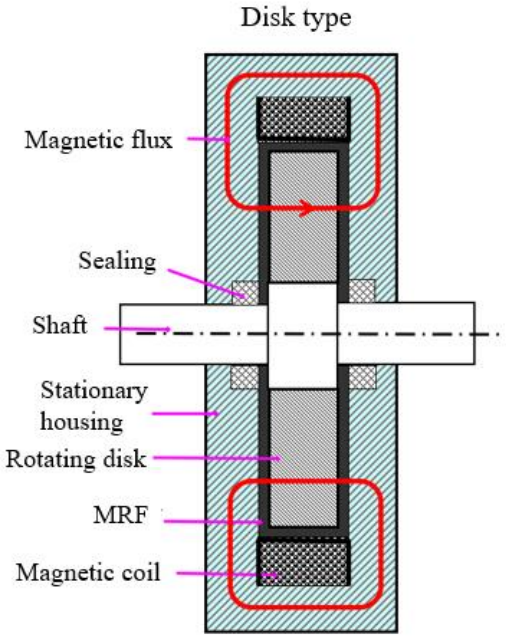

Figure 3.3: Cross view of single disc-type MR brake

[7]

3.2.2. Drum MRB Type

Drum brake has the long cylinder rotor. The magnetic field in this case is applied only in the radial direction since the side housings of the brake are composed of non-magnetic material. Additionally, the housing should be thick in order to prevent the magnetic circuit's bottleneck problem of magnetic circuit. There is a bobbin wall which is wound on the coil, this causes a difficulty in fabricating the brake.

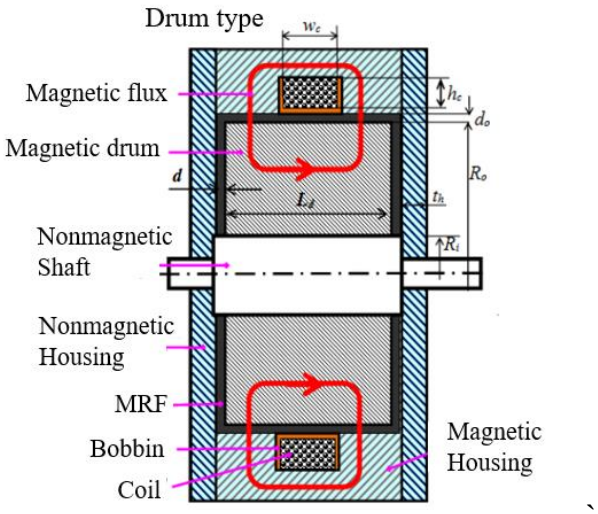

Figure 3.4: Cross view of Conventional drum MR Brake

[7]

3.2.3. Hybrid MRB type

Hybrid MRB is the combination design of the Drum MRB and Disc MRB. It takes the benefits and neglect the disadvantages of both types. The advantage of this type of MRB is that the side housings of hybrid are made of a magnetic material. As a results, the magnetic flux generated by the coil flows not only in the axial direction but also in the radial direction which leads to higher torque.

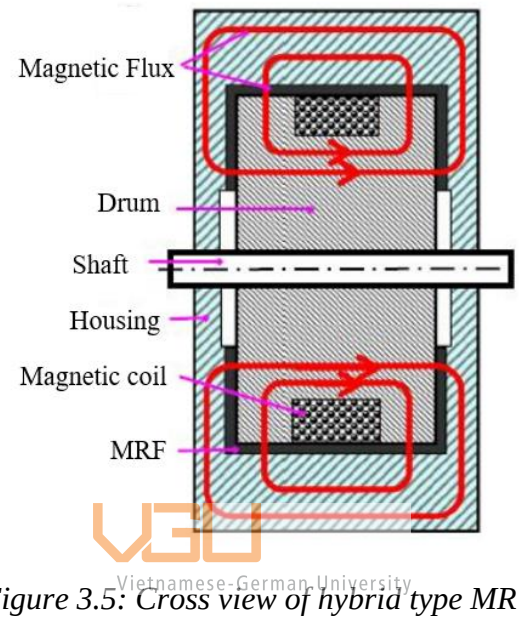

Figure 3.5: Cross view of hybrid type MR brake

[7]

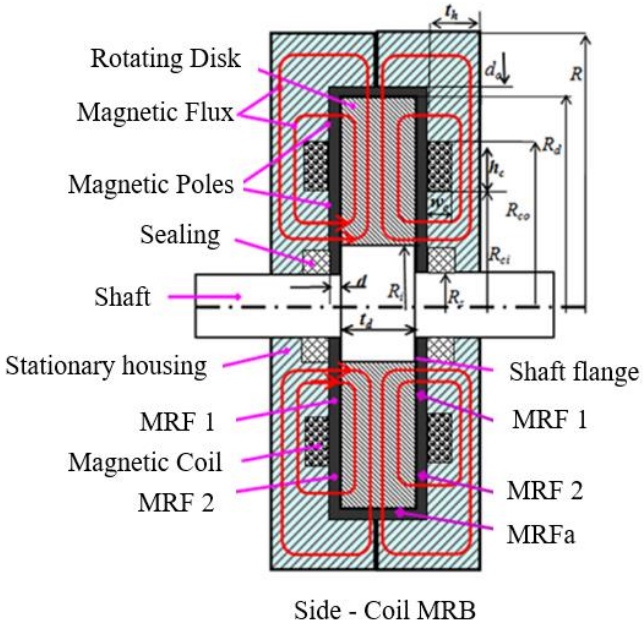

Figure 3.6: Cross view of hybrid Side-coil MR Brake

[7]

3.2.4. Optimal MRB model for Electric Scooter

3.2.4.1. Choosing MRB

With variety of MR Brake type, it is necessary to determine the most optimal MRB for electric scooter which is satisfied these conditions (4):

- Light weight
- Easy to disassemble, maintenance and repair (Mechanical simplicity)
- Required small space (radial dimension; R, thickness: L)
- Suitable cost
- Optimally required power

In order to narrow down the type of MRB base on these criteria. Information of optimal design for MRB types which have been done is considered.

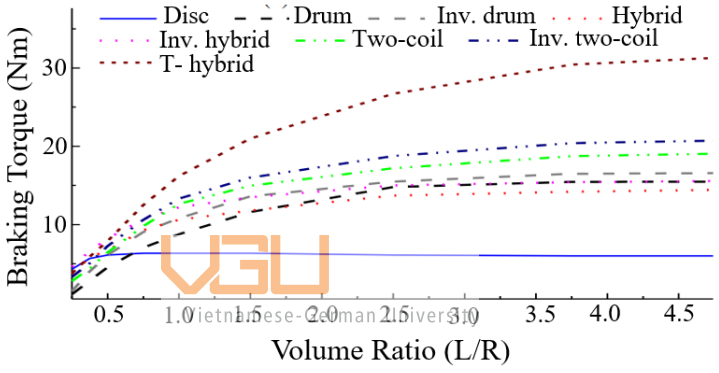

R = 40

Figure 3.7: Braking torque of the optimized MRBs featuring MRF-140-CG when the torque ratio is 20

[4]

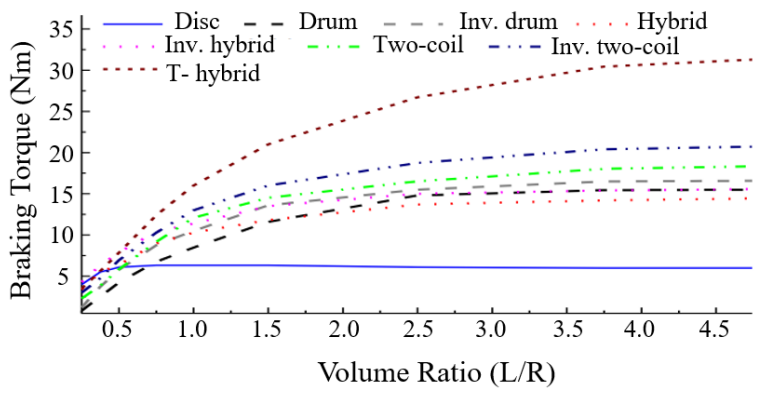

Figure 3.8: Braking torque of the optimized MRBs featuring MRF-140-CG when the torque ratio is 50

[4]

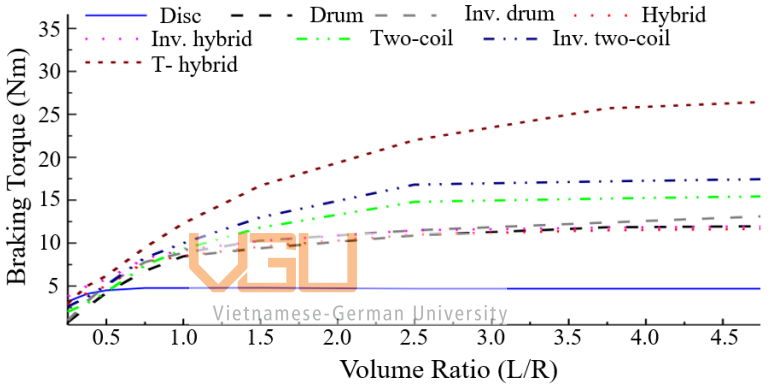

Figure 3.9: Braking torque of the optimized MRBs featuring MRF-132-DG when the torque ratio is 20

[4]

As data of three figures shows, with the same radial dimension and volume ratio, the torque generated by conventional disc, drum type is always smallest. This leads to the neglection of these MRB types in the design. Thus, variants from classical MRB types which are proved to be more efficient are in the list of selecting MRB model for electric scooter:

- Thin wall side-coil includes single coil type and double coils type
- Tooth-shape type
- I-MRB type
- Zigzac flux MRB

Among these types, the best models will be chosen to do further selection for last decision of MRB design. The comparison between MRBs is able to be made bases on multi researches have been made.

MRB types	Design parameter [mm]	Characteristics
TSR_MRB	**Coil:** Inner radius R_{cin}=15.4, Width t_c=5.7; Height h_c,=7.2; No. of turns: 2(126)=252 **Housing:** R=27.4 (t_o=2.0), L=34, t_h=4.2, **Disc:** Inner radius R_0=6.4, Thickness t_d= 2.0, Tooth Height: h=3.5, Tooth peak thickness: l_p=1.5, Tooth bottom thickness l_{tb}=1.76, Distance between teeth l_{bd}=2.7 (l_{pd}=2.96), Outer radius R_d=24.8 (Outer tooth peak thickness 1.6) **MRF duct gap**: d=0.6	Max. Torque: 10.09*Nm* Mass: 0.62kg Off-state Torque: 0.025*Nm* Power Consumption.: 15*W* Coil Resistance(*Ω*):R_c=1.16
TWSS_MRB	**Coil:** Width w_c=3.5; Height h_c,=9.5; Radius R_{ci}=39; No. of turns: 2*96=192 **Housing:** R=53, t_{ho}=3.6, L=22.7, t_w=0.5 **Disc:** Radius R_i=27.5, R_d=51; Thickness t_d= 6.4 **MRF duct gap**: 0.6	Max. Torque: 9.92 *Nm* Mass: 1.56kg Off-state Torque: 0.074*Nm* Power Cons.: 30*W* Coil Resistance(Ω):R_c=2.2
TWDS_MRB	**Coil:** Width $w_{c1} \cong w_{c2}$=4; Height $h_{c1} \cong h_{c2}$=6.2 Radius R_{c1i}=24.4, R_{c2i}=41.4; No. of turns: 2*(77+77)=308; **Housing:** R=52.8, t_{ho}=2.9, L=20, t_w=0.5 **Disc:** Radius R_i=15, R_d=50.2; Thickness t_d= 4.4 **MRF duct gap**: 0.6	Max. Torque: 9.94*Nm* Mass: 1.34kg Off-state Torque: 0.0768*Nm* Power Cons.: 36.6*W* Coil Resistance(*Ω*): R_{c1}=1.53, R_{c2}=1.92

Table 3.1: Optimal solutions of Tooth-shape MRB, Single-coil and Double-coil thin-wall MRB

(Van Bien Nguyen, Le Dai Hiep, Quoc Hung Nguyen, Quy Duyen Do, Huu Minh Hieu Do, Seung-bok Choi, 2021) [8]

In Table 3.1, TSR_MRB is Tooth-shape MRB, TWSS_MRB and TWDS_MRB are Single-coil and Double-coil thin-wall MRB respectively. The MRF which is used in this table is MRF132-DG. The solutions are conducted at approximate 10 Nm Torque.

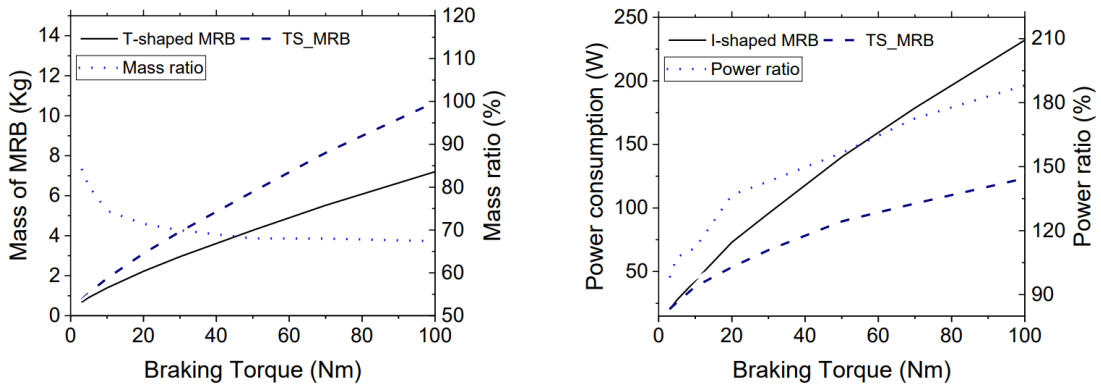

Figure 3.10: Optimal solutions of I-MRB using MRF132-DG

(Nguyen Van Bien, Diep Bao Tri, Vu Van Bo, Le Dai Hiep, Do Quy Duyen, Nguyen Quoc Hung) [9]

Figure 3.10 illustrated the data of the optimal relation of braking torque versus mass and power consumption respectively which is used for comparison between tooth-shaped MRB and I-shaped MRB. The remarkable point of this figure is the relation when the torque is at 10 Nm. Furthermore, this research also states the size of I-shaped MRB which are R = 40 mm, L = 34 mm

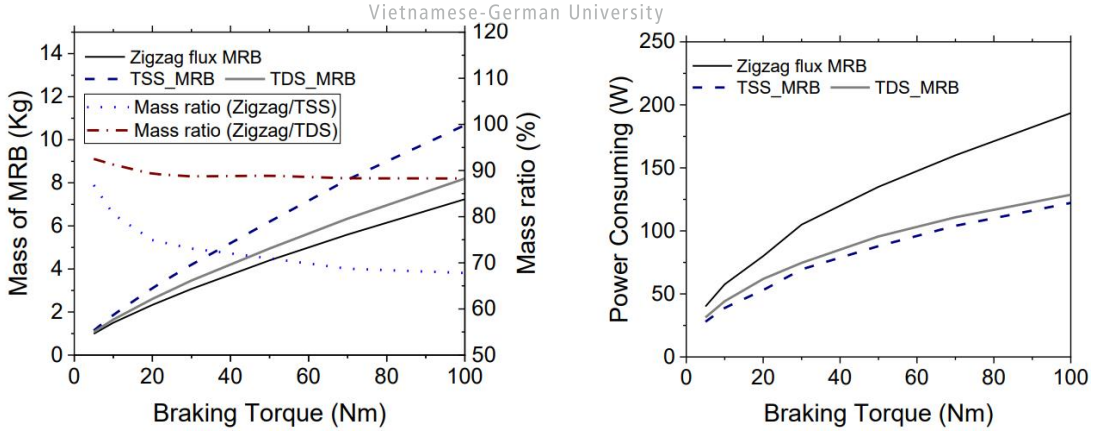

Figure 3.11: Optimal solutions of Zigzag flux MRB, Single-coil and Double-coil thin wall MRB using MRF132-DG.

(Quoc Hung Nguyen, Van Bien Nguyen, Hiep Dai Le, Do Qui Duyen, Weihua Li, Nguyen Xuan Hung, 2021) [11]

The interesting information of Figure 3.11 is also the mass and power consumption of zigzag flux MRB at 10 Nm. Moreover, this study also provides the size of zigzag flux MRB which are R = 55 mm, L = 21 mm.

From Table 3.1, Figure 3.10 and Figure 3.11, a table is made to gather technical parameters of MRB's types which generate 10 Nm Torque by using MRF132-DG.

	Tooth shape	Single-coil TW	Double-coil TW	Zigzag flux	I-MRB
Mass (kg)	0.62	1.56	1.34	1.2	1.3
Required Space (half of cross-section) (mm^2)	931.6	1203.1	1056	1155	1360
Power consumption (W)	15	30	36.6	56.25	37.5

Table 3.2: Technical specifications of MRB's types at 10 Nm by using MRF132-DG

From this information, a comparison among these MRBs is conducted for choosing the most suitable MRB for the electric scooter. The point range is from 1 to 5, in which 1 is lowest potential and 5 is highest potential. The MRB which has the highest total point will be chosen. For each condition (4), 1 point is equal to:

$$\frac{Max - Min}{4} = 1\ point \tag{5}$$

From equation (5) and Table 3.2, a comparison table is able to constructed:

Criteria \ MRB type	Single-coil TW	Double-coil TW	Tooth shape	Zigzag flux	I-MRB
Small required space	2.5	4	5	3	1
Light weight	1	2	5	2.5	2
Mechanical simplicity	2	2	2.5	3.5	4
Low cost	1	3.5	3.5	3.5	4
Low power consumption	3.5	3	5	1	3
Total	10	14.5	21	13.5	14

Table 3.3: Comparison of MRB's types

As can be seen in the table, the Tooth shape MRB has the highest point which is 21. Consequently, the best MRB types for the electrical vehicle is Tooth shape MRB.

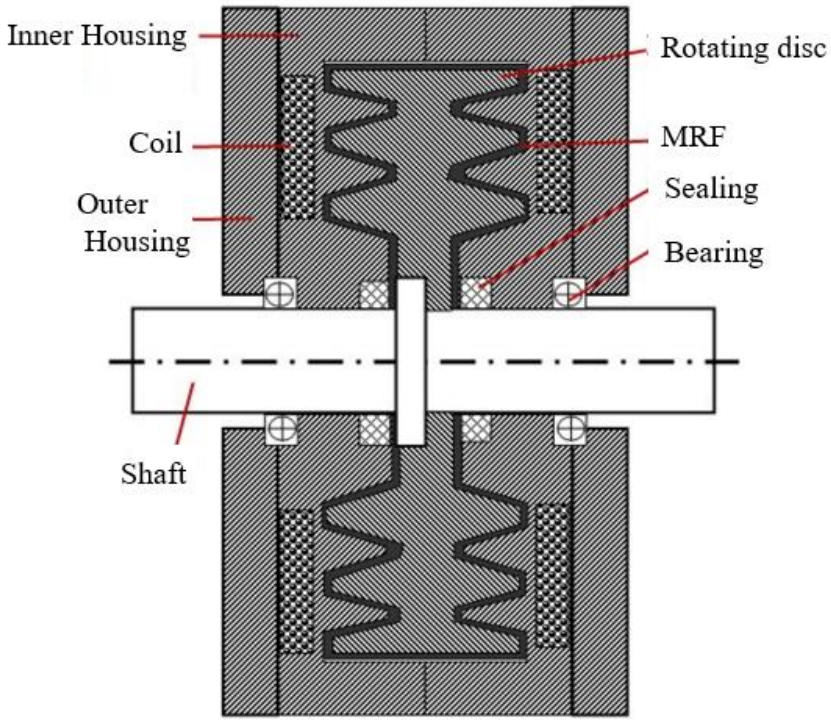

Figure 3.12: Cross view of Tooth shape MRB

3.3. Design requirements

In order to design suitable MR brake for the vehicle, these technical parameters have to be determined.

3.3.1. Required braking Torque

The required braking torque is an important factor to consider when designing a brake system for electrical scooter. The MR brake's braking torque is assumed to be independent of vehicle's speed for required torque calculation. The energy conversation equation for the electric scooter can be determined by ignoring insignificant friction like tire-road friction and drive-line friction:

$$\frac{MV_c^{\,2}}{2} = T_b\theta_b = T_b\frac{S_b}{R_w} = T_b\frac{V_c^{\,2}}{R_w 2a_b}$$

Then:
$$T_b = R_w a_b M \quad (6)$$

Where: T_{tb} is the total required braking torque; M is the total mass of electric scooter and driver; R_w is the wheel radius of electric scooter; V_c is maximum speed; S_b is the travelling distance of the vehicle during braking process, θ_b is the angle that the wheel rotates during braking process; a_b is the braking declaration. In motorcycle brake design, a_b is normally set by a_b = 0.75 g = 7.35 m/s^2 (Q H Nguyen & S B Choi, 2012)

[7]. This value of a_b is also assumed to be applicable for the electrical scooter since two types of vehicles have the similar principle. The total mass is equal to the mass of electric scooter plus the mass of loading, from (3) and the total mass can be calculated as M = 175 kg. According to (3) R_W = 0.2125 m. From equation (6) the total required braking torque is around 274 N m (T_{tb} = 274 N m). The safety factor for the brake is set by 1.3. Then the total brake is equal 356.2 N m. The total required braking torque is split into two terms which is 55% for the front brake and 45% for the rear brake. Which are respectively T_{fb} = 195.91 N m and T_{rb} = 160.29 N m. Since this project's goal is to design the MR brakes in order to replace the conventional brake for electric scooter, T_{fb} and T_{rb} are two important parameters.

3.3.4. Available Space

3.3.4.1. For back wheel

One important specification that should be considered when design the MR brake for the back wheel of the electric scooter is the thickness of MRB (L). An old brake version of the vehicle has already set the limit for the thickness of brake which is 45 mm (L_{max} = 45 mm). If L exceed 45 mm, the brake will touch the frame.

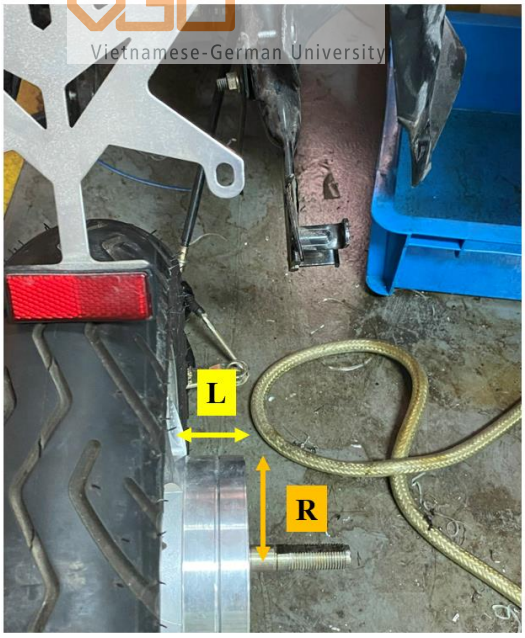

Figure 3.13: Available space of the back wheel

The radius of the brake also has to be inside the hub in the figure. The hub has the inner diameter 55 mm, which means radius R of MRB must be equal or smaller than 55 mm. Moreover, the diameter of the rear wheel is 12 mm.

3.3.4.2. For front wheel

Front wheel mechanism has 1 shaft which has the diameter of 11.99 mm to hold the wheel. This shaft is standstill and fixed to the frame by bolt join, only the wheel rotates.

Figure 3.14: Front wheel's shaft

The front wheel consists of two bearings for rotating, there are also 3 joints on the wheel to connect to the old disc brake. These joints will be used again for attaching the MRB later. The available space for the front MRB is also depend on radius (R) and thickness (L). The thickness of front MRB is set the same as the back MRB which is 45 mm. The radius R in this case is equal or less than 110 mm in order to not touch the frame of the wheel.

Figure 3.15: Front wheel

3.3.5. Allowance working temperature of MRB

As in MR Brake, the MRF is always contact with the housing and the discs or drum. The MRB is continuously subjected to a very high shear rate over the time. As a result, even if there is no magnetic field applied, the temperature of MRB will be potentially high which could decrease the efficiency of MRF. For safety reason, the steady temperature of MRB produced by the friction at zero magnetic field while the electric scooter constantly travelling at 50 km/h is taken into account. Furthermore, the heat increases due to a repetitive braking process also need considering.

In order to make sure that the temperature of MR fluid during the working process do not exceed the peak allowable temperature, the constraint equation in the research of Q H Nguyen and S B Choi is using in this study:

$$T_{MR} = T_{env} + \frac{T_{b0} V_c}{h A_b R_w} + \Delta T_b \leq T_{max} = 130^0 C \tag{7}$$

(Q H Nguyen & S B Choi, 2012) [7]

Where: T_{max} is the maximum allowable working temperature of MRF which is set at 130 ^{0}C. T_{env} is the temperature of the ambient environment which is assume to be 25 ^{0}C in this study. A_b is the area of the outer surfaces of the MRB structure. R_w and V_c are same as equation (4). ΔT_b is the temperature generated by a repeated braking of the MR brake, this value is set at $\Delta T_b = 10^0$C in this thesis. h is the heat transfer coefficient which is influenced by the ambient air's velocity. According to Q H Nguyen & S B Choi [7], the heat transfer coefficient is about 75 W (m^2 K^{-1}) when the vehicle is travelling at 120 km/h (8). There is a study by Avaraham Shitzer which show the relation between the heat transfer coefficient and the wind speed.

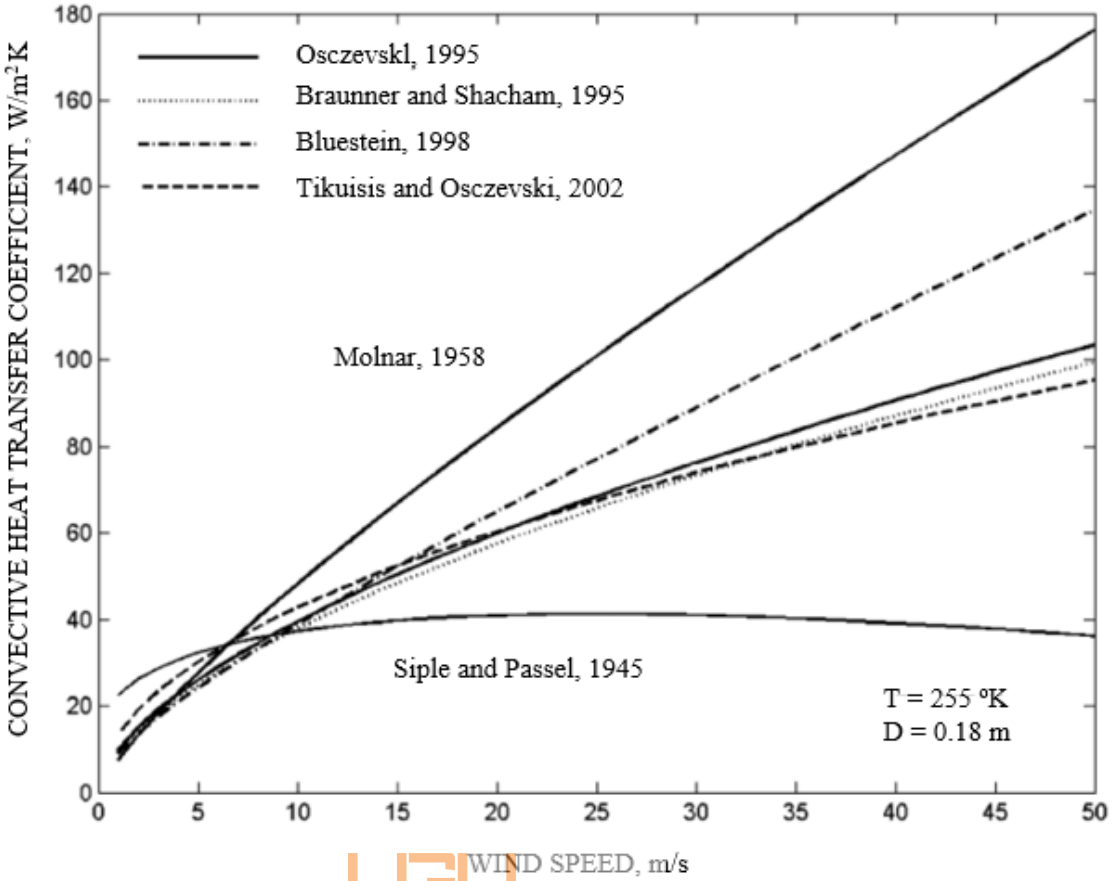

Figure 3.16: Convective heat transfer coefficients versus wind speed

(Avaraham Shitzer, 2006) [12]

Regardless of Siple and Passe line, the figure illustrates the increasing of heat transfer coefficient by the wind speed. For simplicity, this relation is assumed to be linear in this thesis. Combined with the reference value from (8). The heat transfer coefficient for electric scooter travels at 50 km/h is set by 31.25 W (m^2 K^{-1}).

After modifying and putting all the known values in the equation (7), the constraint equation of the temperature of MRF becomes

$$\frac{T_{b0}V_c}{hA_bR_w} \leq 100^0C \tag{9}$$

3.3.6. Material

3.3.6.1. MRF

At the moment, there are three types of MRF that can be accessible which are MRF-122-2EG, MRF-132-DG and MRF-140-CG.

MR fluid	Bingham model
MRF-122-2ED	$\mu_0 = 0.075$ Pa s; $\mu_\infty = 2.8$ Pa s; $\alpha_{s\mu} = 4.5\ \mathrm{T}^{-1}$ $\tau_{y0} = 12$ Pa; $\tau_{y\infty} = 25\,200$ Pa; $\alpha_{st_y} = 2.9\ \mathrm{T}^{-1}$
MRF-132-DG	$\mu_0 = 0.1$ Pa s; $\mu_\infty = 3.8$ Pa s; $\alpha_{s\mu} = 4.5\ \mathrm{T}^{-1}$ $\tau_{y0} = 15$ Pa; $\tau_{y\infty} = 40\,000$ Pa; $\alpha_{st_y} = 2.9\ \mathrm{T}^{-1}$
MRF-140-CG	$\mu_0 = 0.29$ Pa s; $\mu_\infty = 4.4$ Pa s; $\alpha_{s\mu} = 5\ \mathrm{T}^{-1}$ $\tau_{y0} = 25$ Pa; $\tau_{y\infty} = 52\,000$ Pa; $\alpha_{st_y} = 3\ \mathrm{T}^{-1}$

Table 3.4: Rheological properties of MR fluids

As can be seen on the table, the model MRF-122-2ED has smallest yield stress which could not provide enough moment for MR brake. For the MRF-140-CG, it has high yield stress as well as viscosity. However, with the high viscosity, it is very hard for this fluid flow into the MRF gaps. Because of this, the MRD-140-CG is not suitable for making MR brake.

The MRF-132-DG has medium yield stress and viscosity which is the best option for making MRB. This model is chosen for the MRB of electrical scooter

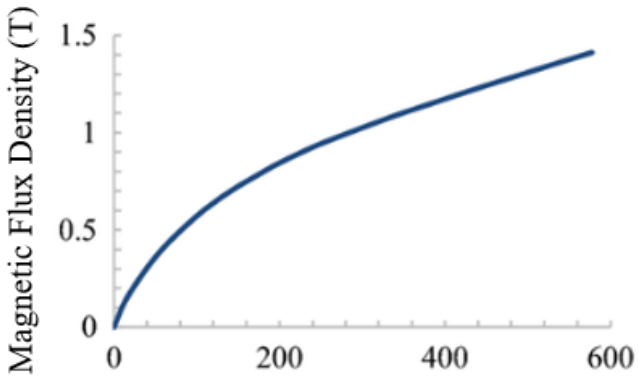

Figure 3.17: B-H curve of MRF-132-DG

(Subash Acharya & Hemantha Kumar, 2019) [13]

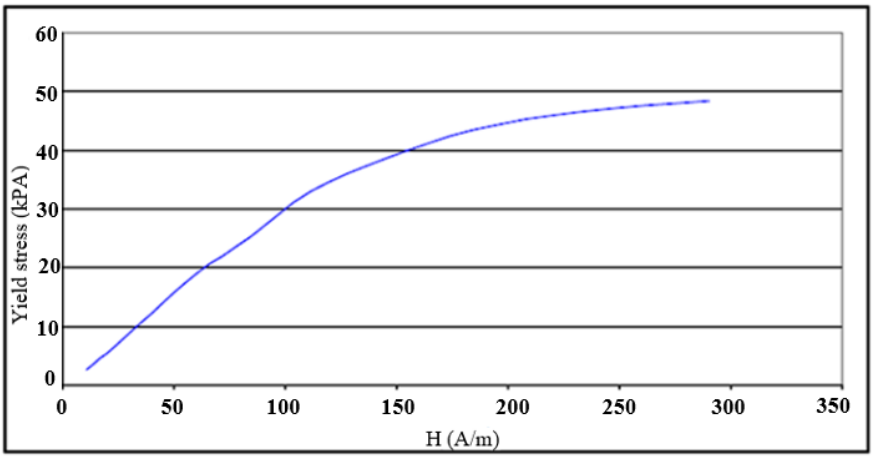

Figure 3.18: Specification of MRF-132-DG

(Zahurin Samad & Maher Yahya Salloom) [14]

3.3.6.2. MRB

C45 steel is chosen to made the housing and the disc of MRB brake since it is commercial steel, easy to buy with the low cost. Furthermore, C45 also has high magnetic conductivity. Some specification of C45 is

- Tensile Strength: 525 MPA
- Yield Strength: 530 MPA
- Shear modulus: 8000 MPA
- Hardness (Brinell): 170

The shaft of MRB will be made by inox in other to neglect the magnetic flow from the coil.

For the coil of MRB, the Copper is used as its well-known high electrical conductivity.

3.3.7. Key design summary

Specification \ MRB		Front MRB	Back MRB
Necessary Torque (N.m)		195.51	160.29
Available Space	Maximum radius (mm)	110	55
	Maximum Thickness (mm)	45	45
Maximum Temperature (celsius) of MRF		130	130
Type of MRB		Tooth-shape 1 coil	Tooth-shape 1 coil
Material of housing and disc of MRB		C45 steel	C45 steel
Material of the coil		Cooper	Cooper
Type of MRF		MRF-132-DG	MRF-132-DG

Table 3.5: Key design for Electric Scooter's MRB

3.4. Proposed configuration of Tooth-shape MR brake and its principle

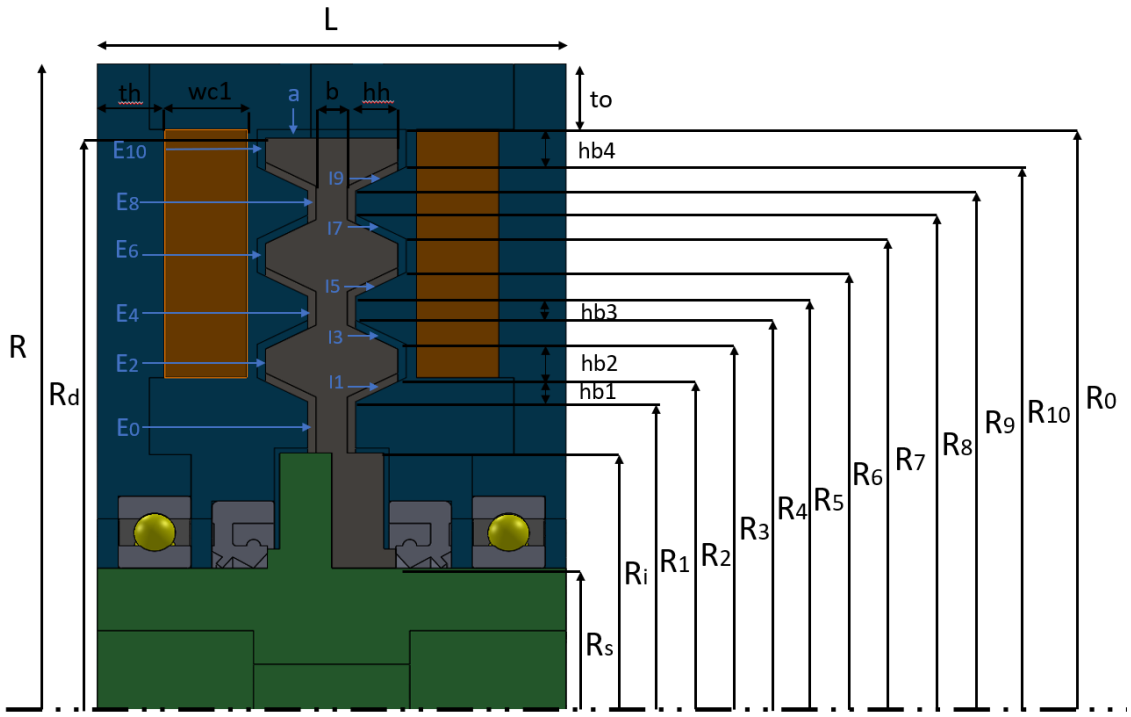

Figure 3.19: Geometric parameters of the Tooth-shaped MR Brake

The tooth-shaped MR Brake consists of two magnetic coils, each coil is placed on each side of the brake housing. The rotor of the MRB in this case is in tooth shaped. Rs is the radius of the shaft on which the brake is placed. R_i is the disc inner radius, the gap between Rs and Ri is necessary space to attach the brake on the shaft by bolt joints. R_d is the disc outer radius. b is the disc thickness and hh is the tooth height. R_2 is the coil inner radius and R_0 is the coil outer radius, wc_1 is the coil thickness. R_1, R_2, R_3, R_4, R_5, R_6, R_7, R_8, R_9, R_{10} are parameter value which are adjusted by the tooth peak length hb2, the length from base to peak of tooth hb1, the distance between teeth hb3 and the top tooth peak length hb4. The outer housing thickness is t_o and the side housing thickness is t_h. The gaps between disc and housing will be filled with MRF. All parameters in the Figure 3.18 are going to be used in the calculation of braking torque as well as the optimization part of the brake later.

3.4.1. Mathematic model of braking torque of tooth-shaped MRB

The calculation of braking torque of tooth-shaped MRB was carried out by the research "Design and Experimental Evaluation a novel magneto-rheological brake with tooth

shaped rotor" [8]. The mathematic model of braking torque from that research is applied to tooth-shaped MRB in this thesis since two model have the same principle.

The total braking torque of the tooth-shaped MRB is the derived as following:

$$T_b = 2(\sum_{i=1,3,5,7,9} T_{Ii} + \sum_{j=0,2,4,6,8,10} T_{Ej}) + T_a + 2T_s + 2T_{br} \quad (10)$$

Where:

T_{Ii} is the induced torque in an inclined duct of MRF which is denoted by "I" in Figure 3.18. In order to see how the inclined torque is constructed. An annular element of the MRB is introduced

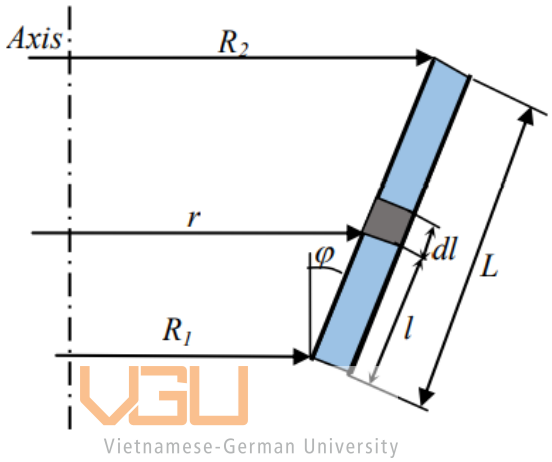

Figure 3.20: Annular ring element in the inclined duct

$$T_{Ii} = 2\pi(R_i^2 l + R_i l^2 sin\varphi + \frac{1}{3} l^3 sin^2\varphi)\mathrm{T}_{yIi} + \frac{\pi}{2}\mu_{Ii}\frac{l}{d}(4R_i^3 + 6R_i^2 l sin^2\varphi + 4R_i l^2) \quad (11)$$

$$\mathrm{i} = 1,3,5,7,9$$

T_{Ej} is the induced torque in a radial duct (end-face duct) which is denoted by "E" in Figure 3.18

$$T_{Ej} = \frac{\pi\mu_{Ej}R_{j+1}^4}{2d}\left[1 - \left(\frac{R_j}{R_{j+1}}\right)^4\right]\Omega + \frac{2\pi\mathrm{T}_{yEj}}{3}\left(R_{j+1}^3 - R_j^3\right); \quad (12)$$

$$j = 0.2.4.6.8.10$$

T_a is friction torque acting on a cylindrical face of the rotor in the corresponding annular duct which is denoted by "a" in Figure 3.18

$$T_a = 2\pi R_d^2(b + 2hh)(\mathrm{T}_{ya} + \mu_a\frac{\Omega R_d}{d_o}) \quad (13)$$

T_s is the lip-seal friction torque which is derived as:

$$T_s = 0.65(2R_s)^2\Omega \quad (14)$$

T_{br} is the friction of the deep groove ball bearing which can be neglected since it is very small.

In equation (11), (12), (13), (14), R_i and R_j are the radius to the odd point and even point in Figure 4.1, l and φ are the length and the angle of the inclined duct. T_{yI}, T_{yE} and T_{ya} are respectively the yield stress of MRF in the I_i, E_j, and a gap. μ_{Ii}, μ_{Ej} and μ_a are corresponding post yield viscosity. d is the duct gap size. Ω is the angular speed. R_d is the radius of the MRB disc, b and hh are showing in the figure 3.18, d_o is the cylindrical gap size and R_s is the shaft radius.

The rheological properties of MRF which are yield stress T_y and post-yield viscosity μ are assumed to be performed as the equation (2) when the magnetic flux density across the MRF duct changes. Then, two following equations can be derived:

$$T_y = T_{y\infty} + (T_{y0} - T_{y\infty})\,(2e^{-B\alpha_0} - e^{-B\alpha_\infty}) \quad (15)$$

$$\mu = \mu_\infty + (\mu_0 - \mu_\infty)\,(2e^{-B\alpha_0} - e^{-B\alpha_\infty})$$

3.4.2. Mathematic model of MRF-based mechanisms

The purpose of the MRF-based mechanisms is to find the relation between the electric power supply and the mechanical torque of the MR Brake. Furthermore, this mechanism also provides the mean to control the torque by the electric current.

In order to solve the modeling of MRF, the result equations from the research "Optimal Design Methodology of Magnetorheological Fluid Based Mechanisms" [4] is applied. The field intensity across the MRF volume H_{mr} and the magnetic flux density B_{mr} are respectively formulated as follow:

$$H_{mr} = \frac{N_{turns} I}{l_{mr}} \quad (16)$$

$$B_{mr} = \mu_0 \mu_{mr} H_{mr} \quad (17)$$

Where: I is the applied current, for safety reason the applied current is limited at 2.5 A. l_{mr} is the effective length of the MRF which means the length of MRF gaps have the magnetic field in it. μ_0 and μ_{mr} are the magnetic permeability of the free space ($\mu_0 = 4\pi 10^{-7}$ Tm/A) and of MRF respectively. N_{turns} is the number of turns of the coil. N_{turns} can be approximated by following equation

$$N_{turns} = \frac{A_c}{A_w} * c \quad (18)$$

Where: A_c is the cross-section area of the coil and A_w is the cross-section area of the coil wire, c is the efficient ratio of the coil wire. Usually, the current density in the area of the coil wire does not fill full 100%. Therefore, the ratio c in this project is assumed to be 0.81.

Typically, in order to determine the MRB performance characteristics, the magnetic flux density B_{mr} should be evaluated. However, the average value should be used since the magnetic flux density B_{mr} along the MRF duct are not constant. By integrating flux density along a defined path, the average magnetic flux density over the MR ducts could be found

$$B_{mr\ averange} = \int_{L_p} B(s)ds \tag{19}$$

Where s is a dummy variable for the integration and B(s) is the magnetic flux density at each node in the path. The path length Lp is used to carry out the integration.

Finally, the power consumption P of the MR Brake can be calculated as:

$$P = I^2 * R_w \tag{20}$$

Where: R_w is the resistance of the coil wire which can be determined by:

$$R_w = N_{turns} * \pi * d_c * \frac{r}{A_w} \tag{21}$$

In this equation, d_c is the average diameter of the coil, r is the resistivity of the coil wire. For a cooper wire, r is set at 0.01726e-6 Ωm.

For the tooth-shaped MRB whose configuration is at figure 4.1, Since this MRB has two coil and from equation (20), equation (21), the power consumption equation for tooth-shaped MRB is:

$$P_{tooth-shaped} = 2 * I^2 * N_{turns} * \pi * dc * \frac{r}{A_w} \tag{22}$$

3.4.3. Mass of the tooth-shaped MR brake

The mass of the tooth-shaped MR brake is mathematically stated as

$$m_b = V_h\rho_h + V_d\rho_d + V_c\rho_c + V_{mr}\rho_{mr} \tag{23}$$

Where m_b is the mass of MR brake, V_h, V_d, V_c, V_{mr} are the volume of the housing, the disc, the coil, the MR fluid respectively. Consequently, ρ_h, ρ_d, ρ_c, ρ_{mr} are the density of the housing, the disc, the coil, the MR fluid. Due to geometric shape, the volume of the disc and the housing of MRB is complicate to derive. For that reason, the total mass of the housing and the disc is calculated as

$$V_h\rho_h + V_d\rho_d = V_b\rho_{c45} - V_{mr}\rho_{c45} - V_c\rho_{c45} \quad (24)$$

Where V_b is the volume of MR brake if it is fully C45 steel which can be easily calculated by radius and thickness of the brake. P_{c45} is the density of C45 steel which is equal to ρ_h and ρ_d. As a result, equation (22) becomes

$$m_b = V_b\rho_{c45} - V_{mr}\rho_{c45} - V_c\rho_{c45} + V_c\rho_c + V_{mr}\rho_{mr} \quad (25)$$

3.5. Optimal design for tooth-shaped MR Brake

As the MRB is attached on the electric scooter, one of important factors is the power consumption of the brake. The amount of this power should not be too much or exceed the power that the electric scooter can supply. From the equation (22), the power consumption of the tooth-shaped MR brake is depended on the size of the coil since other values are all constant and could not be modified. Moreover, figure 3.18 shows that the size of MRB's coil geometrically relate to the size of the housing of the MRB. Thus, the optimal design problem in this study is to find the optimal geometric dimensions of the tooth-shaped MR brake which can create a maximum braking torque as large as the required torque for each wheel. The brake structures are constrained in an annular space which is determined by R_{rear} = 55 mm, L_{rear} = 45 mm for rear brake and R_{front} = 110 mm, L_{max} = 45 mm for front brake. Furthermore, the constraint equation (9) for temperature of the MRF need to be satisfied. The design requirement is showed in the Table 3.5.

In order to solve the optimization problem, the finite element analysis (FEA) integrated with an optimization tool of ANSYS Workbench 19.2 is implemented. In the ANSYS optimization tool, the NLPQL method (Nonlinear Programing by Quadratic Lagrangian) is used to achieve the optimal solution. The NLPQL method is a gradient-based algorithm to provide a refined, local, optimization result. It supports a single objective, multiple constraints and is limited to continuous parameters. The starting point must be specified to determine the region of the design space to explore. To be more specific, the starting point is the start value of design variables. Following dimensions of MRB: the thickness of disc b, the outer housing thickness t_o, the coil thickness wc_1, the tooth height hh, the length from base to peak of tooth hb1, the tooth peak length hb2 and the value denoted by lpk = R_i -R_s are design variables.

By using the geometric relations of tooth-shaped MR brake and equations (6), (9), (10), (15), (19), (22), (25), the analysis code file used in optimal design of MRB is conducted. The detail ANSYS code file is put at Appendix section for reference.

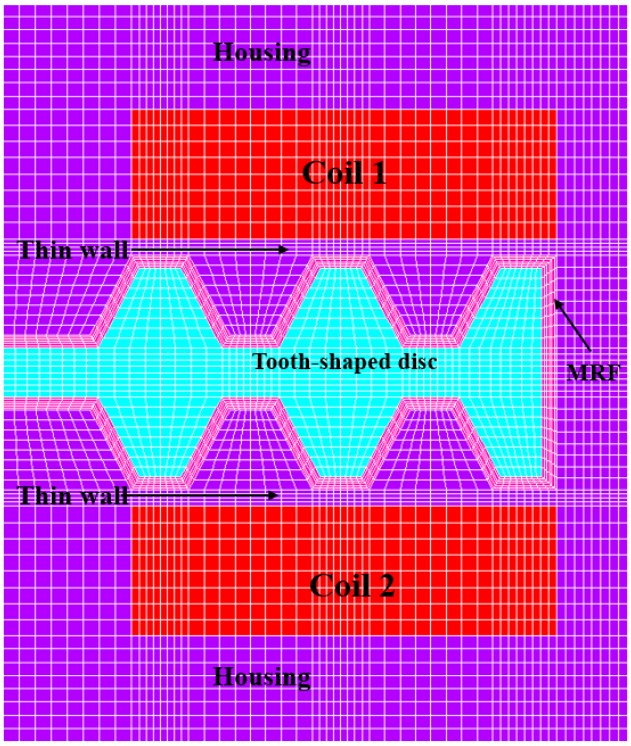

Figure 3.21: Finite element models of tooth-shaped MR Brake

Optimization	
Method Selection	Manual
Method Name	NLPQL
Estimated Number of Design Points	800
Finite Difference Approximation	Forward
Allowable Convergence (%)	0.1
Maximum Number of Iterations	100
Maximum Number of Candidates	3

Table 3.6: Specification of MLPQL method

By considering manufacturing benefit the top tooth peak length hb4 is set at 3 mm. It is noted that the braking torque T_b will increase as the MRF gap size is smaller, however if the gap size is too small, this will lead to difficulty in manufacturing the MRB. Thus, the size of MRF gaps is set at 0.8 mm for horizontal MRF gap and 0.9 mm for vertical MRF gap. Furthermore, the magnitude of the applied current is limited at 2.5 A which means that at 2.5 A, the MRB will achieve a maximum braking torque. The machining

issues are also considered for design variable, which leads to the range of design variables as follow:

Table of Schematic B2: Optimization

	A	B	C	D
1	Input Parameters			
2	Name	Lower Bound	Upper Bound	Starting Value
3	P1 - B	0.003	0.015	0.0035
4	P2 - TO	0.002	0.015	0.0025
5	P3 - WC1	0.003	0.015	0.0035
6	P4 - HH	0.002	0.015	0.0025
7	P5 - HB1	0.0025	0.015	0.003
8	P6 - HB2	0.0025	0.015	0.003
9	P7 - LPK	0.003	0.03	0.0035
10	Parameter Relationships			
11	Name	Left Expression	Operator	Right Expression
*	New Parameter Relationship	New Expression	<=	New Expression

Table 3.7: The range of design variable

In table 3.7, the Lower Bound column means the lower limit value of design variables and the Upper Bound is the upper limit value of design variable and Starting value is the initial value of variable. All the values are at millimeter unit.

Beside the maximum brake torque objective and temperature constraint, there are two more constraint by considering the ability in fabrication, which are the distance between teeth hb3 $\geq$ 2.5 mm and the inclined MRF gap size $d_1 \geq 0.8$ mm. As a result, a complete constraint of optimal design problem is

Table of Schematic B2: Optimization

	A	B	C	D	E	F	G
1	Name	Parameter	Objective		Constraint		
2			Type	Target	Type	Lower Bound	Upper Bound
3	Maximize P11	P11 - TB	Maximize		No Constraint		
4	P13 <= 100	P13 - SV1	No Objective		Values <= Upper Bound		100
5	P8 >= 0.0008	P8 - D1	No Objective		Values >= Lower Bound	0.0008	
6	P9 >= 0.0025	P9 - HB3	No Objective		Values >= Lower Bound	0.0025	
*		Select a Parameter					

Table 3.8: The objective and constraint of optimal design problem

As the constraint radius R of the rear MR brake is smaller than the front MR brake, R_{rear} value is used firstly in the ANSYS optimization tool to see if require braking torque could be achieved. In case that the required torque fails to accomplish, the radius value

of the MR brake R will be slowly increase until the required torque is gained. Thus, the tragedy to obtain the optimal design for both rear MRB and front MRB is illustrated in following flow chart

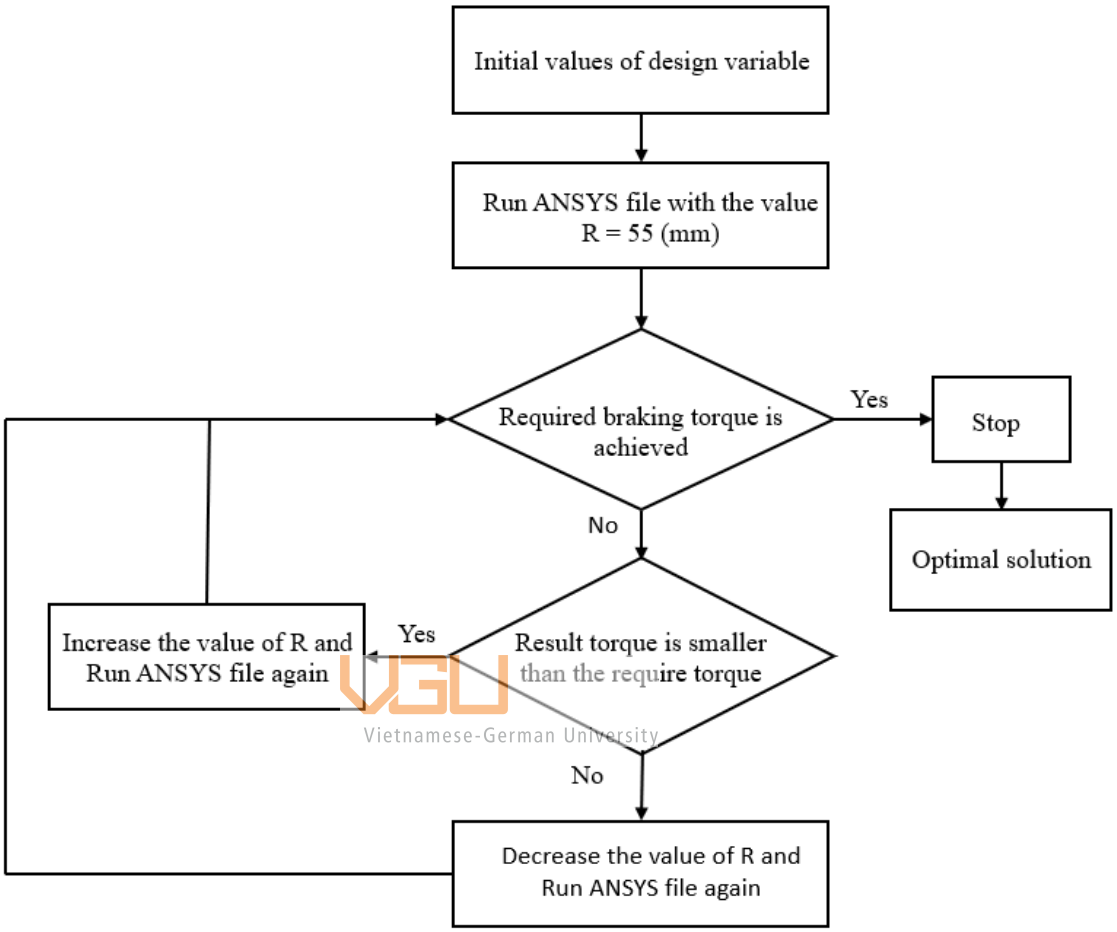

Figure 3.22: Flow chart of method to achieve optimal design parameters of MR Brake

4.2.1. Result of rear tooth-shaped MR Brake

Table of Schematic B2: Optimization				
	A	B	C	D
1	Optimization Study			
2	Maximize P11	Goal, Maximize P11 (Default importance)		
3	P8 >= 0.0008	Strict Constraint, P8 values greater than or equals to 0.0008 (Default importance)		
4	P13 <= 100	Strict Constraint, P13 values less than or equals to 100 (Default importance)		
5	Optimization Method			
6	NLPQL	The NLPQL method (Nonlinear Programming by Quadratic Lagrangian) is a gradient -based algorithm to provide a refined, local, optimization result. It supports a single objective, multiple constraints and is limited to continuous parameters. The starting point must be specified to determine the region of the design space to explore.		
7	Configuration	Approximate derivatives by Forward difference and find 3 candidates in a maximum of 100 iterations.		
8	Status	Converged after 105 evaluations.		
9	Candidate Points			
10		Starting Point	Candidate Point 1	Candidate Point 2
11	P1 - B	0.0035	0.003	0.003
12	P2 - TO	0.0025	0.0039982	0.0040163
13	P3 - WC1	0.0035	0.0078678	0.0078119
14	P4 - HH	0.0025	0.0049162	0.0049952
15	P5 - HB1	0.003	0.0025	0.0025
16	P6 - HB2	0.003	0.0025	0.0025
17	P7 - LPK	0.0035	0.014293	0.014694
18	P8 - D1	0.00057617	0.00080223	0.00080483
19	P9 - HB3	0.00312	0.0015136	0.0015008
20	P10 - PP	98.813	180.33	178.81
21	P11 - TB	61.527	81.487	81.375
22	P12 - MASS	3.2868	3.2905	3.2888
23	P13 - SV1	24.634	28.056	28.167

Table 3.9: Optimal solution of the rear tooth-shaped MRB with R = 55 mm

The table shows that after the optimal solution is found after 105 evaluations with 0.1 % tolerance. However, the maximum braking torque is only 81.487 N.m which do not meet the requirement one. As a result, the radius of the rear tooth-shaped MR brake needs increasing.

When the radius of the rear MR brake is increased to 70 mm (R_{rear} = 70 mm), the optimal result is able to achieve with required maximum braking torque.

Table of Schematic B2: Optimization			
	A	B	C
1	Optimization Study		
2	Maximize P10	Goal, Maximize P10 (Default importance)	
3	P8 >= 0.0025	Strict Constraint, P8 values greater than or equals to 0.0025 (Default importance)	
4	P9 >= 0.0008	Strict Constraint, P9 values greater than or equals to 0.0008 (Default importance)	
5	P12 <= 100	Strict Constraint, P12 values less than or equals to 100 (Default importance)	
6	Optimization Method		
7	NLPQL	The NLPQL method (Nonlinear Programming by Quadratic Lagrangian) is a gradient-based algorithm to provide a refined, local, optimization result. It supports a single objective, multiple constraints and is limited to continuous parameters. The starting point must be specified to determine the region of the design space to explore.	
8	Configuration	Approximate derivatives by Forward difference and find 3 candidates in a maximum of 100 iterations.	
9	Status	Converged after 87 evaluations.	
10	Candidate Points		
11		Starting Point	Candidate Point 1
12	P1 - B	0.0035	0.003
13	P2 - TO	0.0025	0.0043343
14	P3 - WC1	0.0035	0.0076874
15	P4 - HH	0.0025	0.0048507
16	P5 - HB1	0.003	0.0025
17	P6 - HB2	0.003	0.0034754
18	P7 - LPK	0.0035	0.014931
19	P8 - HB3	0.00312	0.0025
20	P9 - D1	0.00057617	0.0008
21	P10 - TB	126.89	164.74
22	P11 - MASS	5.334	5.3494
23	P12 - SV1	38.592	42.212
24	P13 - PP	137.38	273.62

Table 3.10: Optimal solution of the rear tooth-shaped MRB with R = 70 mm

The optimal result is obtained after 87 evaluations with a convergence tolerance 0.1 %. It is observed from the table 3.10 that the braking torque of the optimized brake is 164.74 Nm and the constraint equation of MRF's temperature at a cruising speed of 50 km h^{-1} is satisfied. Both constraints of inclined MRF gap d_1 and the distance between teeth hb3 are also satisfied which have the values respectively 0.8 mm and 2.5 mm. The optimal value of design variables b, t_o, wc1, hh, hb1, hb2, lpk are respectively 3 mm, 4.33 mm, 7.69 mm, 4.85 mm, 2.5 mm, 3.47 mm, 14.93 mm. The mass of the MRB is 5.35 kg and the power consumption is 273.62 W

Radius of the rear MR brake equal 70 mm means that the constraint hub of the old brake must be destroyed. However, removing this hub could damage the motor which locates in the back wheel of electric scooter. For this reason, the optimal tooth-shaped MR

brake of rear wheel is not going to be fabricated. This MR brake configure will be kept for future plan.

4.2.2. Result of front tooth-shaped MR Brake

Based on the referent value of optimal rear MR brake's radius, the optimal radius of the front tooth-shaped MR brake is found which is 75 mm. This value does not exceed constraint value of front MRB which is 110 mm. Thus, the front MR brake could be easily manufactured without any large change of the front wheel mechanism. Furthermore, in order to fabricate the front MRB later, there is one more constraint added to the optimal design problem which is $R_i \geq 37$ mm and the value of R_s has to be equal to 25 mm. The reason for these changes will be explained in the Chapter 4 of this thesis. As a result, the optimal solution of front MR brake is

Table of Schematic B2: Optimization

	A	B	C	D
1	Optimization Study			
2	Maximize P13	Goal, Maximize P13 (Default importance)		
3	P9 >= 0.0008	Strict Constraint, P9 values greater than or equals to 0.0008 (Default importance)		
4	P10 >= 0.0025	Strict Constraint, P10 values greater than or equals to 0.0025 (Default importance)		
5	P11 >= 0.037	Strict Constraint, P11 values greater than or equals to 0.037 (Default importance)		
6	P15 <= 100	Strict Constraint, P15 values less than or equals to 100 (Default importance)		
7	Optimization Method			
8	NLPQL	The NLPQL method (Nonlinear Programming by Quadratic Lagrangian) is a gradient-based algorithm to provide a refined, local, optimization result. It supports a single objective, multiple constraints and is limited to continuous parameters. The starting point must be specified to determine the region of the design space to explore.		
9	Configuration	Approximate derivatives by Forward difference and find 3 candidates in a maximum of 100 iterations.		
10	Status	Converged after 102 evaluations.		
11	Candidate Points			
12		Starting Point	Candidate Point 1	Candidate Point 2
13	P1 - B	0.0035	0.003	0.003
14	P2 - TO	0.0025	0.004314	0.0042928
15	P3 - WC1	0.0035	0.0078998	0.0077249
16	P4 - HH	0.0025	0.0048507	0.0048507
17	P5 - HB1	0.003	0.0025	0.0025
18	P6 - HB2	0.003	0.0034754	0.0034754
19	P7 - LPK	0.0035	0.0053352	0.0053565
20	P8 - DD	-5.9993E-05	0.00048769	0.00048769
21	P9 - D1	0.00057617	0.0008	0.0008
22	P10 - HB3	0.00312	0.0025	0.0025
23	P11 - RI	0.03786	0.037	0.037
24	P12 - PP	150.24	307.94	301.24
25	P13 - TB	153.86	199.89	199.77
26	P14 - MASS	6.1267	6.1611	6.1581
27	P15 - SV1	58.4	65.436	65.498

Table 3.11: Optimal solution of the front tooth-shaped MRB with R = 75 mm

From the table, it can be seen that the optimal solutions are achieved after 102 evaluations with a convergence tolerance 0.1 %. There are 2 optimal result which are Candidate point 1 and Candidate point 2. The different between 2 Candidates is very little, however, when manufacturing the braking torque will not be achieved the value as great as optimal result. For this reason, Candidate point 1 is chosen as the optimal design of front tooth-shaped MR brake.

The optimal values of design variables b, t_o, wc1, hh, hb1, hb2, lpk are respectively 3 mm, 4.31 mm, 7.89 mm, 4.85 mm, 2.5 mm, 3.47 mm, 5.33 mm. The maximum braking torque value is 199.89 Nm, this value is larger than the required one which is 195.51 Nm. The constraint equation of MRF's temperature at a cruising speed 50 km h^{-1} is also fulfilled. By using the geometric relation of the tooth-shaped MR brake which is shown in figure 3.18, the optimal parameter of front MR brake is able to be derive

Parameters	Optimal Value
Disc thickness b (mm)	3
Outer housing thickness to (mm)	4.31
Coil thickness wc1 (mm)	7.89
Tooth height hh (mm)	4.85
Length from base to peak of tooth hb1 (mm)	2.5
Tooth peak length hb2 (mm)	3.47
Distance between teeth hb3 (mm)	2.5
Top tooth peak length hb4 (mm)	3
Horizontal gap size d (mm)	0.8
Vertical gap size do (mm)	0.9
Inclined gap size d1 (mm)	0.8
Drum inner radius Ri (mm)	37
Shaft radius Rs (mm)	25
Mass (kg)	6.16
Braking torque (N.m)	199.89
Number of coil-turns (turns)	806
Power consumption (W)	307.94

Table 3.12: Optimal parameters of the front tooth-shaped MRB

The mass of traditional rear brake and disc brake of electric scooter are usually around 0.24 kg and 0.103 kg respectively. Thus, the mass of designed tooth - shaped MRB is much heavier than other traditional brake due to the necessary of material for forming the brake. However, with the advantages of MRB that are mentioned in Chapter 1, the

application of MRB on electric scooter is still potential with some improvement in the future.

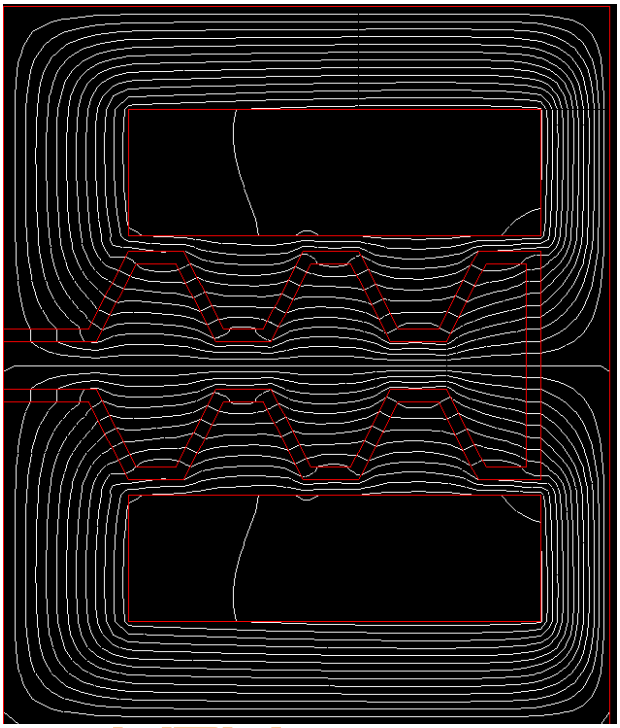

Figure 3.23: Magnetic flux line path in the optimal front MRB

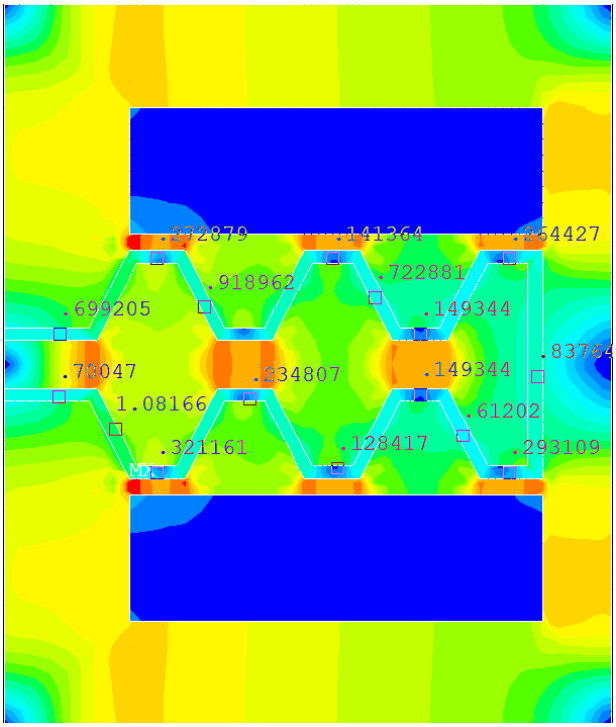

Figure 3.24: Magnetic flux density in the optimal front MRB

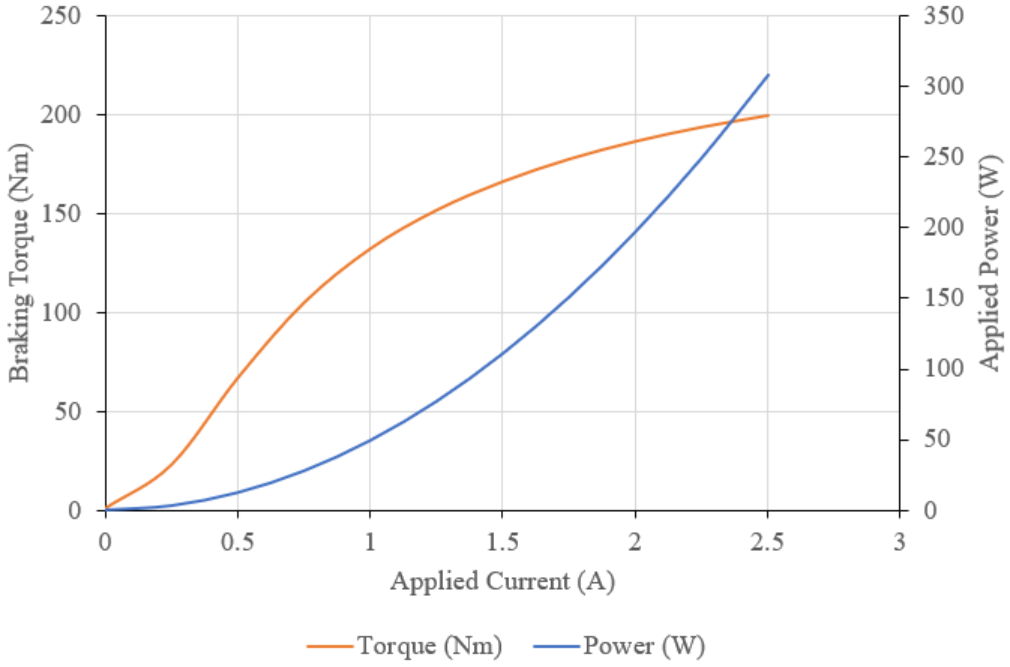

Figure 3.25: Theorical braking torque and power consumption of tooth-shaped MRB repects to applied electric current

Chapter 4: Detailed design of prototype MR brake

4.1. Overview of detail design of front MR brake

Although all necessary parameters of front tooth-shaped MR brake are found in table 3.2, the MR brake still needs some mechanical components and modifying for application on electric scooter. Thus, this section will present a detail structure of MRB as well as a method of assembling it on the front wheel. By using Solidwork software, the mechanism of front tooth-shaped MR brake is able to be made.

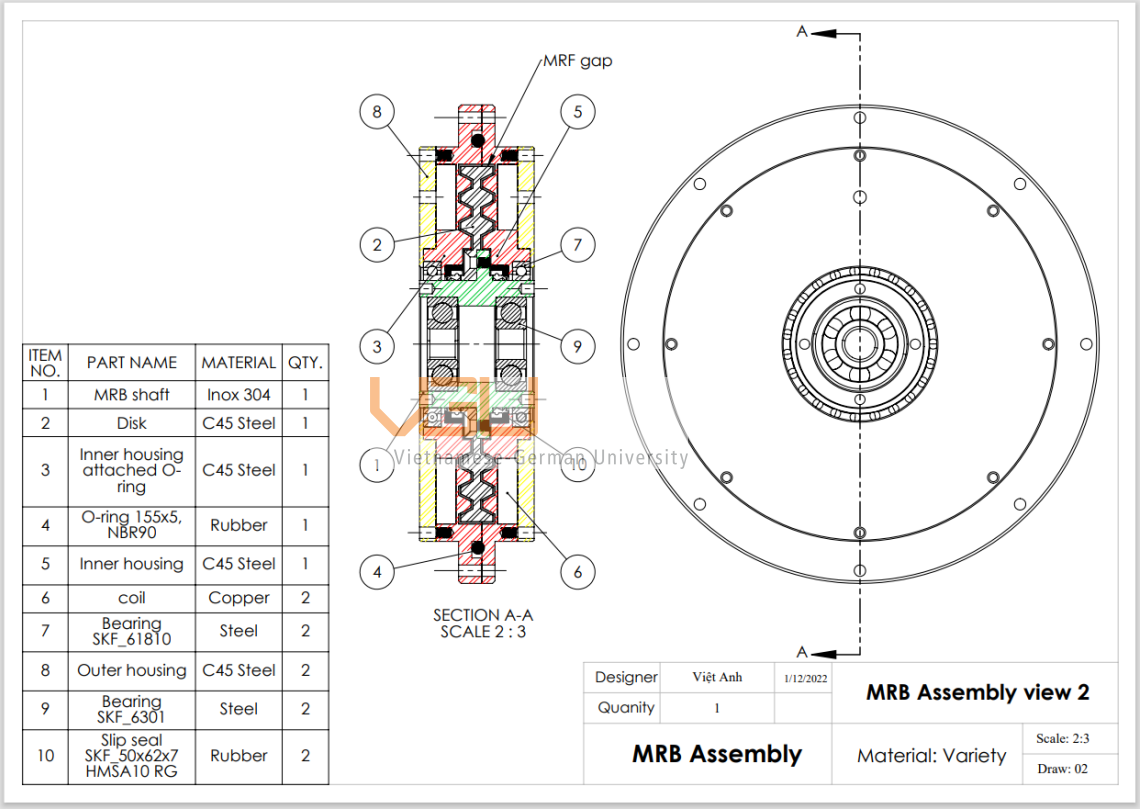

ITEM NO.	PART NAME	MATERIAL	QTY.
1	MRB shaft	Inox 304	1
2	Disk	C45 Steel	1
3	Inner housing attached O-ring	C45 Steel	1
4	O-ring 155x5, NBR90	Rubber	1
5	Inner housing	C45 Steel	1
6	coil	Copper	2
7	Bearing SKF_61810	Steel	2
8	Outer housing	C45 Steel	2
9	Bearing SKF_6301	Steel	2
10	Slip seal SKF_50x62x7 HMSA10 RG	Rubber	2

Figure 4.1: Section view of front MR brake assembly

When it comes to the connection of MR brake to Front wheel, the conceptual design is made also by Solidwork which consists of: the front wheel, the hub connector, pins, tooth-shaped MR brakes, retain ring and washer. The connection hub is attached to the front wheel by bolt joints and the MR brake is joined to the connection hub by small pins. The retain ring and washers are used to secure the bearings in place.

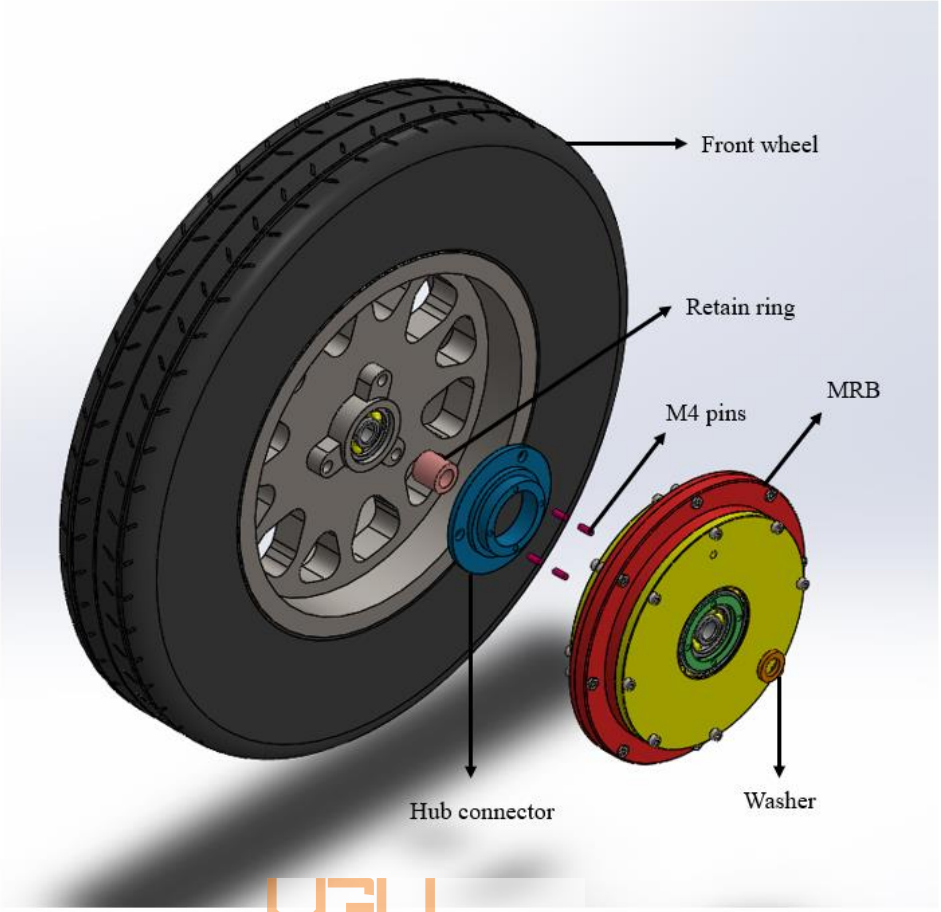

Figure 4.2: Conceptual design of Front MR brake system

To achieve two designs as figure 4.1 and figure 4.2, the following design approach was used

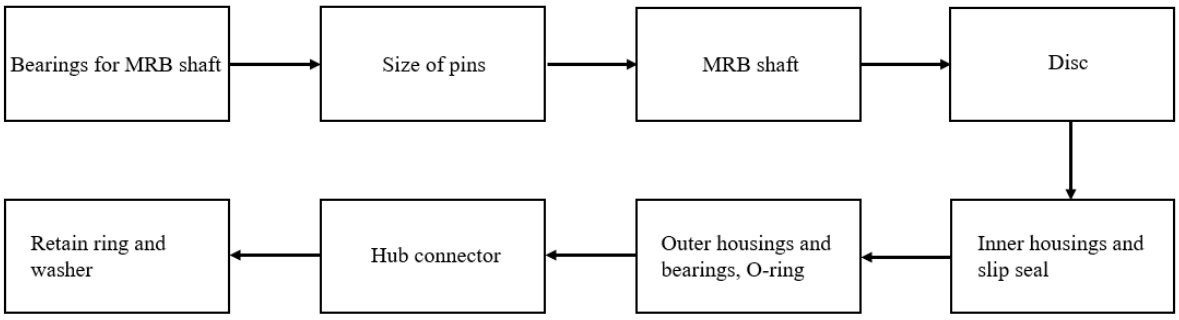

Figure 4.3: Detail design procedure

The design approach is an alternation between components of MR brake and components for connection of front brake system. Thus, this will ensure that the MR brake is fit in available space of the front wheel.

4.2. Mechanism of the front tooth-shaped MR brake

4.2.1. Shaft of tooth-shaped MR brake (MRB shaft)

The MRB shaft is where the MR brake placed on and it also provides the rotation motion for the disc of MRB. This shaft rotates according to the front wheel and the front wheel is rotated around a fix front shaft by using bearings, which means the MRB shaft should be in hollow shape to install bearings either. The outer radius of MRB shaft is denoted as R_s in table 3.12. The inner radius of the shaft is chosen according to the outer radius of front wheel's bearings. The reason for why the bearings of front wheel and MRB shaft's ones need to be similar is to ensure that the disc of MR brake rotate at the same speed with the front wheel. The bearings of the front wheel have similar technical dimensions the model SKF_6301 of SKF deep groove ball bearings.

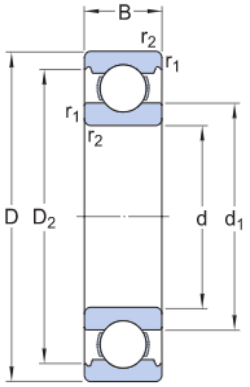

Dimensions

d	12 mm	Bore diameter
D	37 mm	Outside diameter
B	12 mm	Width
d_1	≈ 19.51 mm	Shoulder diameter
D_2	≈ 31.48 mm	Recess diameter
$r_{1,2}$	min. 1 mm	Chamfer dimension

Figure 4.4: Technical dimensions of SKF_6301 deep groove ball bearing

(SKF, 2022) [15]

Consequently, two SKF_6301 deep groove ball bearings are installed inside the MRB shaft. Thus, the value of inner diameter of MRB shaft is 37 mm. Furthermore, there are some requirements in order to place bearings which need to be satisfied when designing MRB shaft

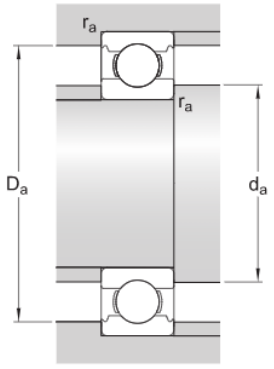

Abutment dimensions

d_a	min. 17.6 mm	Diameter of shaft abutment
D_a	max. 31.4 mm	Diameter of housing abutment
r_a	max. 1 mm	Radius of shaft or housing fillet

Figure 4.5: Requirement for installing SKF_6301 deep groove ball bearing

[15]

The outer radius of the MRB shaft is determined by the diameter of pins (see figure 4.2). The diameter of pins in this design is 4 mm which lead to the fact that the outer radius of MRB shaft must be larger than 22.5 mm. As a result, the outer radius R_s in this case is chosen to be 25mm. This is the reason why there is a constraint $R_s \geq 25$ in the optimal design problem of the front tooth-shaped MR brake.

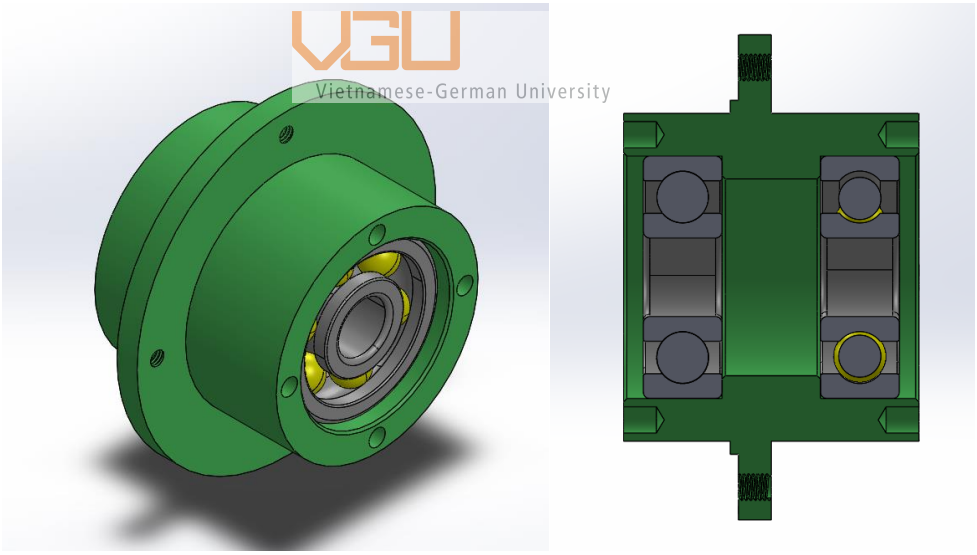

Figure 4.6: MRB shaft with SKF_6301 deep groove ball bearing CAD

The MRB shaft is designed to have a round flange at the middle in order to connect with the disk of MR brake later. The material for MRB shaft is 304 inox which is non-magnetic material. Thus, this material will prevent the magnetic flux of MRB from transferring through the MRB shaft.

4.2.2. Tooth-shaped disc

It is necessary for the disc to have enough space at the base in order to be fixed with the MRB shaft by bolt joint and this space is denote as R_i - R_s (see figure 3.18). Due to the type of bolts in this design is M4 and the head of this bolt is compulsory to place fully inside the round flange of the disc, R_i must larger than 37 mm.

With all dimension is determined in table 3.12, the design of the disc of MRB is easy to make and the material for the disc is C45 steel.

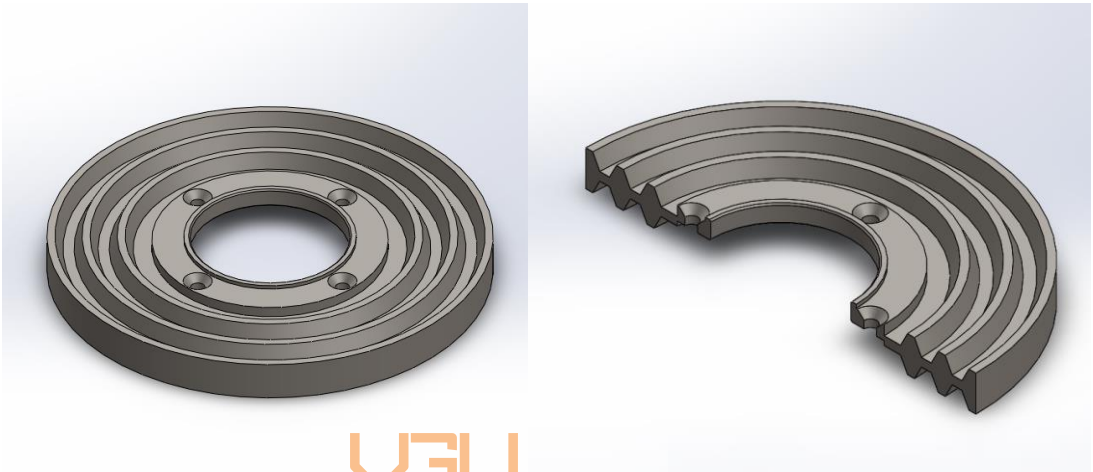

Figure 4.7: CAD of tooth-shaped disc

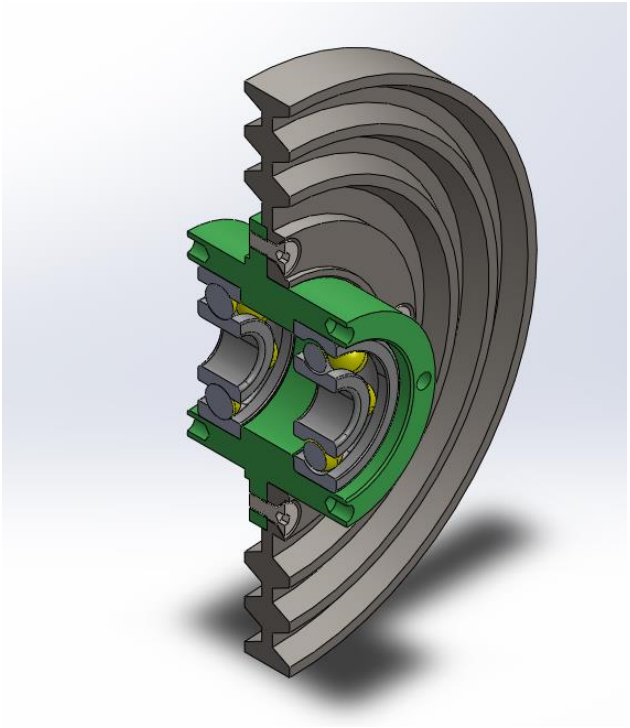

Figure 4.8: Section view of connection between MRB shaft and tooth-shaped disc

4.2.3. Inner housing, coil, slip seals, O-ring and bearings

The total housing of the MR brake is separated into 2 parts that are inner housing and outer housing. The material for both inner and outer housing is C45 steel. The inner housing combines with the disc to create the gaps to retain the MRF inside, moreover, each half of the inner housing is where the coil is placed. Slip seals and O-ring play an important role in preventing the MRF from leaking out when half of inner housing are assembled to each other.

4.2.3.1. Slip seals

The chosen slip seals should have the value of inner diameter be same as value of the MRB shaft's diameter which is 50mm. One more considered factor when choosing slip seal is the thickness of it. The thinner the slip seal is, the better for the MR brake structure since the thickness of the front MR brake is only 45 mm. Thus, the model SKF_50x62x7 HMSA10 RG from SKF is selected since it is satisfied both conditions.

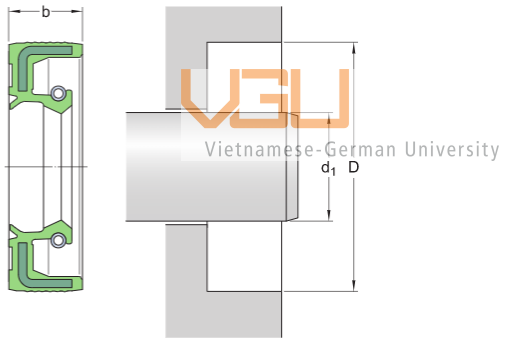

Dimensions

d_1	50 mm	Shaft diameter
D	62 mm	Housing bore diameter
b	7 mm	Seal width

Application and operating conditions

Operating temperature	min. -40 °C
Operating temperature	max. 100 °C
Operating temperature, short periods	max. 120 °C
Circumferential speed	max. 7.84 m/s
Rotational speed	max. 3 000 r/min
Pressure differential	0.03 N/mm²

Figure 4.9: Technical specification of SKF_50x62x7 HMSA10 RG slip seal

[15]

4.2.3.2. O-ring

While the slip seal prevents MRF from leaking out horizontally, the O-ring help restrain the MRF annularly. The inner diameter of the O-ring has to larger than the diameter of

the front MR brake which is 150 mm. As a result, the model O-ring 155x5 NBR90 from Lemming company is the most suitable for the front MR brake.

O-ring dimension	
Inside diameter	155
Cross section	5
Details	
Seal type	O-ring
Material type	NBR90

Table 4.1: Technical specifications of O-ring 155x5 NBR90

(Lemming, 2022) [16]

There is also a requirement for the structure of inner housing when installing O-ring 155x5 NBR90

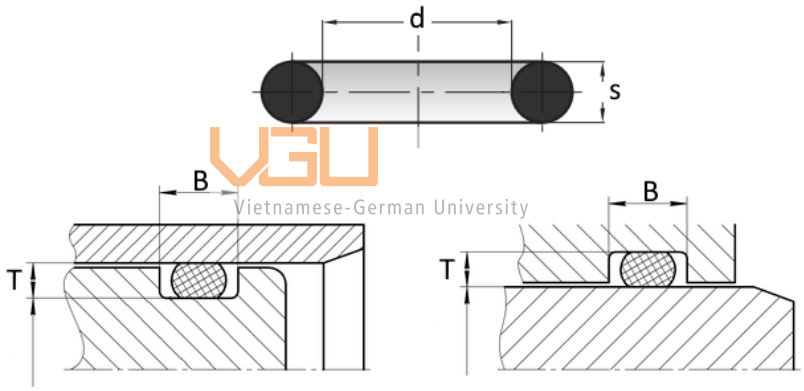

Figure 4.10: O-ring groove

O-ring groove is where the O-ring is placed in. When determining the width of the groove, these followings have to be considered: O-ring diameter, oval form formed after assembly, the free space which is necessary to ensure even pressure. It is also important to prevent the groove from overfilling. Thus, the O-ring should fill it to a maximum of 85%, leaving room for possible increase in volume.

s O-ring thickness	T groove depth	B groove width
1,5	1,1	1,9
1,6	1,2	2,1
1,78	1,3	2,3
2	1,5	2,6
2,4	1,8	3,1
2,5	1,9	3,2
2,62	2	3,4
3	2,3	3,9
3,53	2,75	4,5
4	3,15	5,2
5	4	6,5

Table 4.2: O-ring groove dimension bases on O-ring thickness

[16]

The thickness of chosen O-ring is 5 mm, then the dimension of the groove is showed in the red box.

4.2.3.3. Bearings

The bearings are also placed inside the inner housings in order to make the inner housings be as concentric with the MRB shaft as possible. This will ensure two half inner housings do not lean forward or backward when they are assembled which causes the reduction of MRF gap size. Moreover, the bearings also the housing to stand still while the tooth-shaped disc is rotated. The criteria for choosing bearings of MRB are that they must be fit with the MRB shaft whose diameter is 50 mm and their width need to be as small as possible. The model SKF_61810 deep groove ball bearing is the most suitable for require criteria of MRB and it is used for this design.

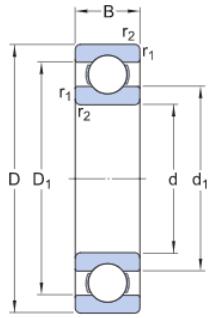

Dimensions

d	50 mm	Bore diameter
D	65 mm	Outside diameter
B	7 mm	Width
d_1	≈ 54.67 mm	Shoulder diameter
D_1	≈ 60.3 mm	Shoulder diameter
$r_{1,2}$	min. 0.3 mm	Chamfer dimension

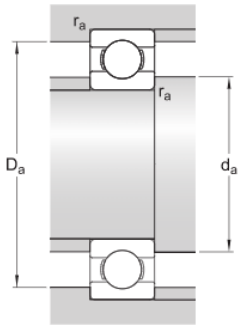

Abutment dimensions

d_a	min. 52 mm	Diameter of shaft abutment
D_a	max. 63 mm	Diameter of housing abutment
r_a	max. 0.3 mm	Radius of shaft or housing fillet

Figure 4.11: Technical dimensions of SKF_61810 deep groove ball bearing [15]

Calculation data

Basic dynamic load rating	C	6.76 kN
Basic static load rating	C_0	6.8 kN
Fatigue load limit	P_u	0.285 kN
Reference speed		20 000 r/min
Limiting speed		13 000 r/min
Minimum load factor	k_r	0.015
Calculation factor	f_0	17.2

Table 4.3: Technical specifications of SKF_61810 deep groove ball bearing [15]

4.2.3.4. Inner housings

Based on table 3.12, figure 4.8, table 4.2 and figure 4.10, the inner housing's geometric shape are able to be modified for installing slip seals, O-ring and bearings. The geometric shape of the coil is also easy to determine by table 3.12.

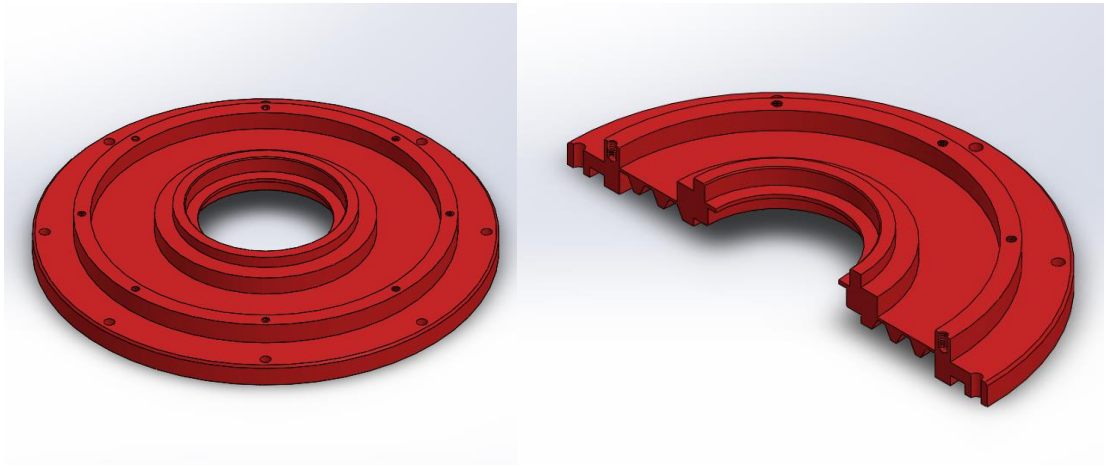

Figure 4.12: CAD of half of inner housing which attach O-ring

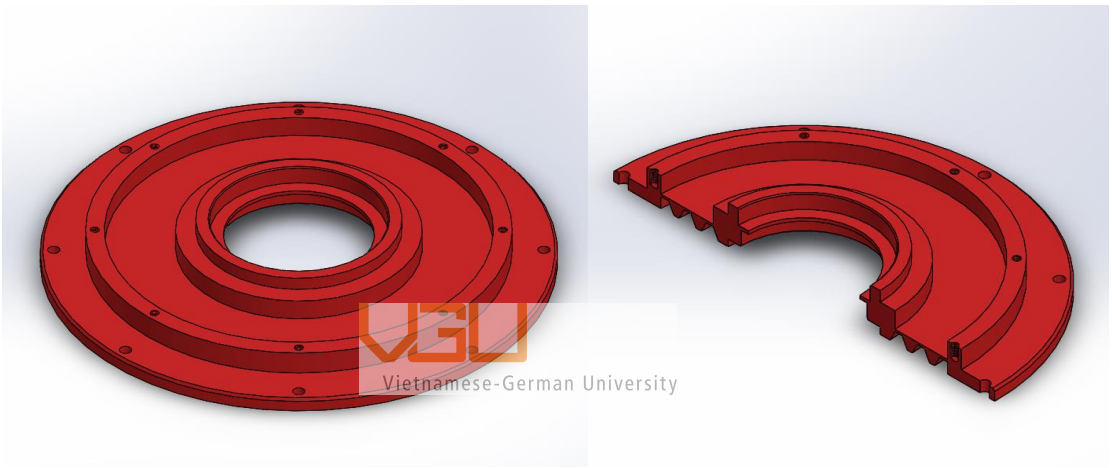

Figure 4.13: CAD of other half of inner housing

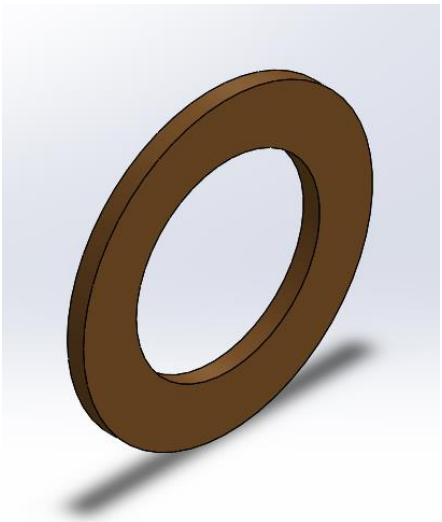

Figure 4.14: CAD of MR brake's coil

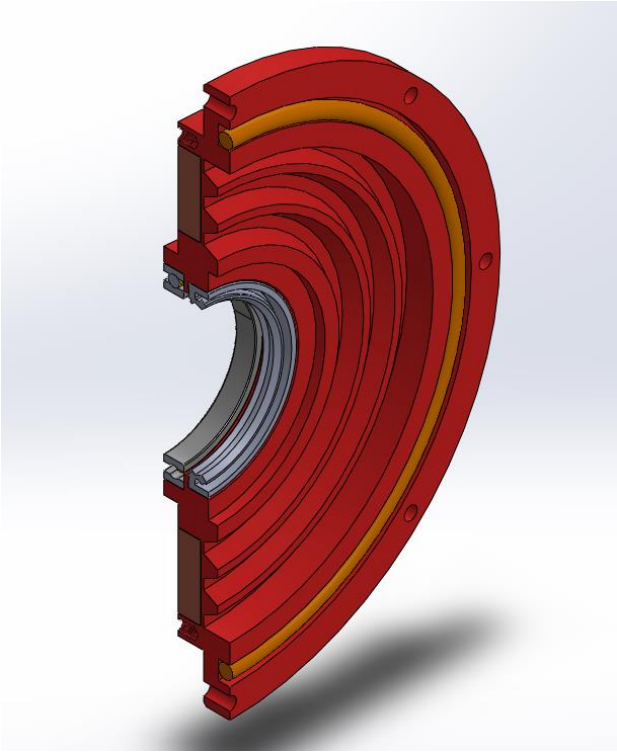

Figure 4.15: Section view of inner housing when installing Slip seal, O-ring, bearing and coil

4.2.4. Outer housing

The outer housing aim to enclose the magnetic flux of MR brake. Furthermore, outer housing also plays a role in sealing the position of the coils and bearings. Then, the shape of the outer housing is also modified based on table 3.12 and the shape of inner housing. There is a small hole on outer housing for the connection of the coil and electric power source.

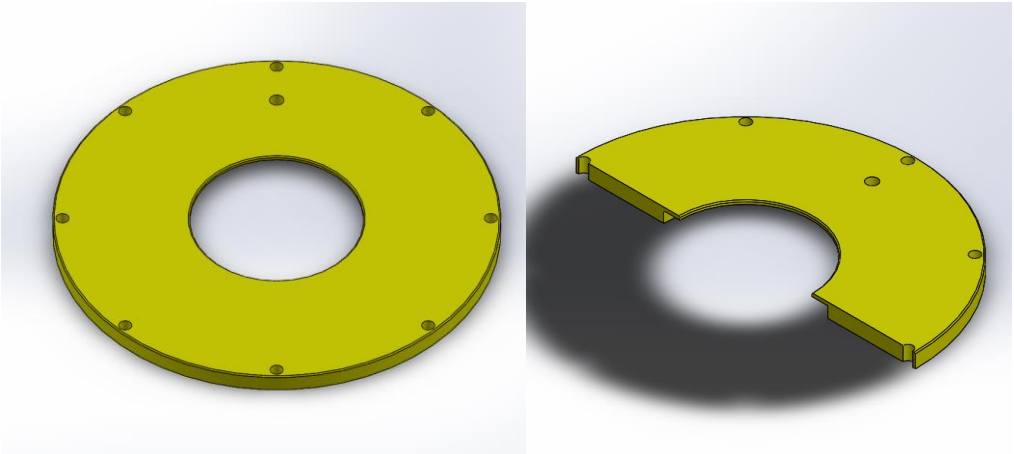

Figure 4.16: CAD of half of outer housing

4.2.5. Assembly of front tooth-shaped MR brake

All components of the tooth-shaped MR brake are assembled together. Inner housing and outer housing connect with each other by 24 M4 DIN 912 hexagon socket head cap screws. The disc is fixed with the MRB shaft by 4 M4 DIN 7991 hexagon socket countersunk head screws

HEXAGON SOCKET HEAD CAP SCREWS DIN 912

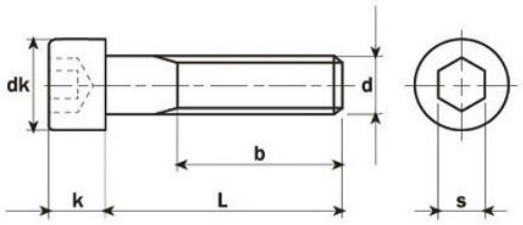

Grades: 8.8 / 10.9 / 12.9 / A2 / A4

d	M3	M4	M5	M6	M8	M10	M12	M14	M16	M18	M20	M22	M24	M27	M30
P	0,5	0,7	0,8	1	1,25	1,5	1,75	2	2	2,5	2,5	2,5	3	3	3,5
b*	18	20	22	24	28	32	36	40	44	48	52	56	60	66	72
dk (max)	5,5	7	8,5	10	13	16	18	21	24	27	30	33	36	40	45
k (max)	3	4	5	6	8	10	12	14	16	18	20	22	24	27	30
s	2,5	3	4	5	6	8	10	12	14	14	17	17	19	19	22

Table 4.4: Specifications of DIN 912 hexagon socket head cap screws

HEXAGON SOCKET COUNTERSUNK HEAD SCREWS DIN 7991

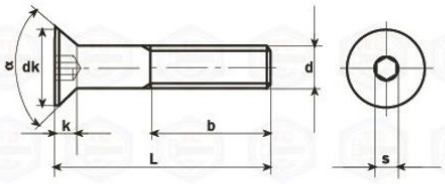

Grades: 8.8 / 10.9 / 12.9 / A2 / A4

d	M3	M4	M5	M6	M8	M10	M12	M16	M20
P	0,5	0,7	0,8	1	1,25	1,5	1,75	2	2,5
b*	12	14	16	18	22	26	30	38	46
dk	6	8	10	12	16	20	24	30	36
k (max)	1,7	2,3	2,8	3,3	4,4	5,5	6,5	7,5	8,5
a	90°	90°	90°	90°	90°	90°	90°	90°	90°
s	2	2,5	3	4	5	6	8	10	12

b*: Size b is a guide value, it amounts on the minimum lenght of the threaded part.
Per diameter (d) are lenghts (L) above de dotted line threaded up to the head.

Table 4.5: Specifications of DIN 7991 hexagon socket countersunk head screws

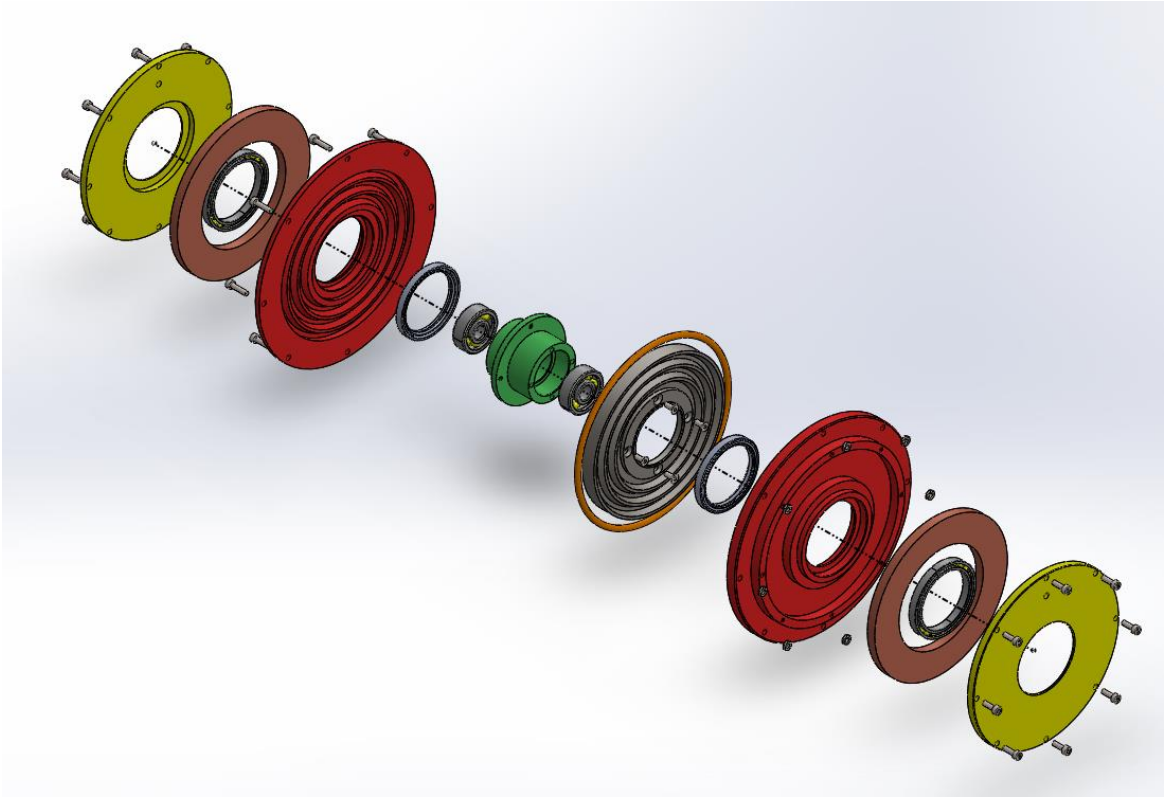

Figure 4.17: Explore view of tooth-shaped MR brake

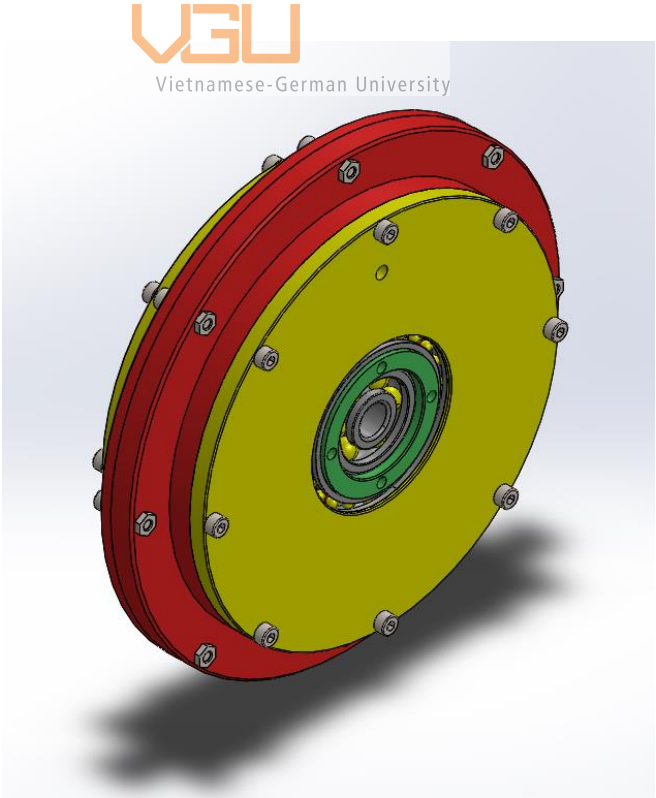

Figure 4.18: CAD of tooth-shaped MR brake

4.3. Mechanism for attaching MRB on front wheel

It can be observed from figure 3.15 that the front wheel has the solid knob which already have has 3 inner thread paths on it. This solid knob is going to be used to connect the MR brake structure to the front wheel later. However, the thickness of the solid knob needs milling to 14.6 mm in order to have enough space to attach the MRB.

Figure 4.19: CAD of the front wheel with adjusting solid knob

In order to assemble the MRB to the front wheel, a hub connector is design. This hub is joined with the front wheel and the MR brake by 3 M8 screws and 4 M4 pins respectively. Consequently, the shape of hub connector is a short hollow shaft which has a round flange at one end to connect with the front wheel. The inner and outer diameter of the other end is designed to be similar with the MRB shaft's ones.

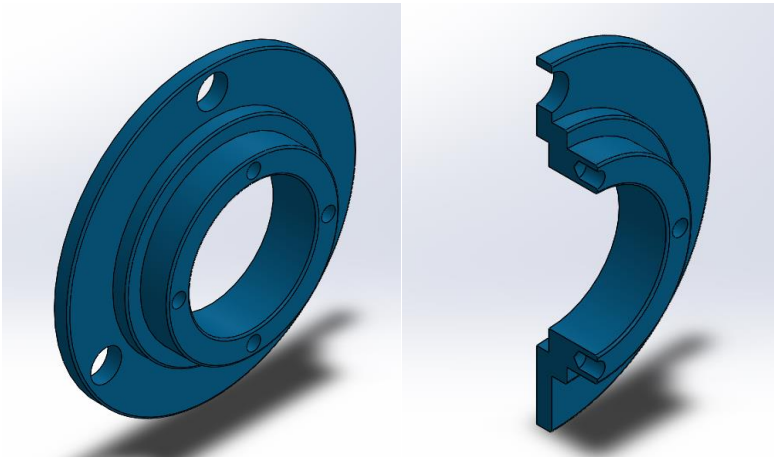

Figure 4.20: CAD of the hub connector

The retaining ring is placed between front wheel's bearing and MRB shaft's bearing which aim to secure the position of them.

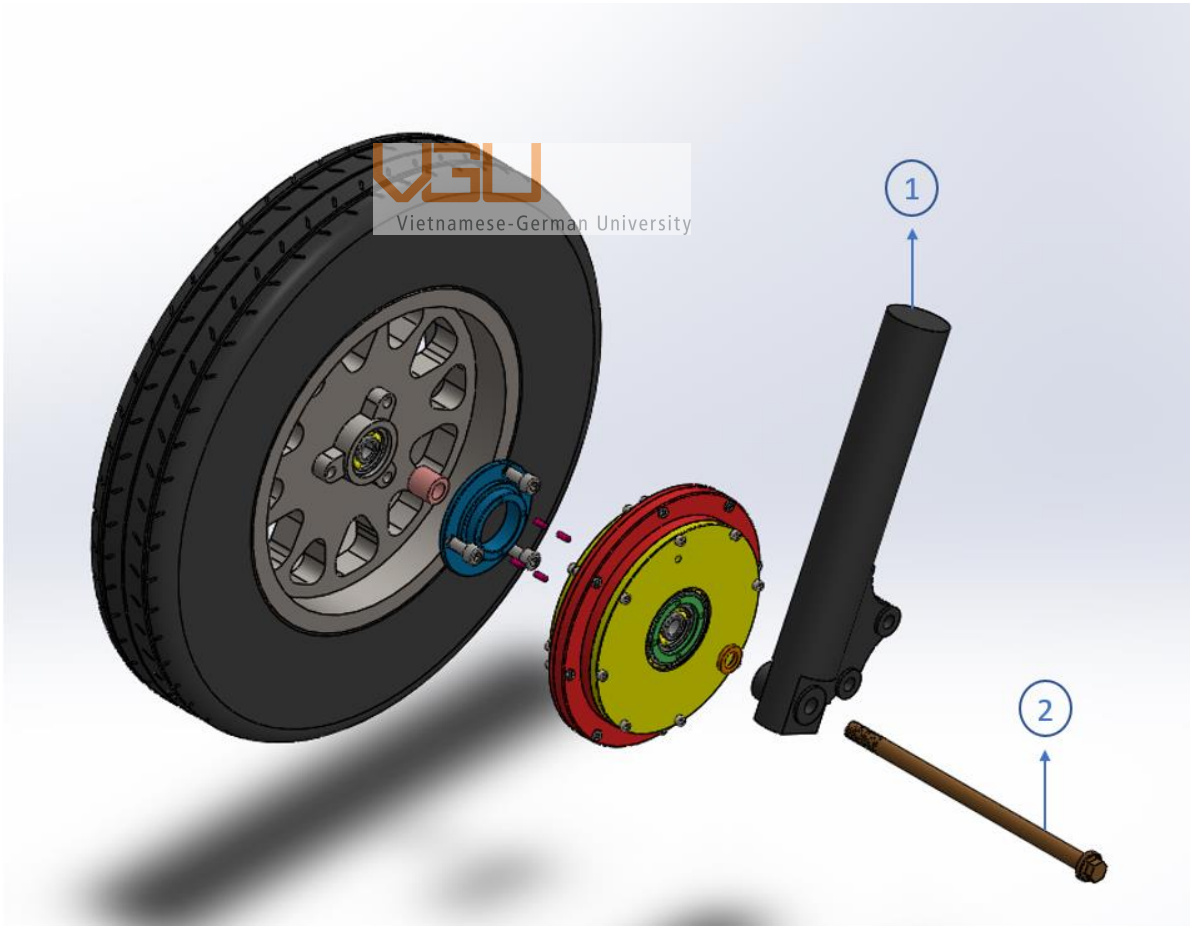

Figure 4.21: Explore view of front wheel with MR brake; 1: Front shaft holder, 2: Front wheel shaft.

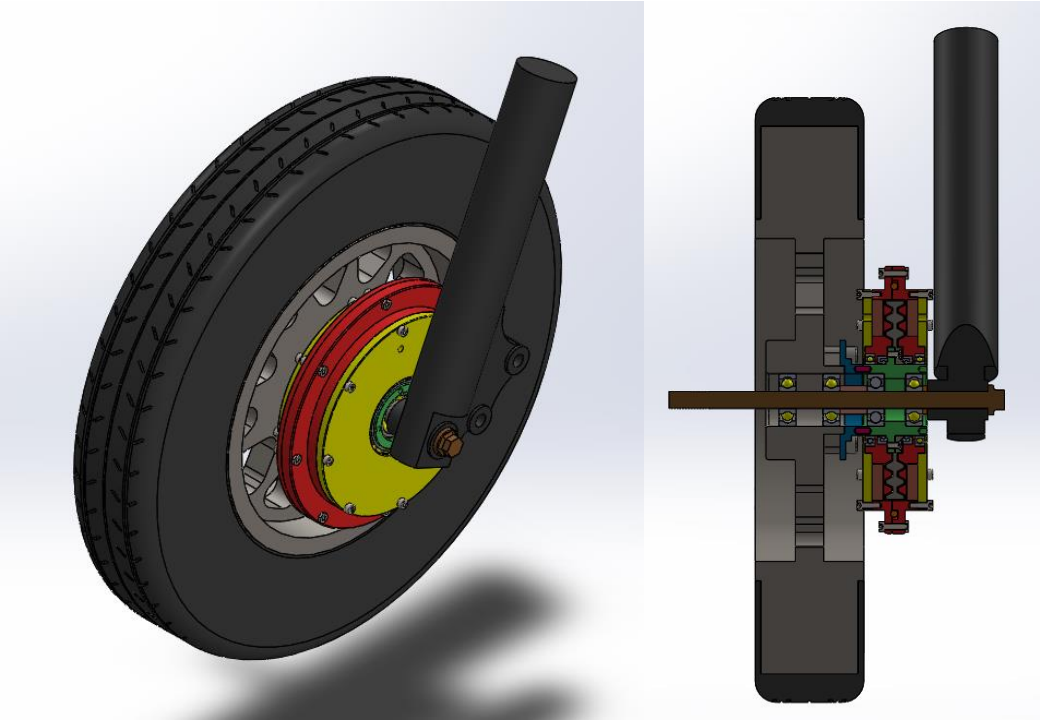

Figure 4.22: CAD of front wheel with MR brake

4.4. Mechanical properties calculation

4.4.1. MRB shaft calculation

When being operating, there will be two main loads in the MRB shaft: Bending stress due to the weight of MR brake system and torsional stress when the MR brake is activated, which is T_b = 199.89 N.m. The torsional stress due to pure rotation of the front wheel can be neglected able since that value is very small. There are two bearings are installed in the MRB shaft, thus these can be treated as pin support and roller support at two ends of MRB shaft. In order to calculate the bending stress of MRB, the maximum bending moment can be derived as

$$M_b = m_b * 9.8 * \frac{L}{2} \quad (26)$$

With: M_b is the bending moment, m_b is the mass of MR brake which is 6.16 kg, L is the length of MRB shaft which is 45 mm. As a result, the value of M_b is 1.36 N.m. For simplifying calculation problem, the MRB shaft is treated as a hollow shaft without considering the round flange with inner diameter d_i = 37 mm, outer diameter d_o = 50 mm.

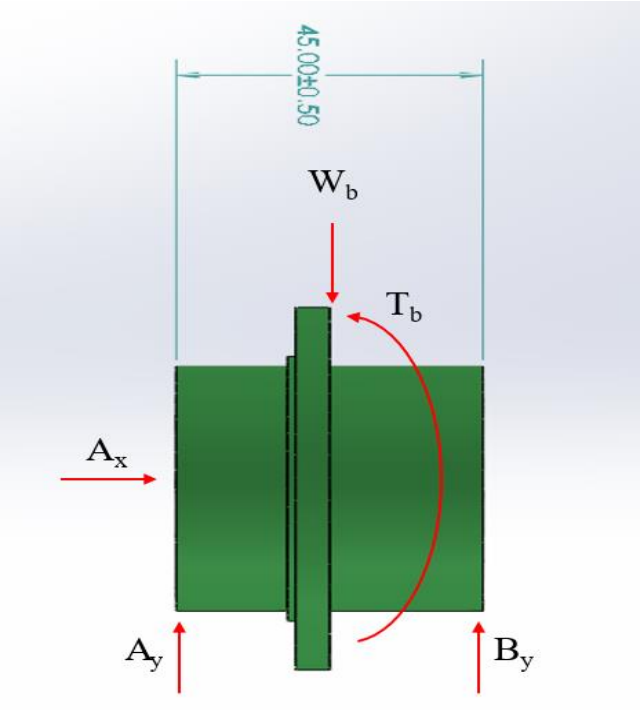

Figure 4.23: Free body diagram analysis of MRB shaft

Bending stress calculation of the hollow shaft:

$$\sigma_b = \frac{32M_b d_o}{\pi(d_o^2 - d_i^2)} \tag{27}$$

Torsion stress calculation of the hollow shaft

$$\tau = \frac{16T_b d_o}{\pi(d_o^2 - d_i^2)} \tag{28}$$

Von-missed stress calculation

$$\sigma_v = \sqrt{\sigma_b^2 + 3\tau^2} \tag{29}$$

Where: σ_b is bending stress, τ is the torsion stress and σ_v is von-missed stress

The condition for the MRB shaft to operate without being failure is

$$\sigma_v \leq \frac{yield\ strenght\ of\ Inox\ 304}{safety\ factor} \tag{30}$$

Result after calculation

Von-missed stress	20.15 MPA
Yield strength	206.8 MPA
Safety factor	10.3

Table 4.6: Result of MRB analysis

It is observed that the safety factor for the MRB brake is 10.3 which is much larger than the required one 1.3. Thus, the design of MRB is approved.

4.4.2. Screw joints at MRB shaft and tooth-shaped disc calculation

As the MR brake is activated, the torsion stress is also taken up by the M4 screw joints which is used to connect the MRB shaft with the tooth-shaped disc. This means that the braking torque is transmitted by shearing force created in the bolts.

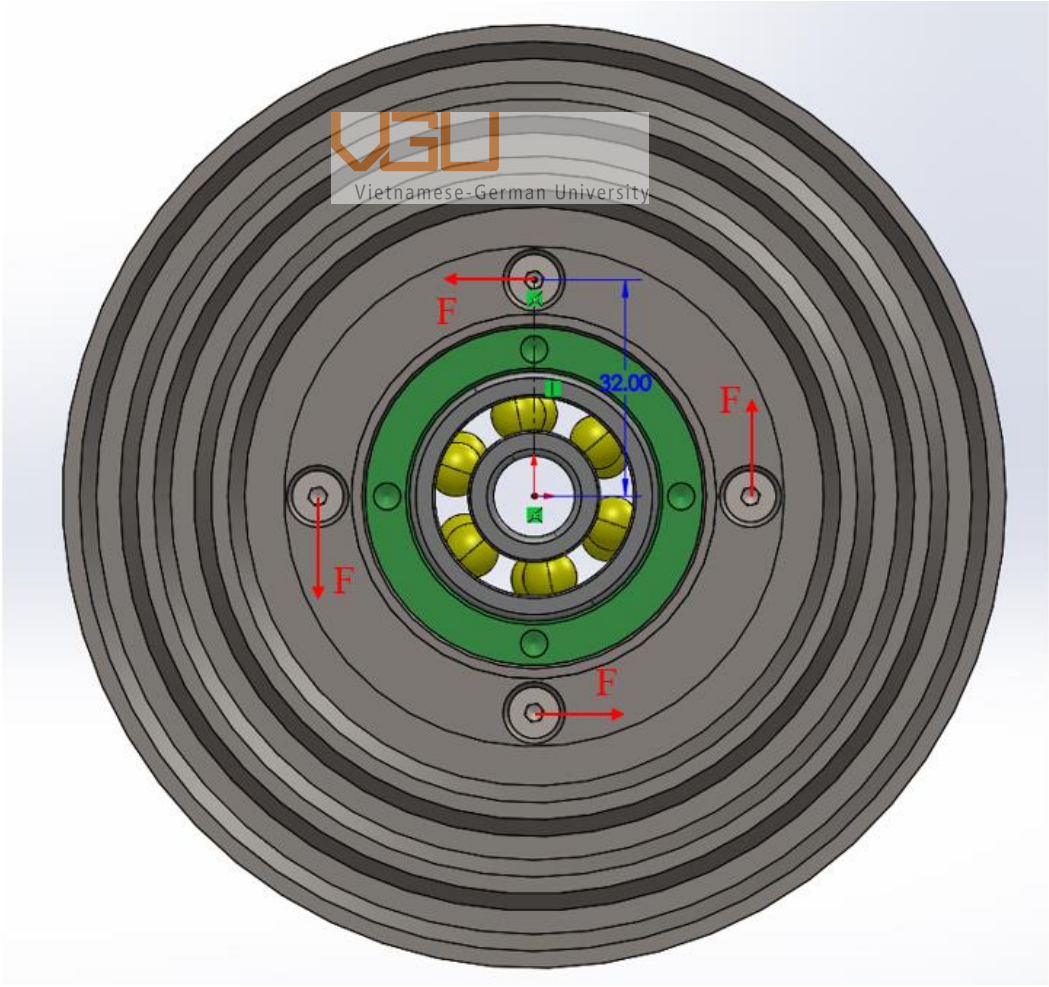

Figure 4.24: Shearing force at the screws

The 8.8 grades M4 screw has following mechanical properties

- Shear stress allow: τ_{allow} = 320 MPA
- Tensile/Bending stress allow: σ_{allow} = 400 MPA

Calculation of force in each M4 screw

$$F = \frac{T_b}{r * n} \tag{31}$$

With: F is the shearing force in each screw, T_b is the braking torque which equal to 199.89 N.m, r is the distance from center to the screw (r = 32 mm) and n is the total of screws (n = 4).

Then the shear stress in each screw can be derived as

$$\tau_b = \frac{F}{\pi * \frac{d^2}{4}} \tag{32}$$

Where: τ_b is the shearing stress, d is the diameter of M4 screw which is 4 mm.

Result after calculation

Shear stress	124.3 MPA
Shear stress allow	320 MPA
Safety factor	2.57

Table 4.7: Result of screw analysis

The safety factor of each screw is 2.57 which is acceptable in this design. Consequently, 4 M4 screws grade 8.8 are valid to be used.

4.4.3. Pin joints calculation

With the same principle as calculating shear stress in bolts, the shear stress at pins can be determined by using equation (31), (32).

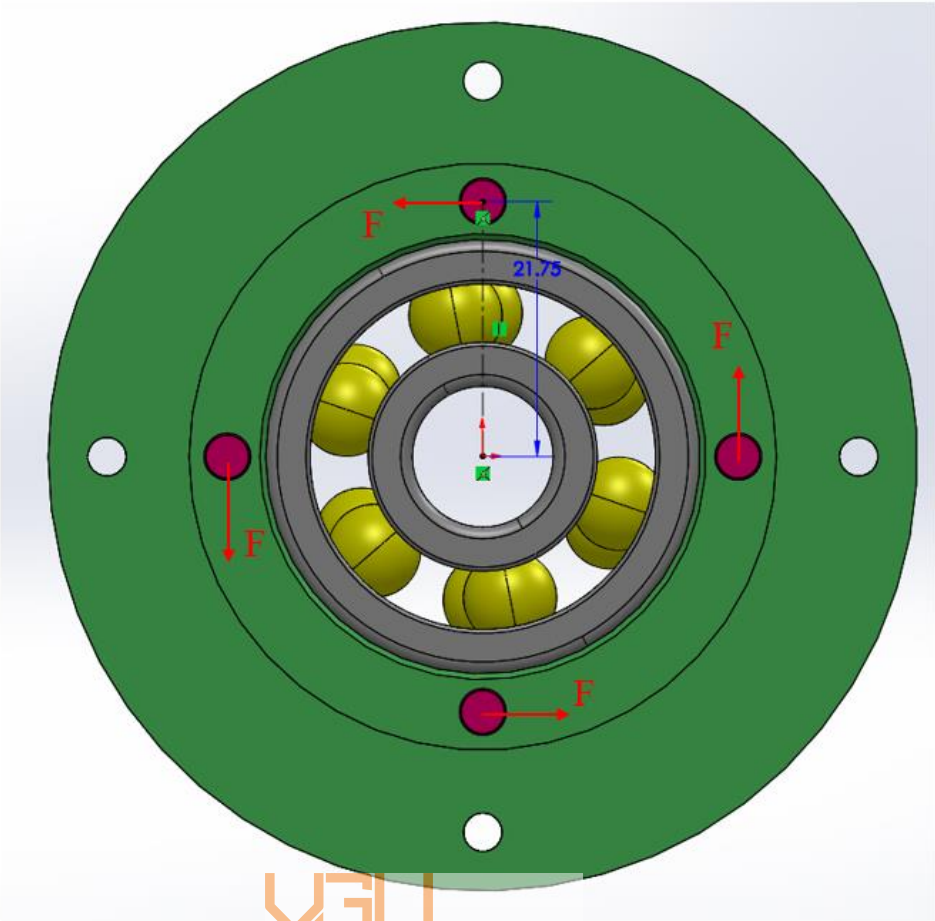

Figure 4.25: Shearing force at the pins

Result after calculation

Shear stress	182.83 MPA
Shear stress allow	320 MPA
Safety factor	1.75

Table 4.8: Result of pin analysis

The safety factor in this case is 1.75 which is still larger than the required one in this design, 1.3. Therefore, 4 pins with 4 mm diameter are acceptable for usage.

4.5. Simulation

The static simulation is made for the main working mechanism of the MRB when it is attached on the electric scooter to see its mechanical properties. The components which

are in the mechanism includes MRB shaft, tooth-shaped disc, hub connector, 4 M4 bolts and 4 pins.

4.5.1. Set up material

C45 steel is applied for material of tooth-shaped disc. Inox 304 is applied for MRB shaft and hub connector, M4 screws and M4 pins.

Property	Value	Units
Elastic Modulus	2.05e+11	N/m^2
Poisson's Ratio	0.29	N/A
Shear Modulus	8e+10	N/m^2
Mass Density	7850	kg/m^3
Tensile Strength	625000000	N/m^2
Compressive Strength		N/m^2
Yield Strength	530000000	N/m^2
Thermal Expansion Coefficient	1.15e-05	/K

Table 4.9: Specification of C45 steel in Solidwork software

Property	Value	Units
Elastic Modulus	1.9e+11	N/m^2
Poisson's Ratio	0.29	N/A
Shear Modulus	7.5e+10	N/m^2
Mass Density	8000	kg/m^3
Tensile Strength	517017000	N/m^2
Compressive Strength		N/m^2
Yield Strength	206807000	N/m^2
Thermal Expansion Coefficient	1.8e-05	/K

Table 4.10: Specification of Inox 304 in Solidwork software

4.5.2. Set up constraint

In reality, the simulated mechanism works in dynamic condition. In order to simulate it in static condition, the stage that exactly when the MR brake activated is considered. Thus, in static simulation, tooth-shaped disc, round flange of hub connector, M4 screws and M4 pins are treated as fix component and the total torque 199.89 N.m is applied to the MRB shaft. The Meshing method is set automatically by the Solidwork software for simplicity.

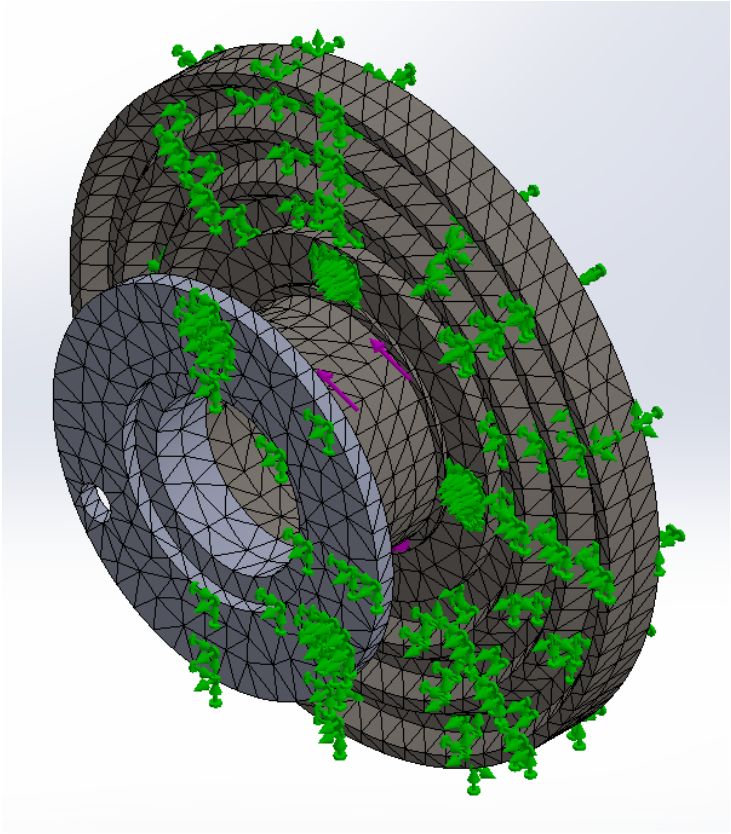

Figure 4.26: Meshing and constraint of simulated model

4.5.3. Result

Model	Assembly of MRB shaft, tooth-shaped disc and hub connector
Maximum Von mises stress	35.79 MPa
Maximum displacement	0.001155 mm
Minimum safety factor	5.8

Table 4.11: Simulation result

As the minimum safety factor of the simulated model is 5.8, which is greater than 1.3 (requirement), this mechanism could be expected to operate on the electric scooter without failure.

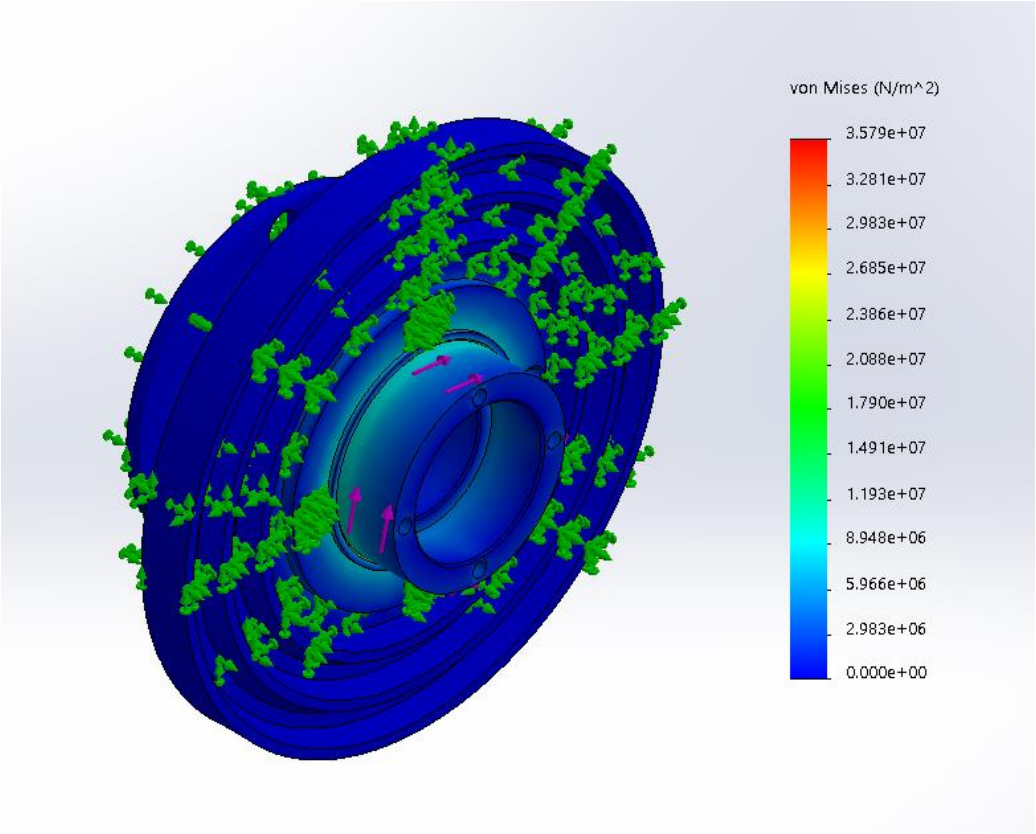

Figure 4.27: Distribution of von mises stress

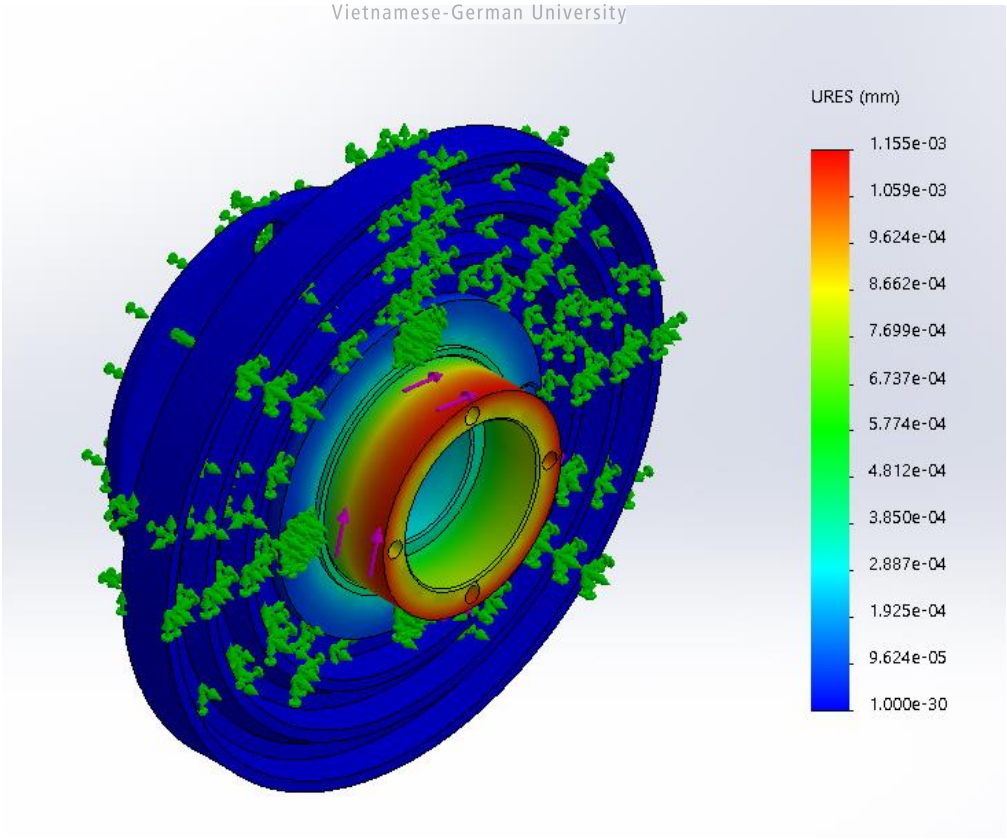

Figure 4.28: Distribution of displacement

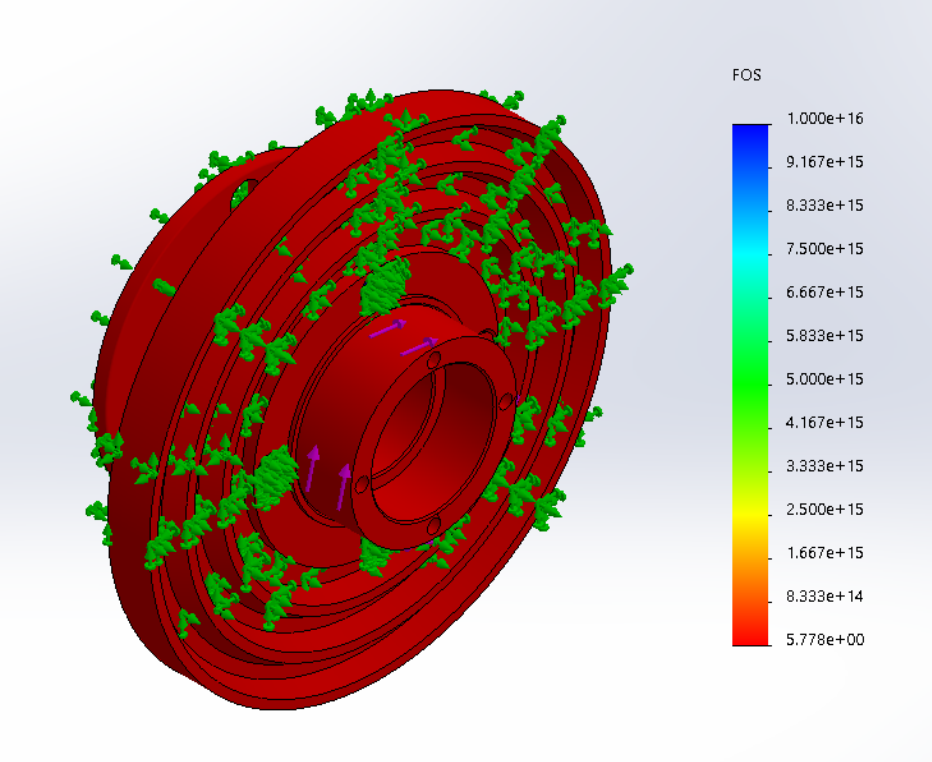

Figure 4.29: Distribution of safety factor

4.6. Drawing

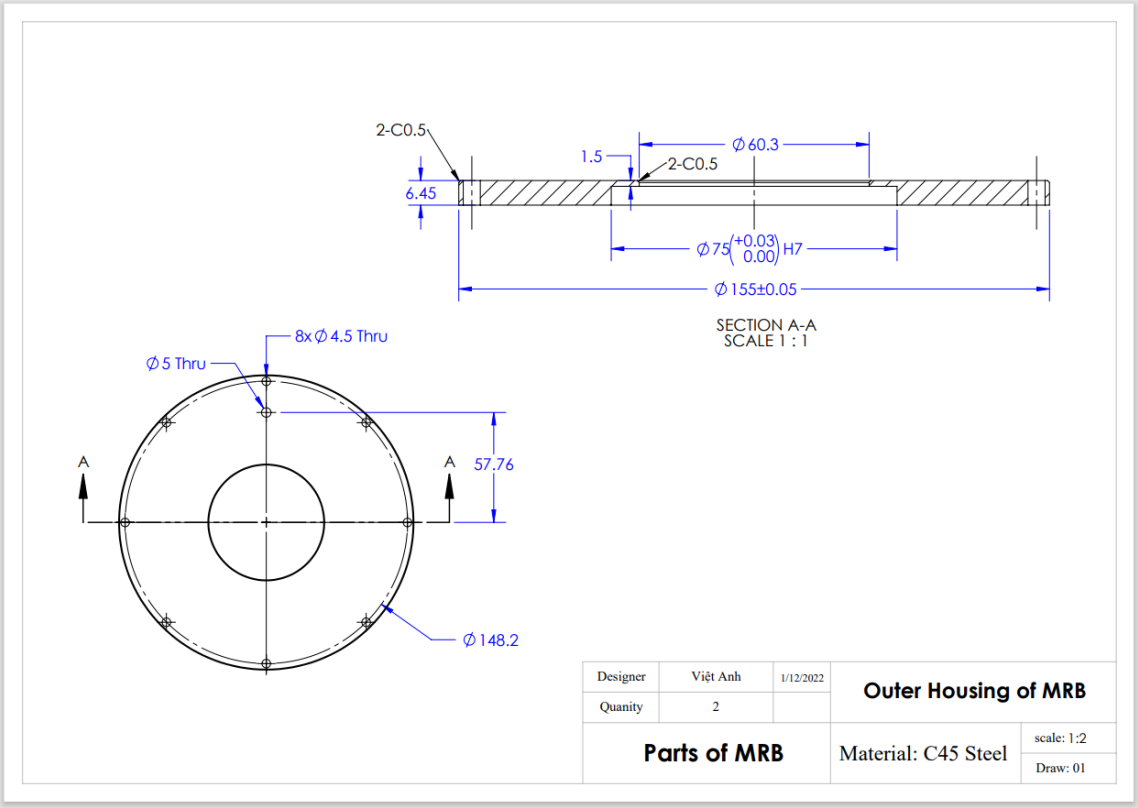

Figure 4.30: 2D drawing of outer housing

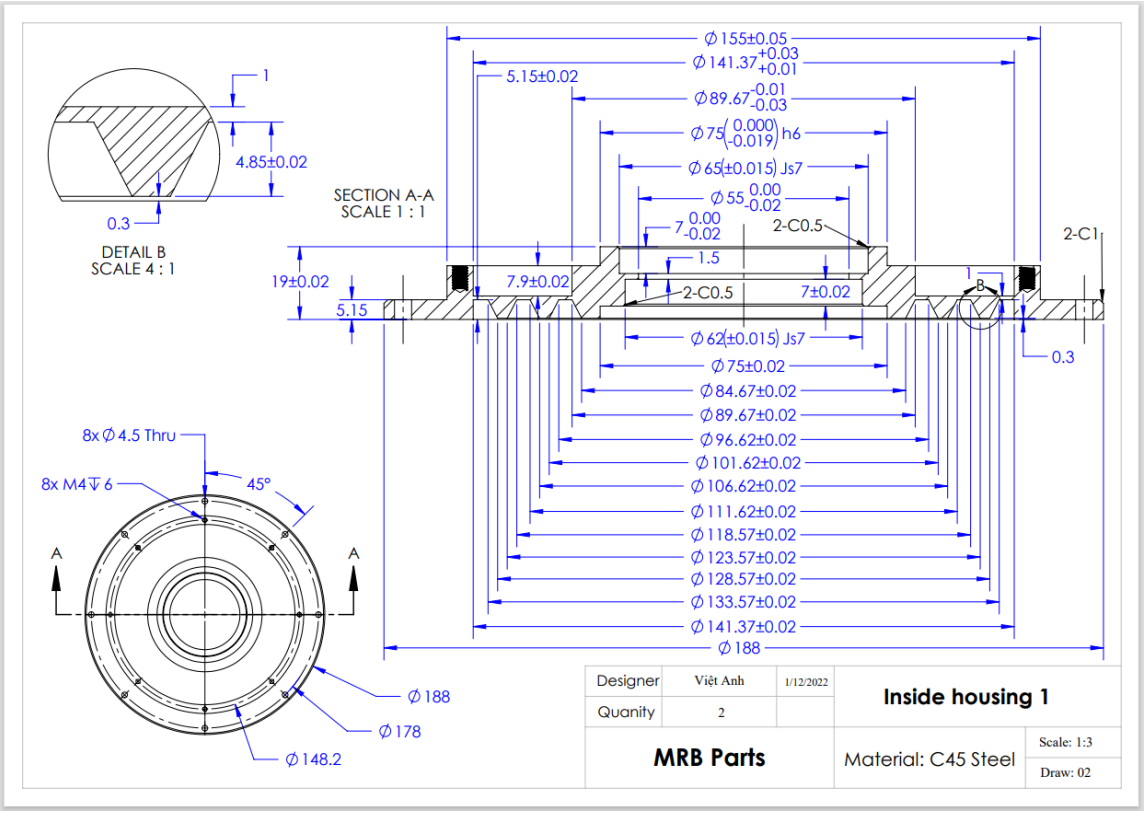

Figure 4.31: 2D drawing of half of inner housing

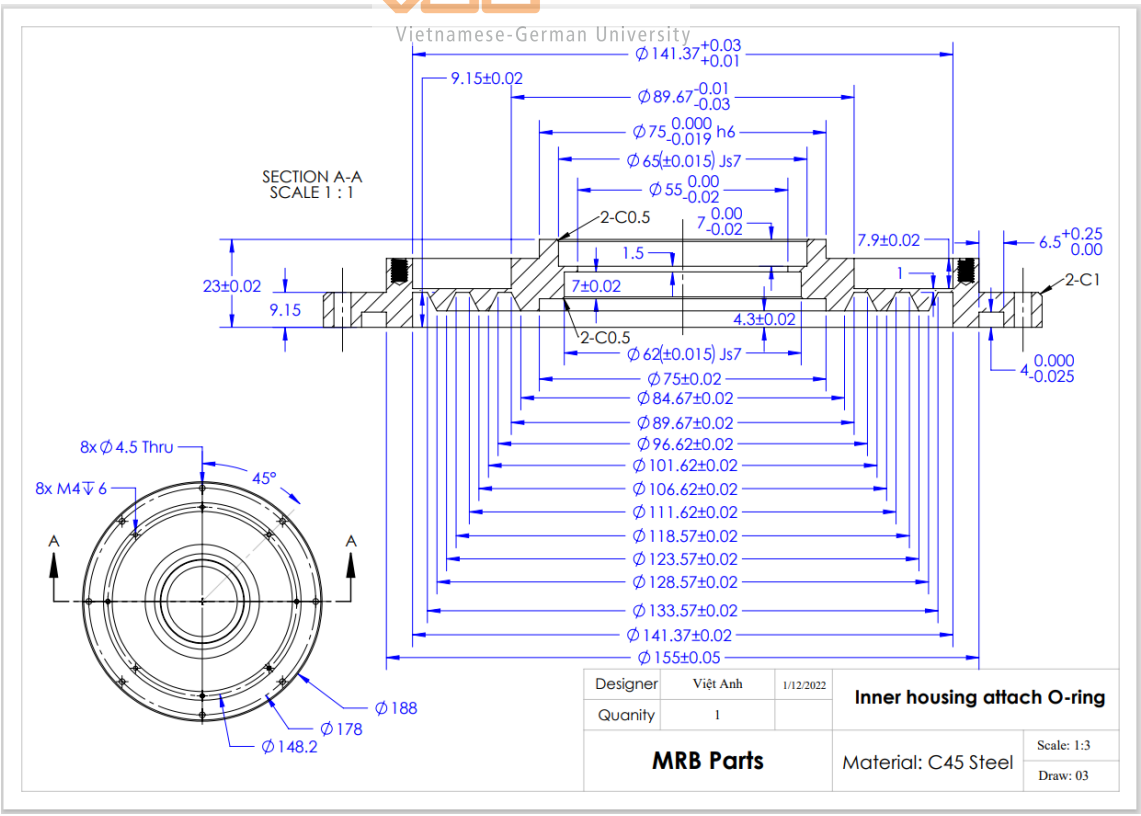

Figure 4.32: 2D drawing of half of inner housing which attach O-ring

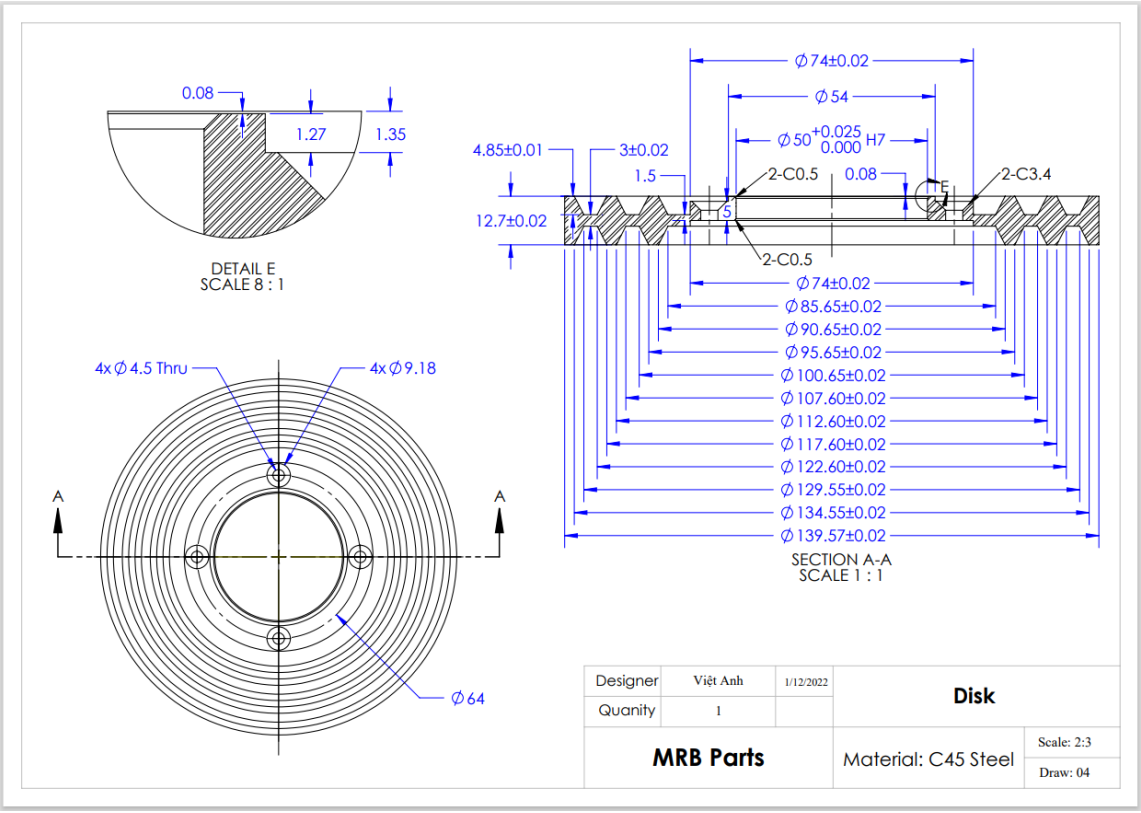

Figure 4.33: 2D drawing of tooth-shaped disc

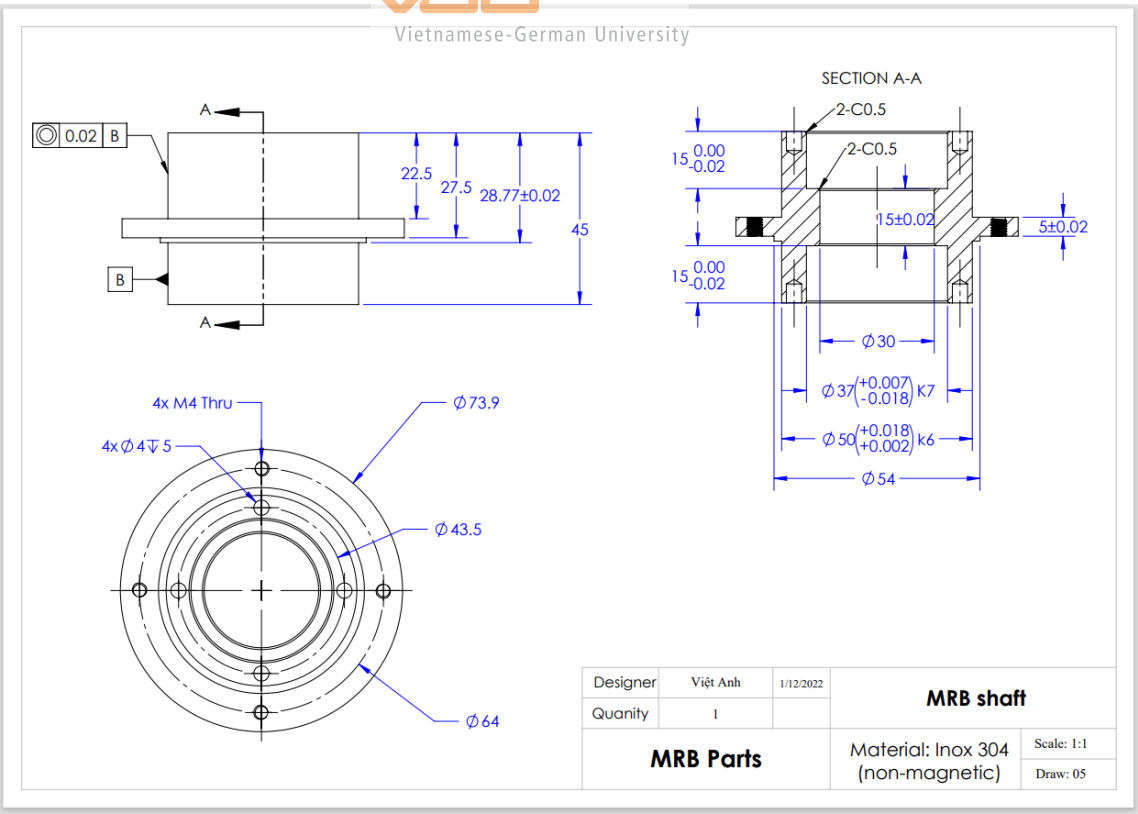

Figure 4.34: 2D drawing of MRB shaft

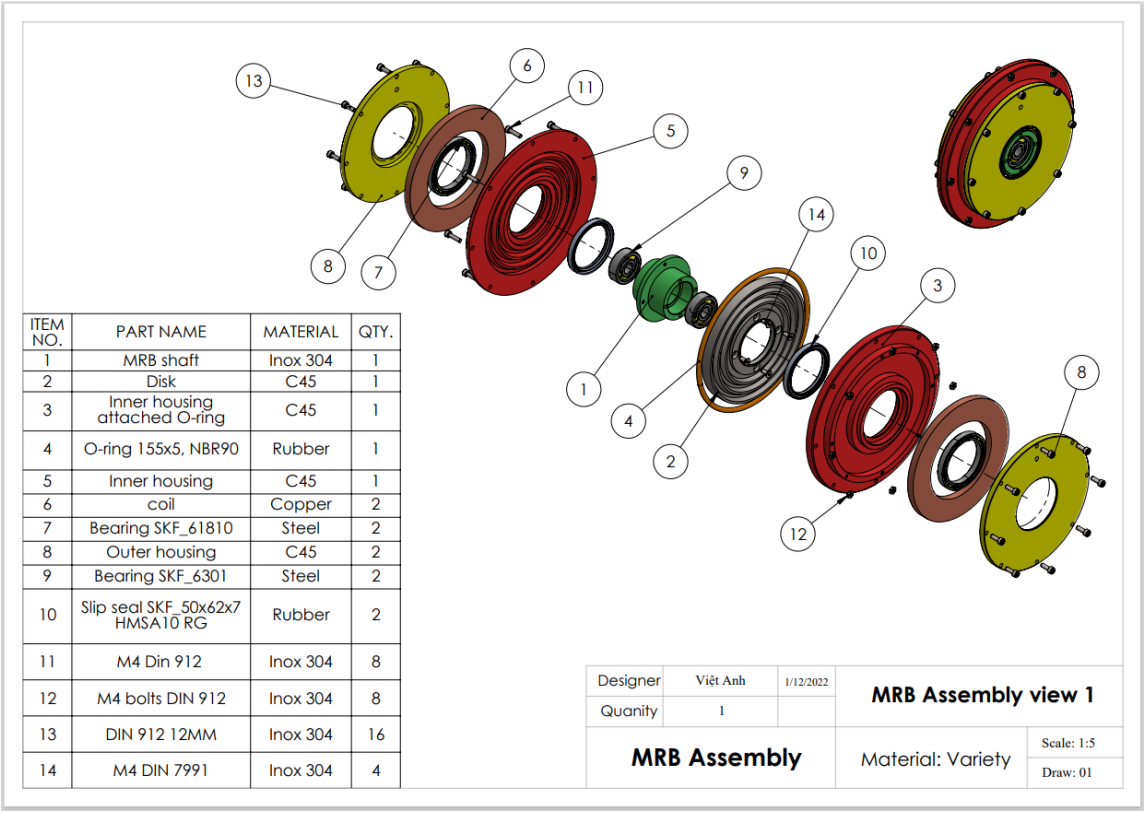

ITEM NO.	PART NAME	MATERIAL	QTY.
1	MRB shaft	Inox 304	1
2	Disk	C45	1
3	Inner housing attached O-ring	C45	1
4	O-ring 155x5, NBR90	Rubber	1
5	Inner housing	C45	1
6	coil	Copper	2
7	Bearing SKF_61810	Steel	2
8	Outer housing	C45	2
9	Bearing SKF_6301	Steel	2
10	Slip seal SKF_50x62x7 HMSA10 RG	Rubber	2
11	M4 Din 912	Inox 304	8
12	M4 bolts DIN 912	Inox 304	8
13	DIN 912 12MM	Inox 304	16
14	M4 DIN 7991	Inox 304	4

Designer	Việt Anh	1/12/2022	**MRB Assembly view 1**
Quanity	1		
MRB Assembly	Material: Variety	Scale: 1:5	
		Draw: 01	

Figure 4.35: 2D drawing of MRB Assembly

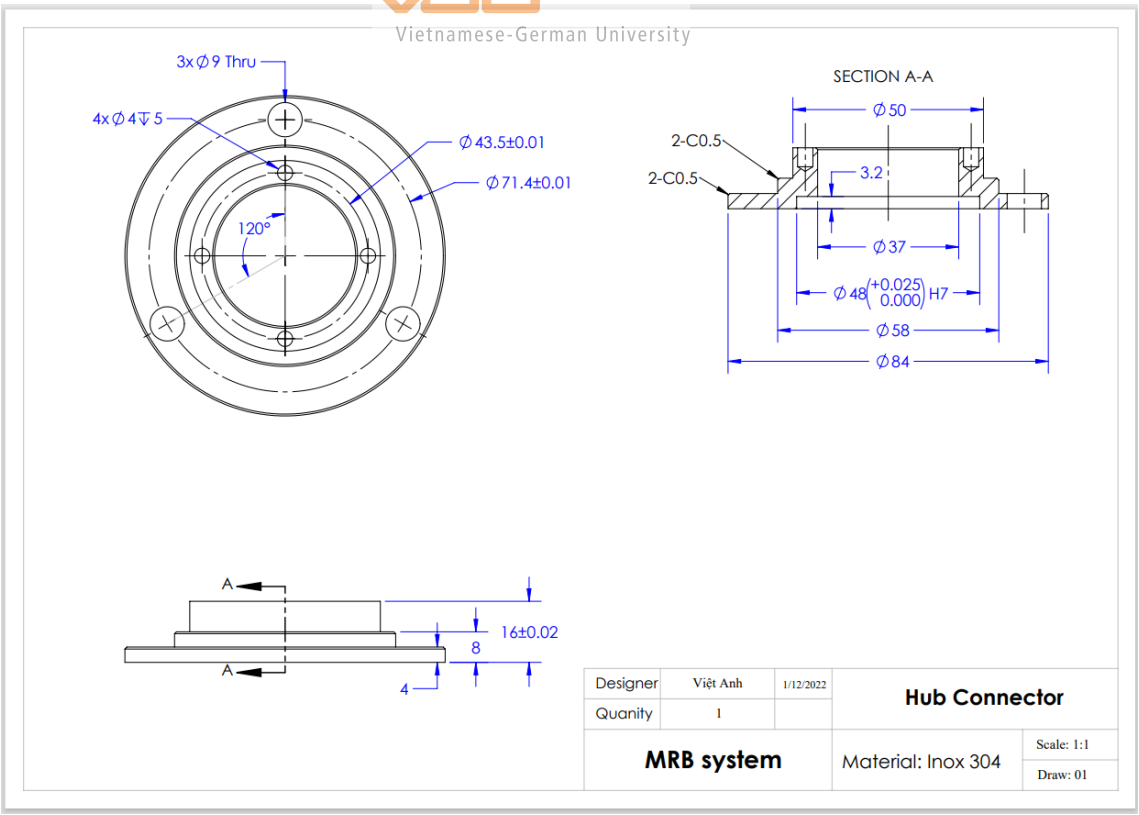

Designer	Việt Anh	1/12/2022	**Hub Connector**
Quanity	1		
MRB system	Material: Inox 304	Scale: 1:1	
		Draw: 01	

Figure 4.36: 2D drawing of hub connector

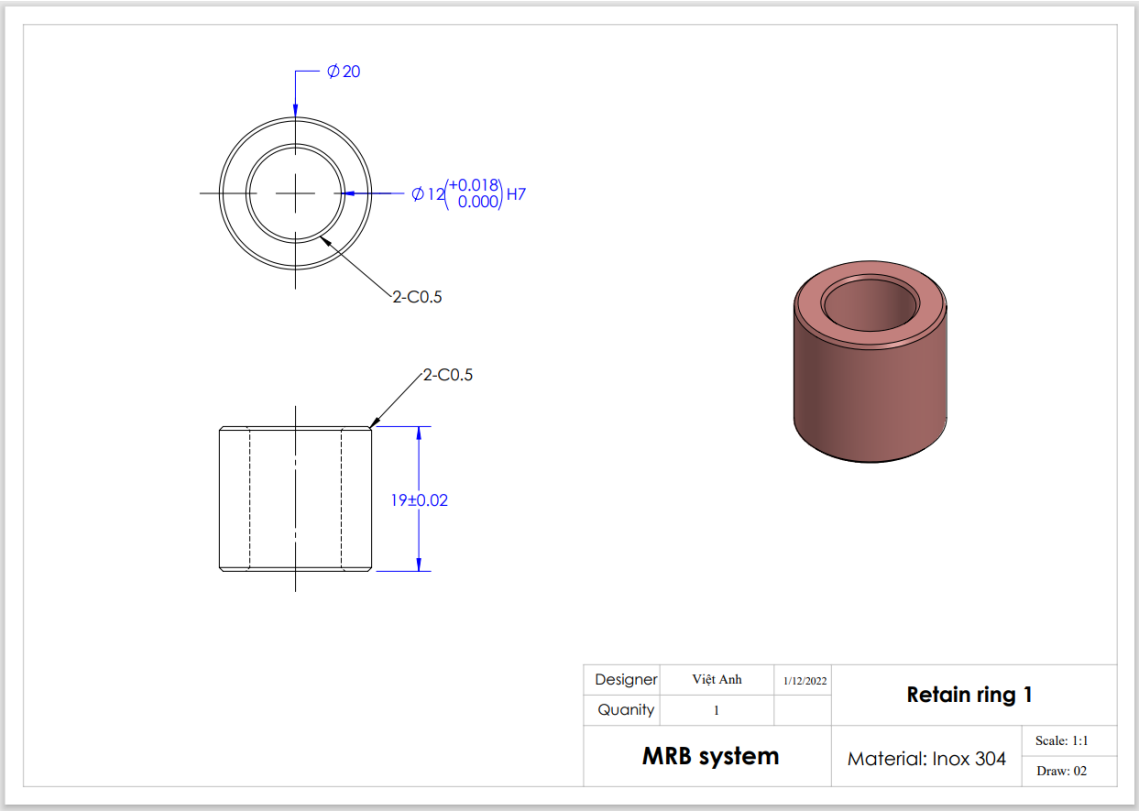

Figure 4.37: 2D drawing of retain ring

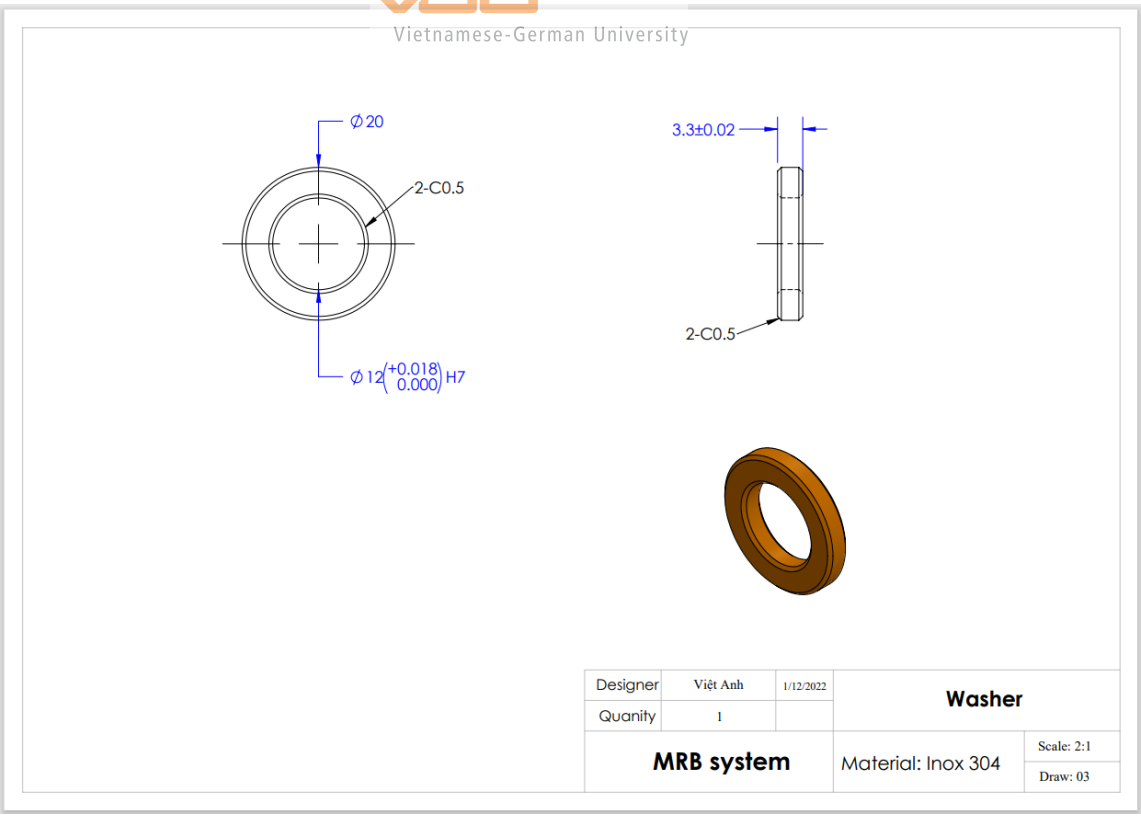

Figure 4.38: 2D drawing of washer

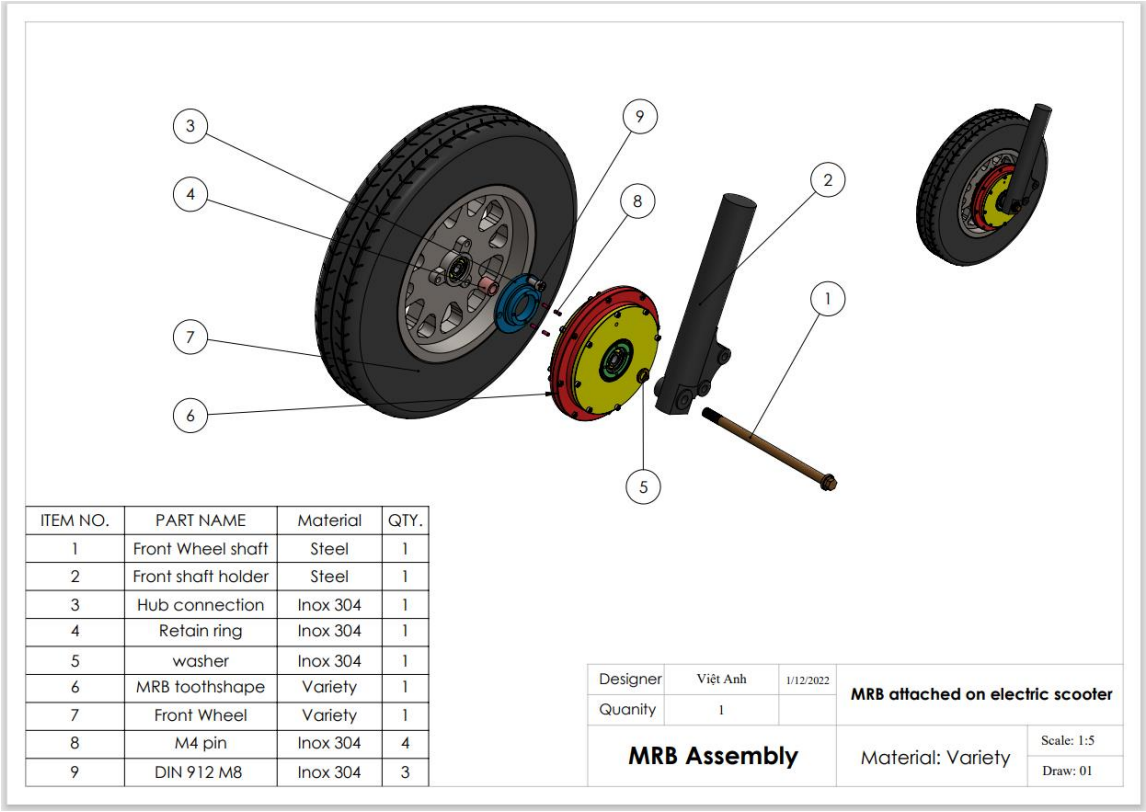

ITEM NO.	PART NAME	Material	QTY.
1	Front Wheel shaft	Steel	1
2	Front shaft holder	Steel	1
3	Hub connection	Inox 304	1
4	Retain ring	Inox 304	1
5	washer	Inox 304	1
6	MRB toothshape	Variety	1
7	Front Wheel	Variety	1
8	M4 pin	Inox 304	4
9	DIN 912 M8	Inox 304	3

Designer	Việt Anh	1/12/2022	MRB attached on electric scooter
Quanity	1		
MRB Assembly	Material: Variety		Scale: 1:5
			Draw: 01

Figure 4.39: 2D drawing of assembly of MRB and electric scooter

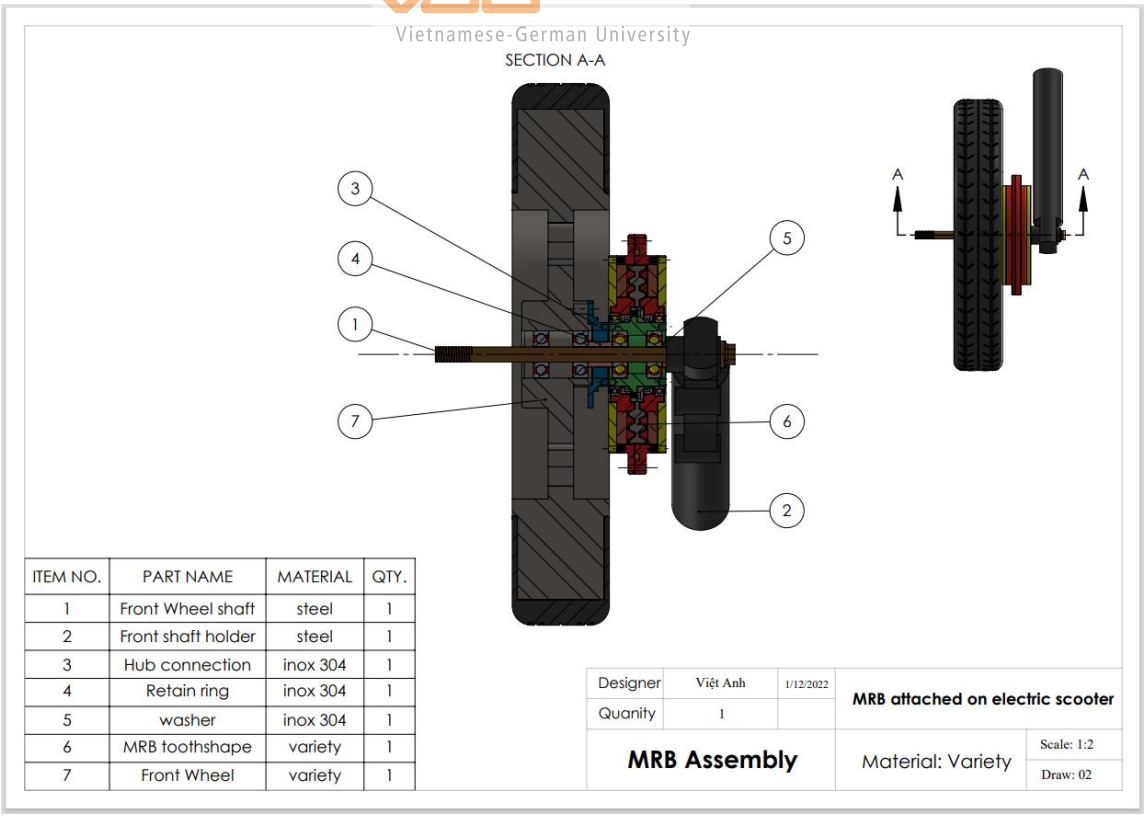

ITEM NO.	PART NAME	MATERIAL	QTY.
1	Front Wheel shaft	steel	1
2	Front shaft holder	steel	1
3	Hub connection	inox 304	1
4	Retain ring	inox 304	1
5	washer	inox 304	1
6	MRB toothshape	variety	1
7	Front Wheel	variety	1

Designer	Việt Anh	1/12/2022	MRB attached on electric scooter
Quanity	1		
MRB Assembly	Material: Variety		Scale: 1:2
			Draw: 02

Figure 4.40: Section view of assembly of MRB and electric scooter

Chapter 5: Conceptual design of experiment

5.1. Experiment model

The purpose of making experiment is to see if the MRB could reach the torque as large as the theorical value. This is the important step before implementing it on the electric scooter.

5.1.1. Motor selection

The motor aims to provide the rotation motion of the MRB shaft. Due to the limited budget of the project, available Panasonic AC servo motor model MSMO42AIUX is selected for the testing model.

Motor model	Panasonic AC servo MSMO42AIUX
Output power	400 W
Current	2.5 A
Voltage	106 V
Maximum output speed	3000 RPM
Rated frequency	200 Hz
Shaft diameter	14 mm

Table 5.1: Specification of Panasonic AC servo motor model MSMO42AIUX

Figure 5.1: Panasonic AC servo motor model MSMO42AIUX

5.1.2. Torque sensor

The torque sensor is the mean for measuring braking torque in this experiment. Due to the high cost of this components, the torque sensor which is available in University's Gpem Lab is adopted. The model of this torque sensor is DR 3000 from Lorenz Messtechnik gmbh. DR 3000 is rotating torque sensors with non-contact transmission which means the torque transducers are supplied as active sensor with integrated measuring amplifier as output signal in Voltage. By the non-contact transmission, the measurement data are transmitted maintenance free and without signal distortion between rotor and stator. Integrated speed/angle measurement is accessible as an option. The rated torque of current DR 3000 sensor is 200 N.m.

Figure 5.2: DR 3000 rotating torque sensor

USB-Torque Sensor DR-3000/DR-3000-P		
Rated torque $\mathbf{M_{nom}}$	N·m	0.1 ... 5000
Accuracy class	% M_{nom}	0.1 (optional 0.05)
Speed resolution	min^{-1}	1
Speed accuracy		1 % full scale ±1 digit
Angle of rotation resolution	degree	0.25
Relative repeatability error in unchanged mounting position **b'**	% M_{nom}	±0.02
Feed-in from USB	VDC	4 ... 6
Current consumption	mA	≤250
Output signal torque	digits	±25000
Output signal speed/angle of rotation	digits	±32511
Control signal excitation		per software
Sample rate	kSample/s	2.5
Electrical connection		Mini-USB-B-Socket IP68, incl. 3 m connection cable to PC
Reference temperature $\mathbf{T_{ref}}$	°C	23
Rated temperature range	°C	5 ... 45
Operating temperature range	°C	0 ... 60
Storage temperature range	°C	-10 ... 70
Temperature effect on zero signal $\mathbf{TK_0}$	% M_{nom}/10 K	±0.2
Temperature effect on characteristic value $\mathbf{TK_C}$	% M_{nom}/10 K	±0.1
Maximum operating torque $\mathbf{M_G}$ (static)	% M_{nom}	150
Torque limit $\mathbf{M_{max}}$ (static)	% M_{nom}	200
Breaking torque $\mathbf{M_B}$ (static)	% M_{nom}	>300
Permissible oscillation stress when subjected to torque $\mathbf{M_{df}}$	% M_{nom}	70 (peak-to-peak)
Level of protection		IP50

Table 5.2: Specification of non-contact transmission rotating torque sensor

(Lorenz Messtechnik gmbh, 2022) [17]

From the table, it is important to notice the permissible oscillation stress when subjected to torque M_{df} since its limit is only 70% of the rated torque (200 N.m) of current torque sensor. This means that the torque must not exceed 140 N.m when it is transmitted through the sensor.

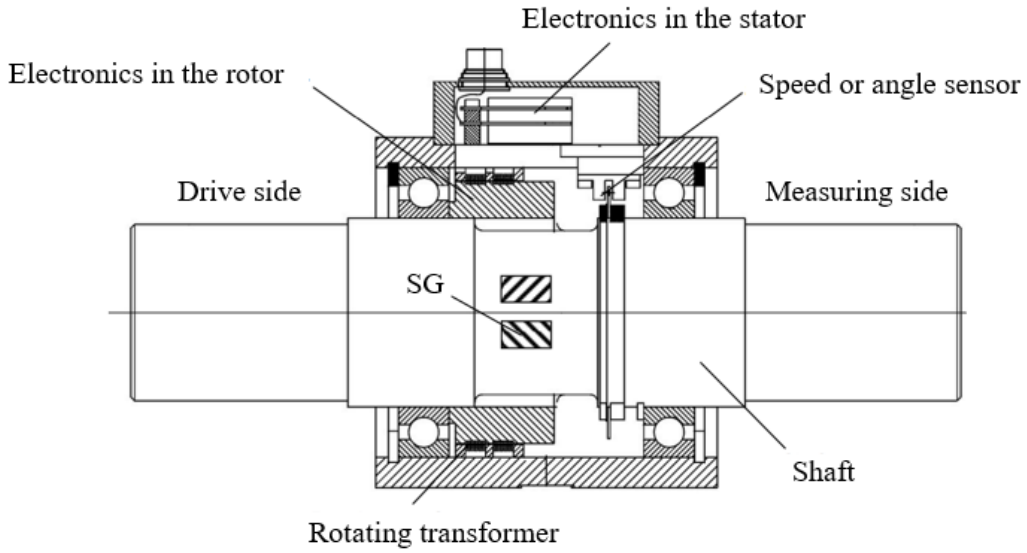

Figure 5.3: Mechanical setup of DR 3000 rotating torque sensor

5.1.3. Spur gears design

There are two considering points when designing the testing model, first, the braking torque of the tooth-shaped MR brake is larger than the allowable measuring torque for the DR 3000 sensor. Second is the MRB shaft could not be connected directly to the shaft of torque sensor since it needs to stay on a fixed shaft for rotating. Thus, a pair of spur gear is designed to encounter these problems. The ratio is set at 1:4, consequently, when the MR brake is activating the torque transmitted through the torque sensor is only approximately 50 N.m. Furthermore, when the motor gets to 3000 RPM, the rotating speed of the tooth-shaped disc is 750 RPM which is respect to when the electric scooter travel at 60 km/h.

The modulus of gears is first determined. Thanks to the Machine Dynamic and Drive System subject in Vietnamese-German University, the suitable modulus is able to be derived bases on the table of relation between power of motor and rotating speed of the gear

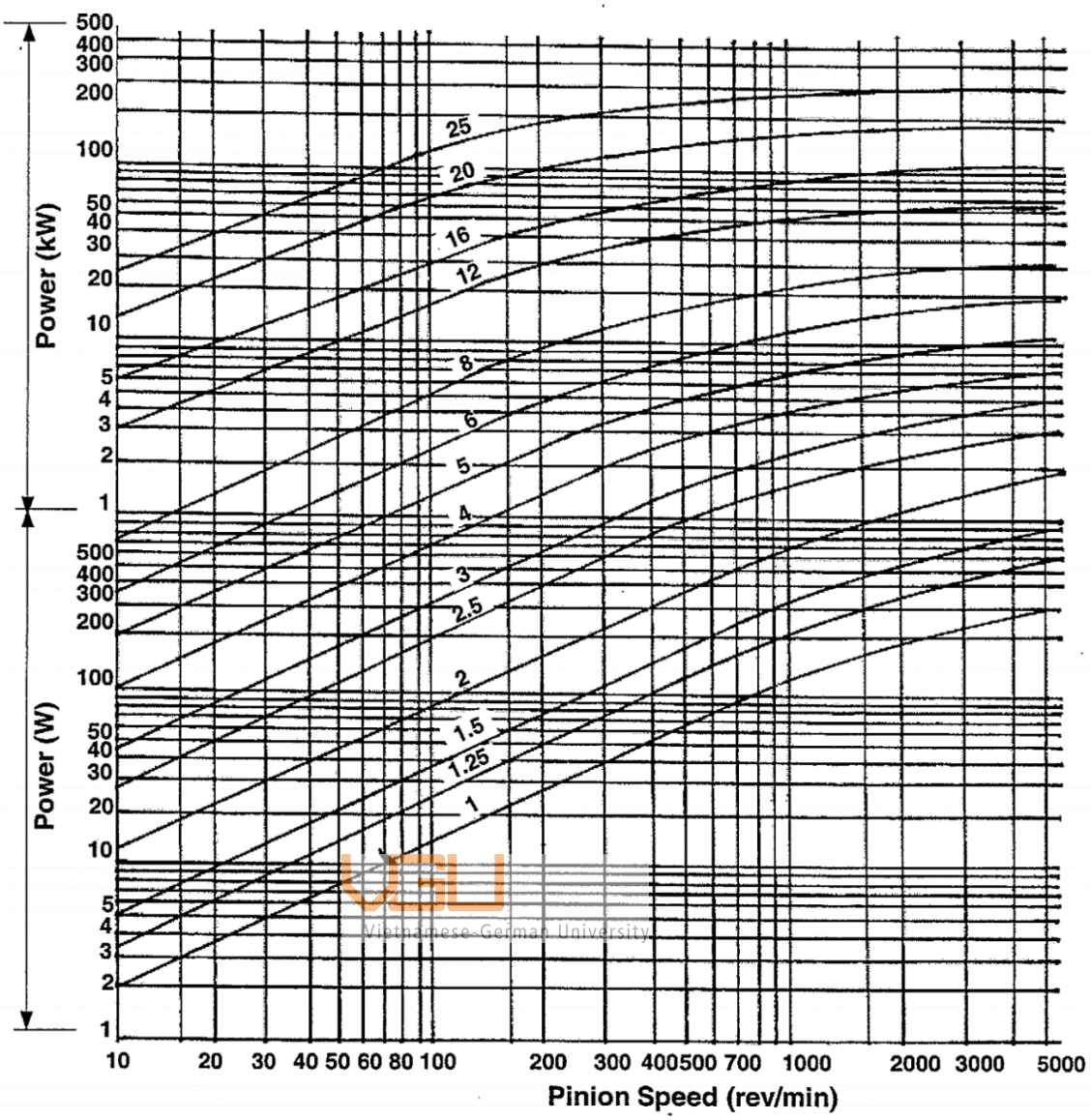

Figure 5.4: Relation between power and pinion speed

According to figure 5.4, the modulus 1.25 is corresponding to 400 W and 3000 RPM. However, for simplicity in machining, the modulus 1.5 is final decision. The pitch diameter of driven gear must exceed the diameter of the MR brake in order to prevent the driving gear from contacting with the housing of MRB. Thus, the diameter of driven gear is set at 192 mm. Then, following equation is used to calculate other parameters of pair of gear

$$\frac{N_{driven}}{N_{driving}} = 4 \tag{33}$$

$$d_{driven} = m * N_{driven} \quad (34)$$

$$d_{driving} = m * N_{driving}$$

$$l = \frac{d_{driven} + d_{driving}}{2} \quad (35)$$

$$8m \leq b \leq 12m \quad (36)$$

In with: m is modulus, N is the number of teeth, d is the pitch diameter of gear, l is the distance between shafts of two gears and b is the thickness of the gear.

Result

Pair of spur gear
m = 1.5
$N_{driving}$ = 32
N_{driven} = 128
$d_{driving}$ = 48 mm
d_{driven} = 192 mm
l = 120 mm
b = 14 mm

Table 5.3: Specifications of pair of spur gear

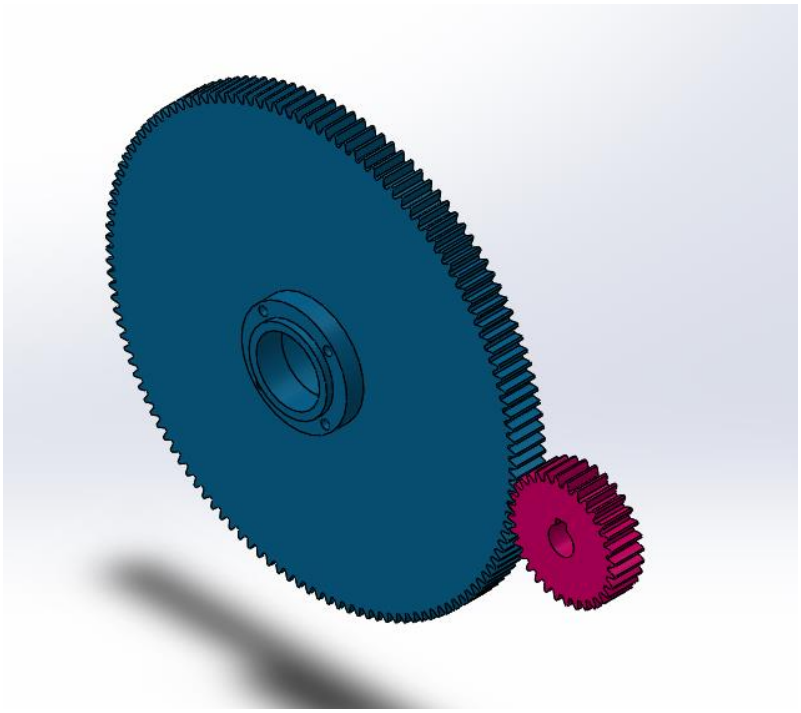

Figure 5.5: CAD of spur gears

The driven gear is design to have space for installing the same bearing model as MRB shaft (SKF_6301), moreover, the driven gear is connected with the MRB shaft also by 4 pins. For the driving gear, the inner diameter of it is 12 mm with a key way for attaching on the driving shaft later.

5.1.4. Driving shaft design

The diameter of the driving shaft is similar with the inner diameter of driving gear which is 12 mm. Then, the key with corresponding with this value of shaft's diameter according to DIN 6885 is

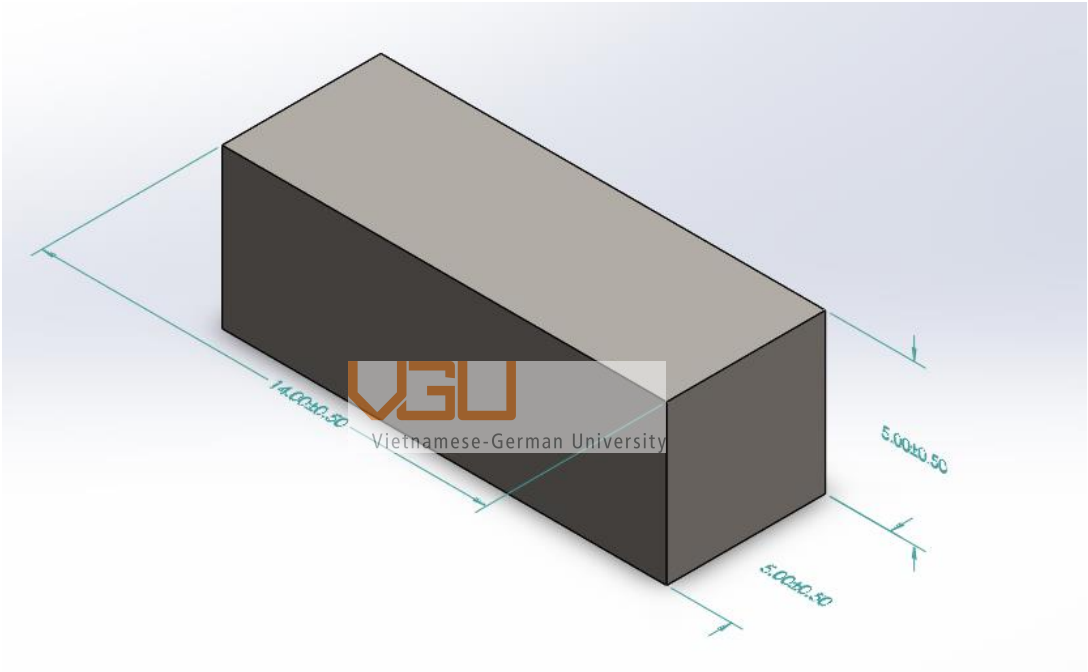

Figure 5.6: CAD of parallel key DIN 6885

Combining with the key way's dimensions of driving gear which is also designed by DIN standardization, the dimensions of driving's shaft key way is determined. Moreover, a bearing is also installed on the driving shaft in order to provide the ability of rotating. The model SKF_3201 ATN9 ball bearing is selected for this function since this is the double row bearing type which is stiffer than normal bearing. Thus, it could maintain the stability of the shaft when the driving gear is loaded.

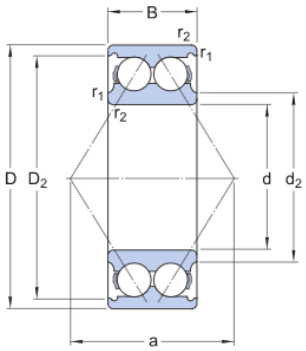

Dimensions

d	12 mm	Bore diameter
D	32 mm	Outside diameter
B	15.9 mm	Width
d_2	≈ 17.2 mm	Recess diameter inner ring shoulder
D_2	≈ 27.7 mm	Recess diameter outer ring shoulder
$r_{1,2}$	min. 0.6 mm	Chamfer dimension inner ring
a	19 mm	Distance pressure point(s)

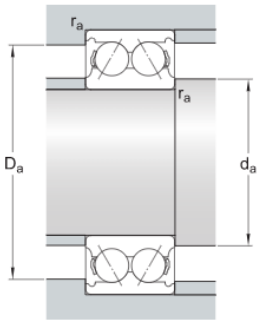

Abutment dimensions

d_a	min. 16.4 mm	Abutment diameter shaft
D_a	max. 27.6 mm	Abutment diameter housing
r_a	max. 0.6 mm	Fillet radius

Figure 5.7: Specification of SKF_3201 ATN9

[15]

Consequently, the driving shaft is designed with the key way and necessary geometric for installing bearing

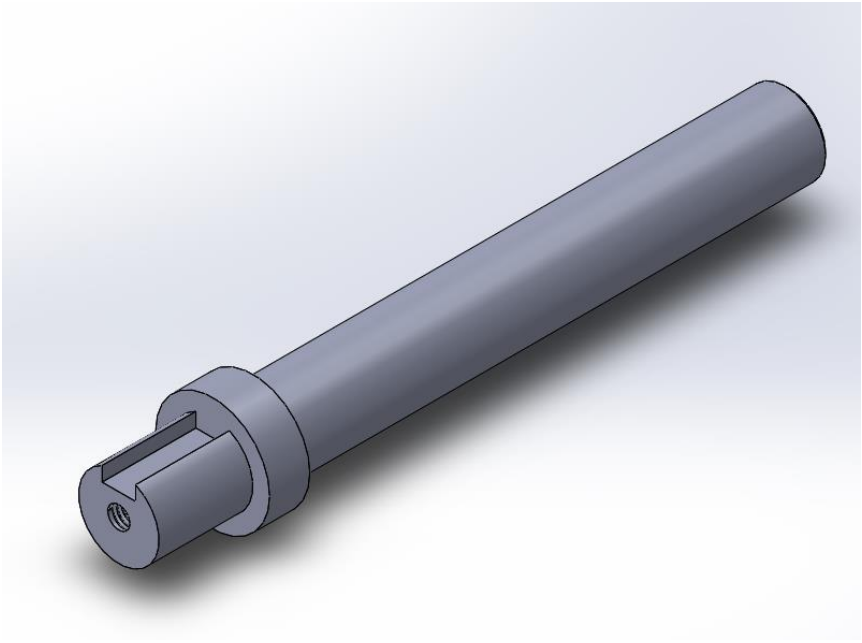

Figure 5.8: CAD of driving shaft

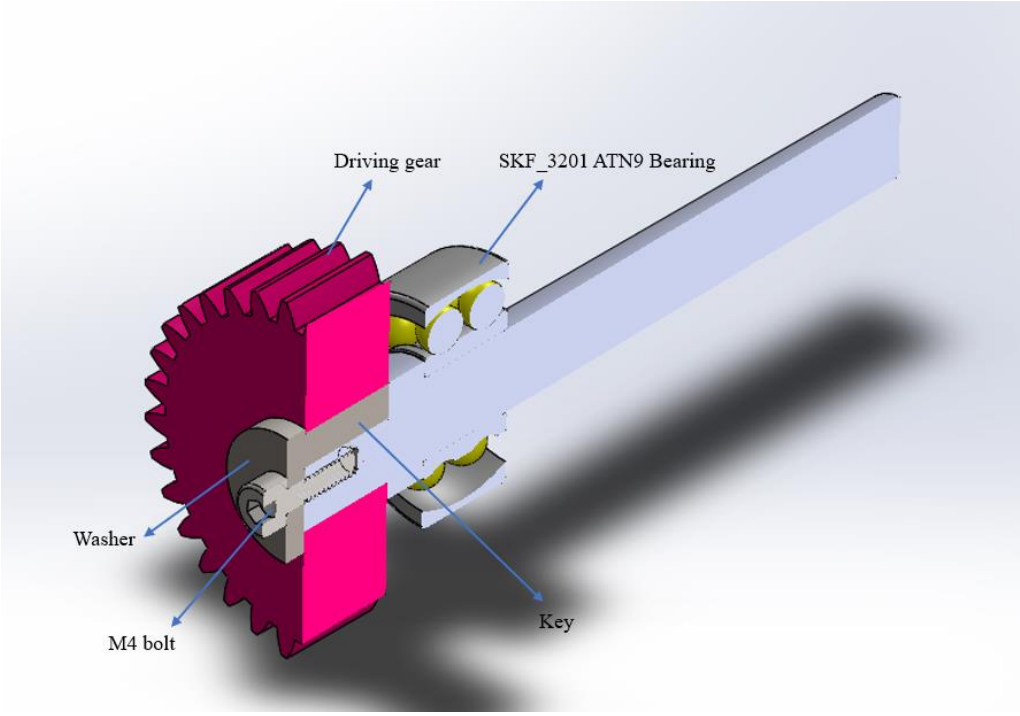

Figure 5.9: Assembly of all components on driving shaft

5.1.5. Driven shaft of testing model

The driven shaft is made use of electric scooter's front shaft and it is where the tooth-shaped and the driven gear is placed on. As discussed in section 5.1.3, the driven gear is connected to the MRB shaft by 4 pins and rotated by SKF_6301 bearing

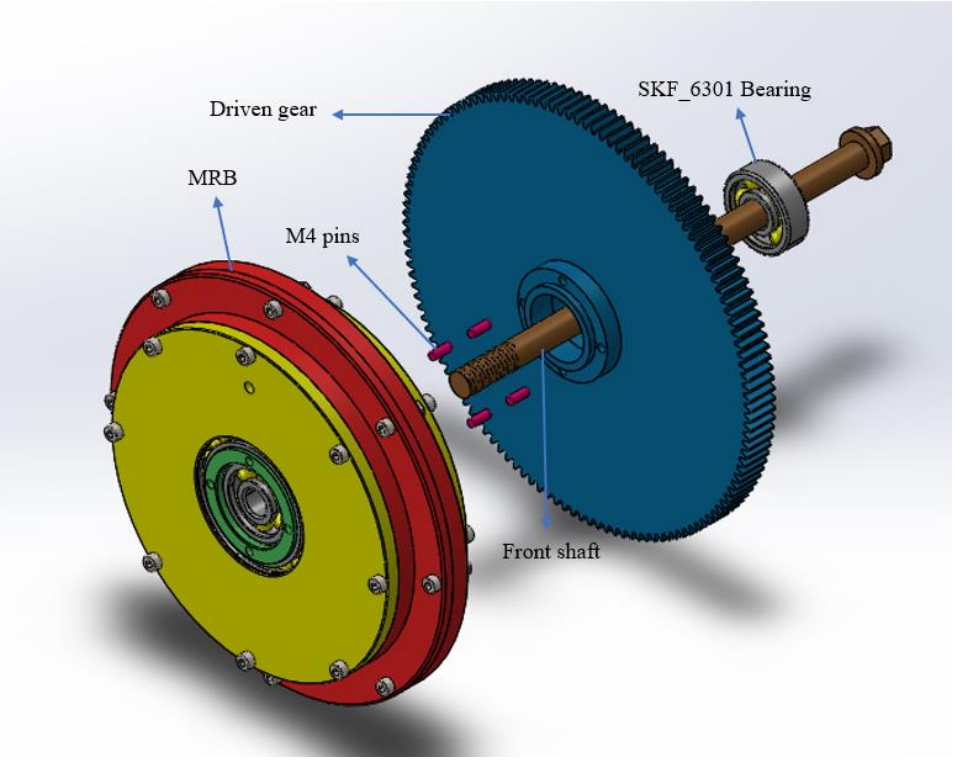

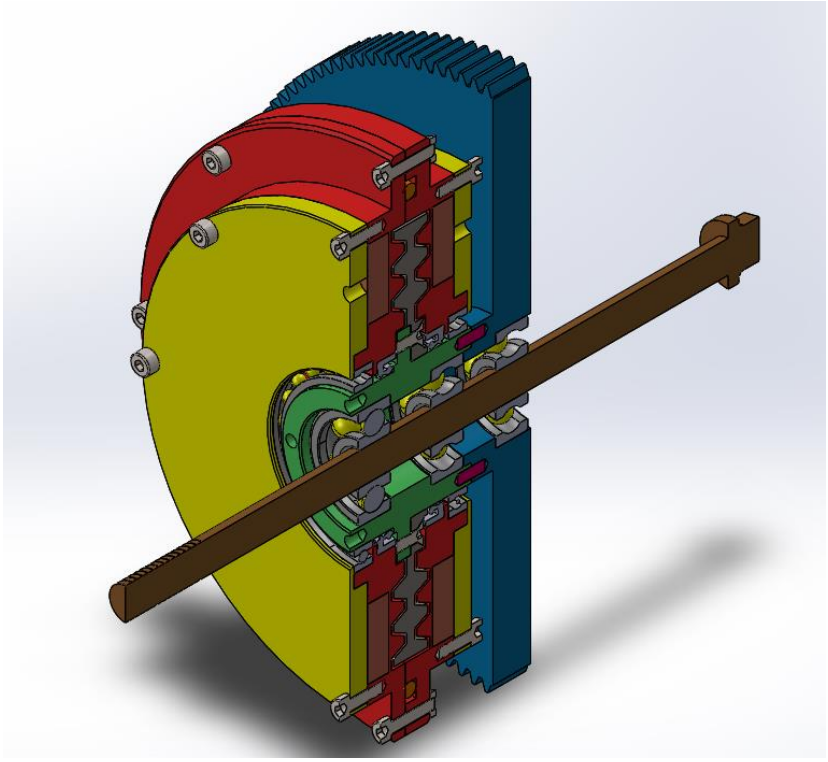

Figure 5.10: Assembly of driven shaft

5.1.6. Coupling selection

The working principles of coupling are to linking different shafts together as well as absorbing mounting errors in connection of shafts for power transmission.

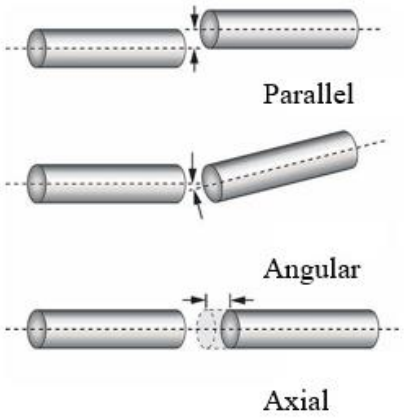

Figure 5.11: Possible misalignment in shaft mounting

There are many types of couplings such as beam coupling, chain coupling, jaw coupling, diaphragm coupling, disc coupling, ... etc. After considering requirements of testing model and project's budget, jaw coupling type is chosen.

Jaw coupling is used for both motion controls and light power transmission and this model allows for backlash-free torque transmission. Accommodation for parallel misalignment typically reaches 0.254 mm and angular misalignment reaches 1 degree. A jaw coupling transmits torque through the compression of an elastomeric spider which is inserted between two intermeshing jaws. This elastomeric spider also gives this coupling some damping capacity.

Two places in the testing model need coupling. First is between driving shaft and torque sensor, second is between torque sensor and motor. The diameter of driving shaft, torque sensor's shaft and motor's shaft are respectively 12 mm, 32 mm and 14 mm.

For linking purpose of those shafts, clamp jaw coupling model DJC 55CRD from DURI JDC is selected.

Figure 5.12: DJC 55CRD coupling

Product No.	Standard inner diameter (D1, D2) (mm)																													
	3	4	4.5	5	6	6.35	7	8	9.525	10	11	12	14	15	16	18	19	20	22	24	25	26	28	30	32	35	38	40	45	50	60
DJC-14□	•	•	•	•																										
DJC-20□		•	•	•	•	•	•	•	•	•																				
DJC-25□				•	•	•	•	•	•	•	•	•																		
DJC□-30□					•	•	•	•	•	•	•	•	•	•	•															
DJC□-40□								•	•	•	•	•	•	•	•	•	•	•												
DJC-55□										•	•	•	•	•	•	•	•	•	•	•	•	•	•	•	•					
DJC-65□												•	•	•	•	•	•	•	•	•	•	•	•	•	•	•	•			
DJC-80□														•	•	•	•	•	•	•	•	•	•	•	•	•	•	•		
DJC-95□																		•	•	•	•	•	•	•	•	•	•	•	•	
DJC-100□																		•	•	•	•	•	•	•	•	•	•	•	•	•

Table 5.4: Inner diameter range of DJC 55CRD coupling

(Dai Hoa Phu, 2022) [18]

DJC-55 coupling has flexible range of inner diameter which is from 10 mm to 32 mm. Thus, DJC 55CRD coupling is valid for shafts mounting purpose of the testing model

Product No.	Dimension (mm)						Tightening Screw		Rated. Torque	Max. Torque	Max. RPM	Moment of inertia	Torsional Stiffness	Angle	Parallel	End play	Mass
							Size	Torque									
	A	L	W	B	C	F	M	N · m	N · m	N · m	min^{-1}	kg · m^2	N·m/rad	°	mm	mm	g
DJC-55CRD	55	30	78	14	2	10.5	M6	13	60	120	11,000	1.6×10^{-4}	4,000	1	0.1	$^{+1.4}_{0}$	330

Table 5.5: Specification of DJC 55CRD coupling

[18]

5.1.7. Holders

After having all dimensions of components in testing model, holders for motor, torque sensor, driving shaft and driven shaft are designed. The most important thing is all the shafts must be concentric.

5.1.7.1. Holder for the motor

The holder for the motor has an L shape with 4 M5 horizontal holes to attach the motor by bolt joints. There are also 2 M10 vertical holes on the bottom plane of the holder to fix it with the base later.

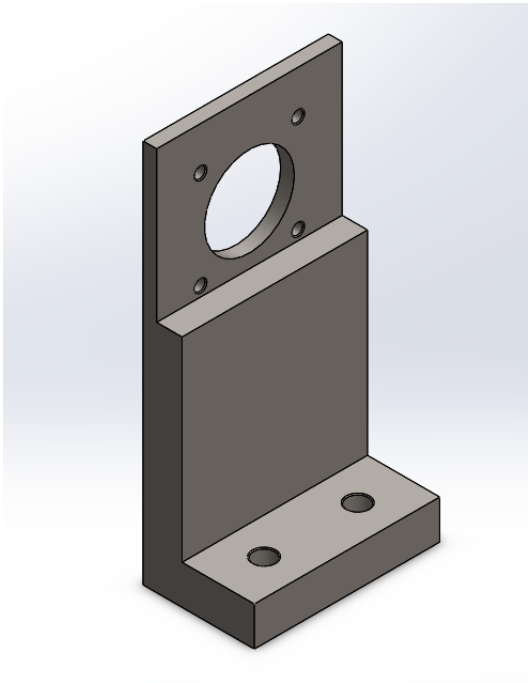

Figure 5.13: Holder of motor

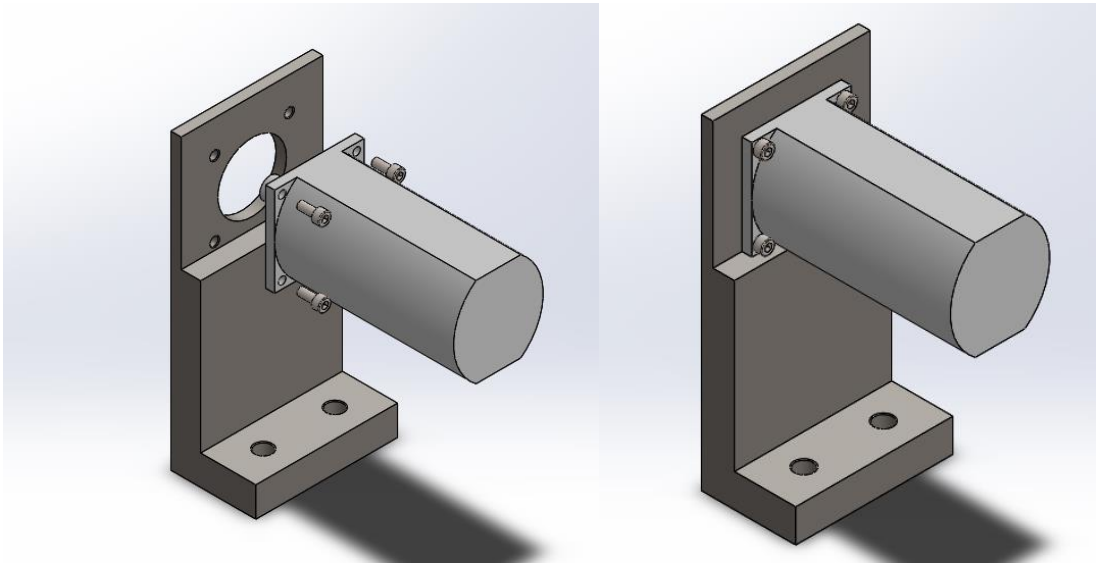

Figure 5.14: Assembly of motor and its holder

5.1.7.2. Holder for the torque sensor

As the torque sensor already have had the screw hole at the bottom, the holder for the torque sensor is designed according to it. As a result, the shape of the holder has 4 M8 vertical screw holes to attach torque sensor, 2 M9 holes for the fixtures and 4 M10 vertical screw holes to fix with the base of system.

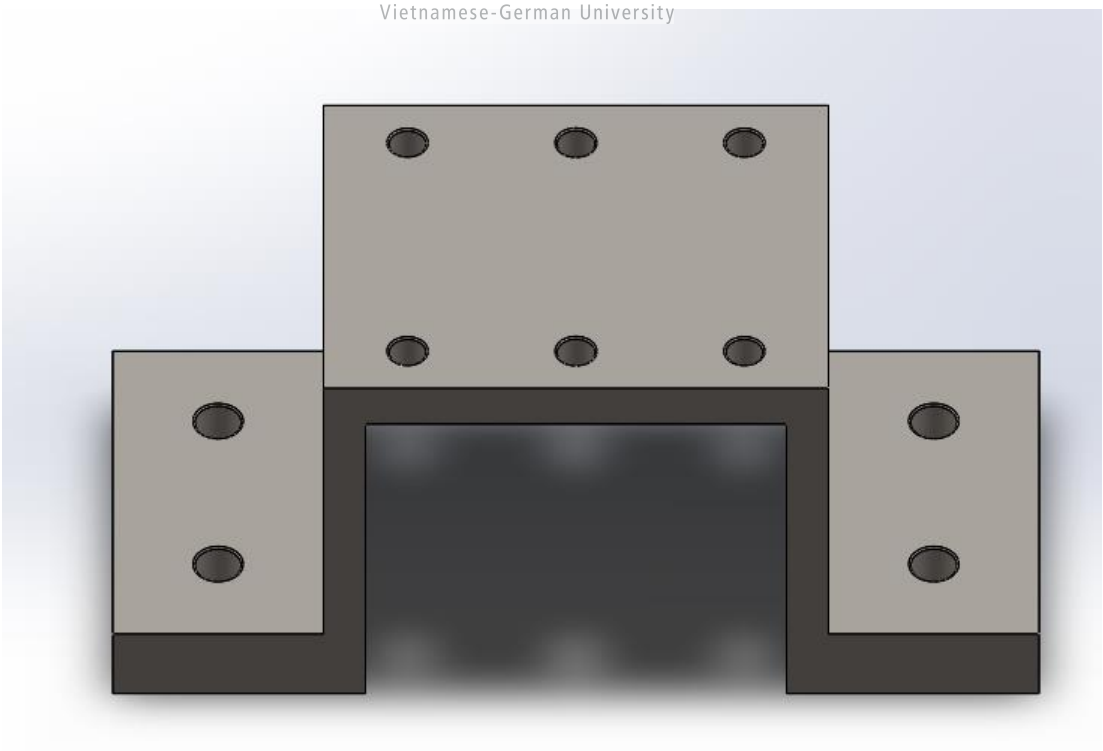

Figure 5.15: Holder for torque sensor

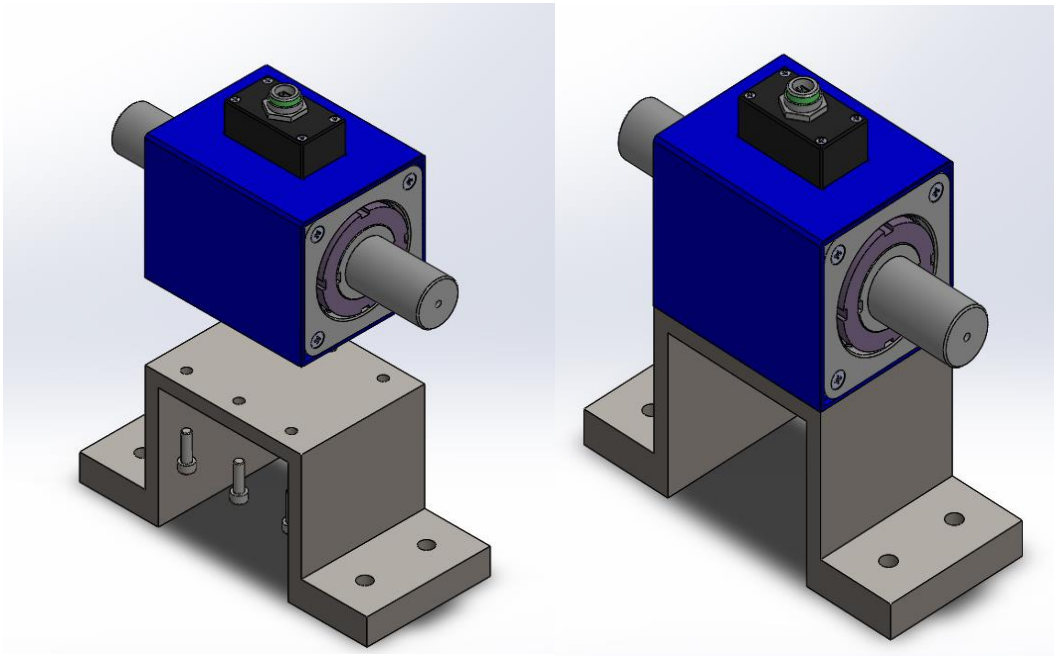

Figure 5.16: Assembly of torque sensor and its holder

5.1.7.3. Holder for driving shaft and driven shaft

The driven shaft needs two holders to be placed on. The first holder of driven shaft is made to contain the driving shaft also. Thus, the distance between 2 vertical holes of the second holder must be equal to the necessary distance between two gears. The hole where the driving shaft is placed is modified for installing bearing.

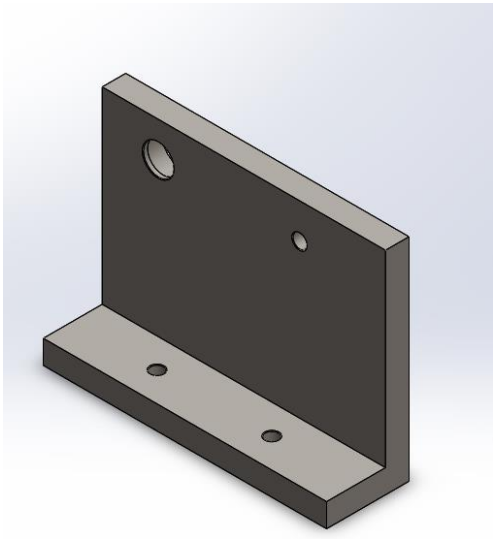

Figure 5.17: First holder of driven shaft

The second holder of driven shaft also aims to fix the housing of the MR brake which prevent it from rotation by using 3 M4 screws.

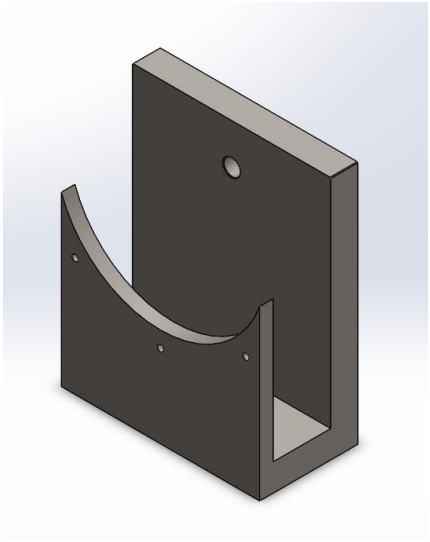

Figure 5.18: Second holder of driven shaft

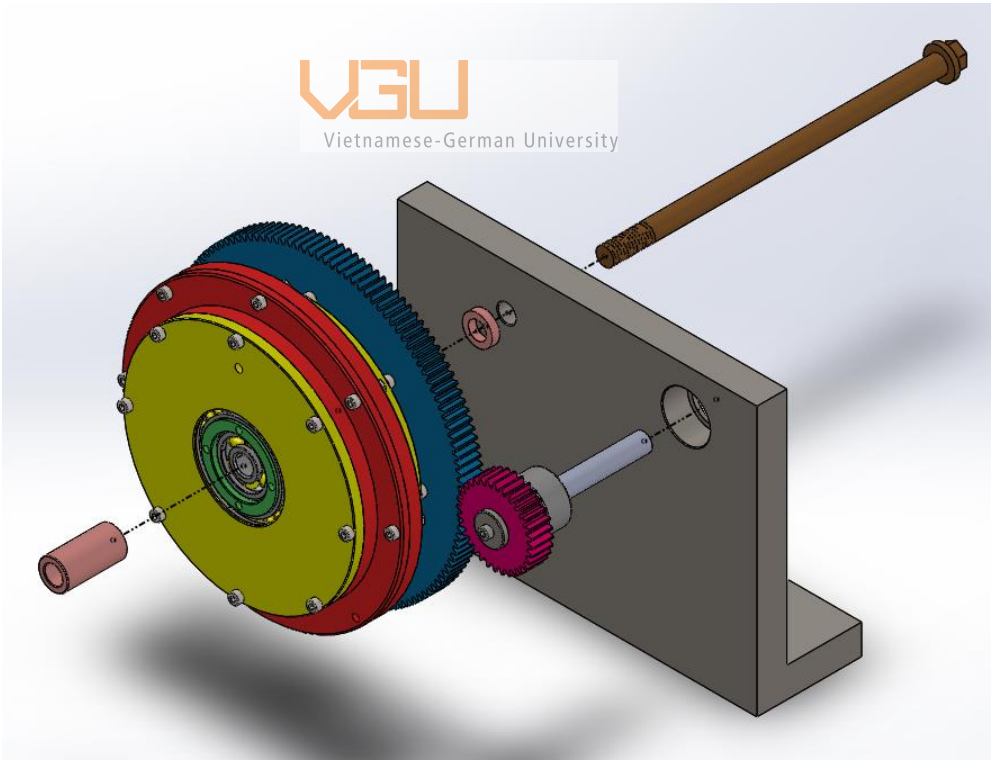

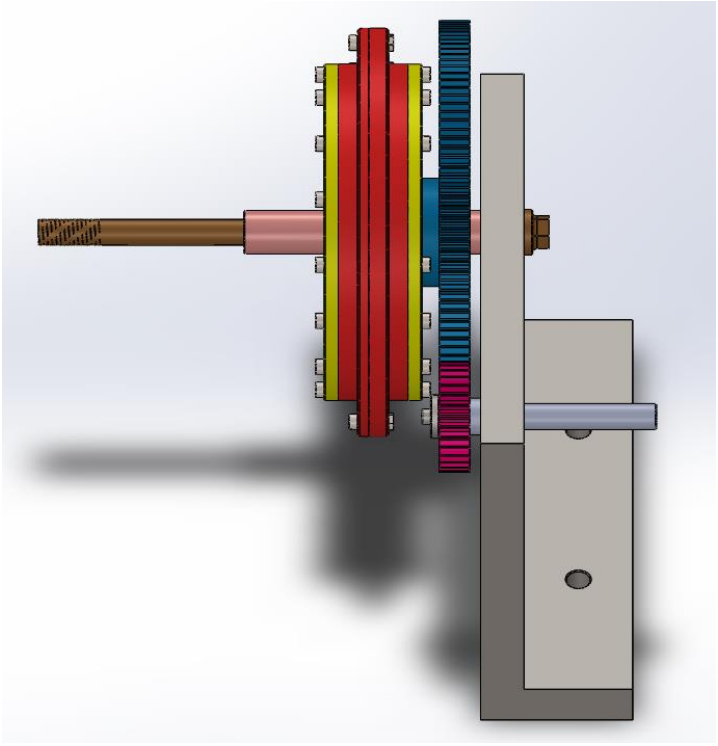

Figure 5.19: Assembly of driving shaft, driven shaft and second holder

Two retaining rings are added to secure the bearings of MRB shaft and driven gear. Then the second holder is installed with 3 M4 screws to fix the housing of MRB.

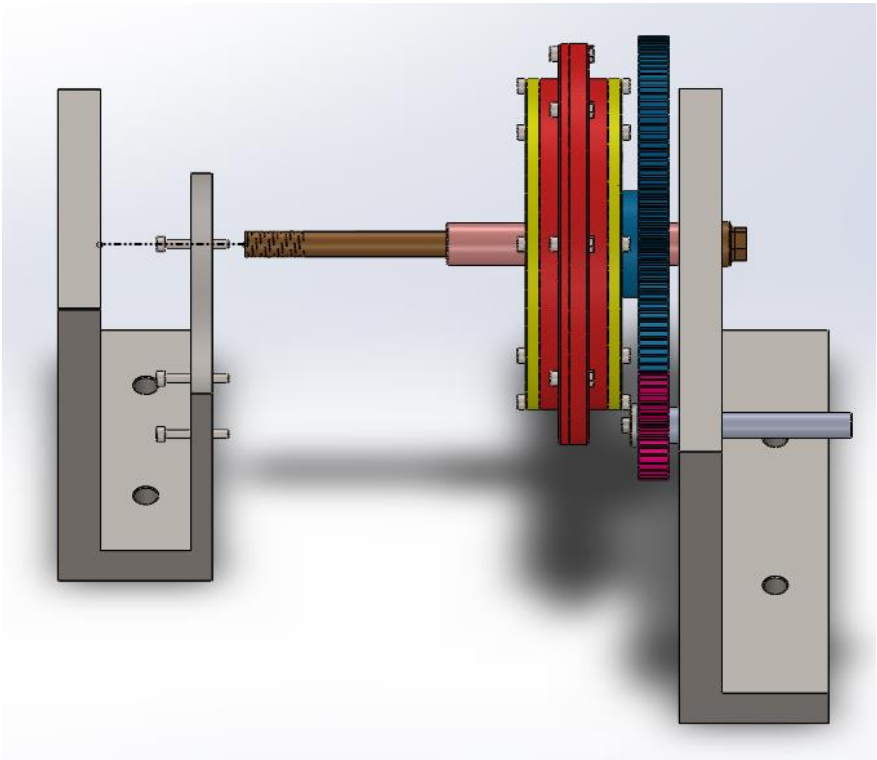

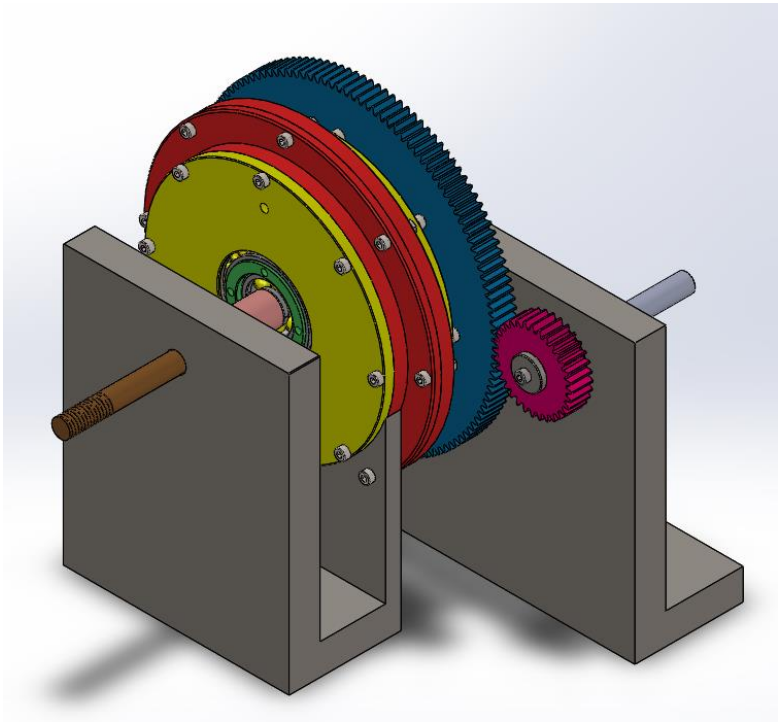

Figure 5.20: Full assembly of driven shaft, driving shaft and holders

5.1.7.4. Base of system

After all holders are determined, the rectangle base is designed with M10 holes corresponding to holes of previous holders. There are two M11 holes in order to insert the connection screws of torque sensor.

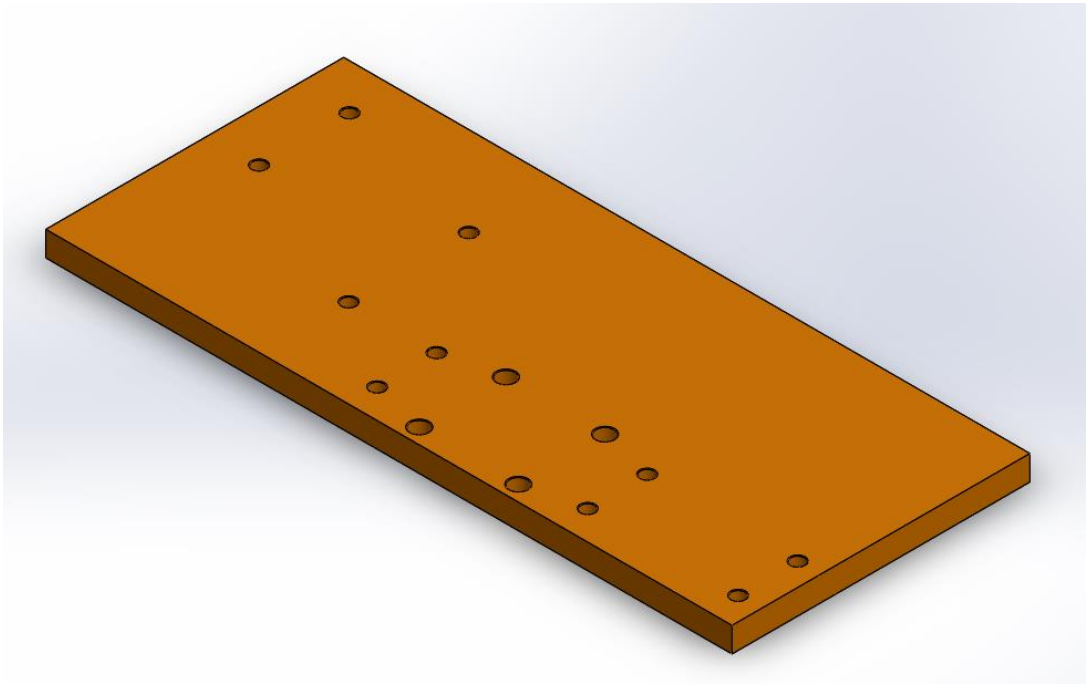

Figure 5.21: The base of system

5.1.8. Full detail of experiment model

The couplings are added to connect the driving shaft and torque sensor's shaft as well as the motor's shaft and torque's shaft. All components of testing model are then mounted to the base of system by M10 bolts and screws. The end retain ring and M12 nut are added to secure the position of drive shaft.

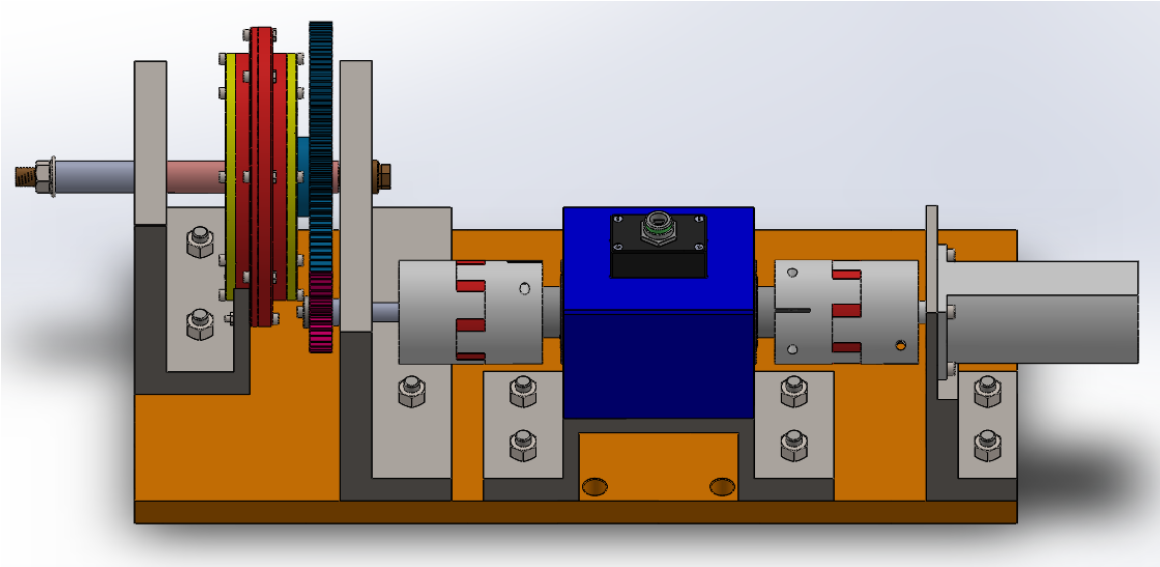

Figure 5.22: Testing model

With the specification of Panasonic AC servo motor model MSMO42AIUX as table 5.1, this motor could only produce enough torque to make the disc of the MRB rotate without the applied electric current. As a result, this testing model is only able to measure the yield stress of the MRF in the tooth-shaped brake without any effect of electric current. For that reason, the second version of testing model is designed in order to measure the braking torque of the MRB when the electric current is applied.

5.2. Second version of testing model

To solve the lack of input torque when the MRB is activated, the motor is replaced by a round crank. The crank will be rotate by man power. This will allow the testing model to measure the maximum torque of the MR brake.

Figure 5.23: Crank

The ball bearing units KP002 is selected for supporting the rotation of the crank. The specification of KP002 model is in the red box of the following picture.

P series with seat

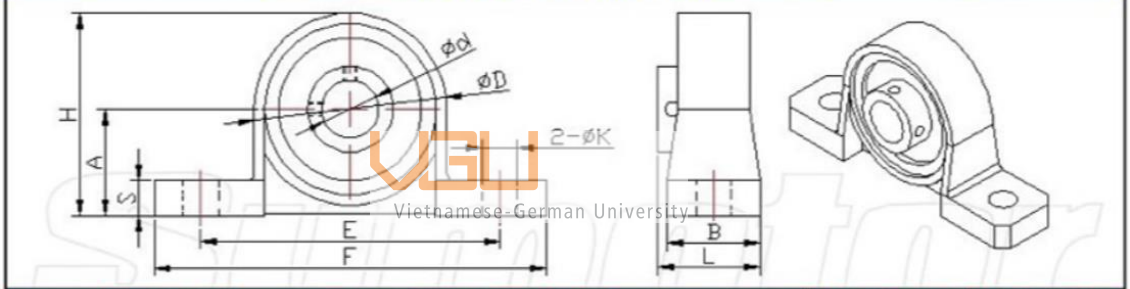

Model	Bore(mm)	Dimension (mm)									Hex. Socket Screws	Net Weight (g)
	d	A	H	E	F	S	D	B	L	K		
P08	8	15	29	42	55	5	27	13	15	5	2 x M2.5	37
P000	10	18	35	52	67	6	33	16	19	6.5	2 x M4	66
P001	12	19	38	56	71	6	38	16	19	6.5		80
P002	15	22	43	62	80	7	42	16	20	6.5		100
P003	17	24.5	47.5	67	85	7	46	18	20	7		135
P004	20	28	55	80	100	9.5	54	20	25	10	2 x M5	215
P005	25	32	62	90	112	10	60	20	25	10		265
P006	30	37	71	106	132	11	67	26	30	12.5		385

Table 5.6: Specification of P series ball bearing units

Since the crank has a 15.5 mm hole with key way and the bore diameter of the ball bearing units is 15 mm, a shaft is designed to connect the crank with the coupling in testing model with the diameter of two ends respectively 15 mm and 15.5 mm.

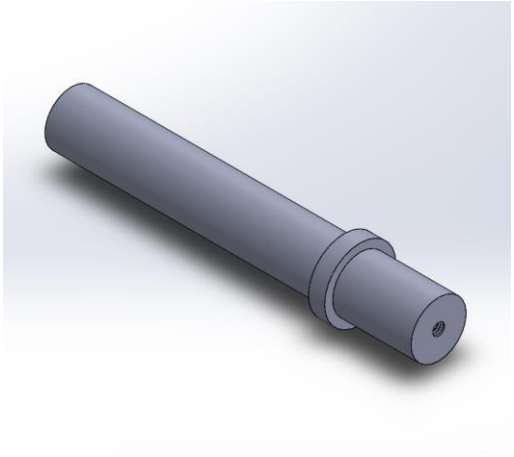

Figure 5.24: Crank shaft

Then a crank holder is made to attach all above element, the design of the crank holder guarantees that the crank shaft is concentric with the coupling in order to assembly with each other.

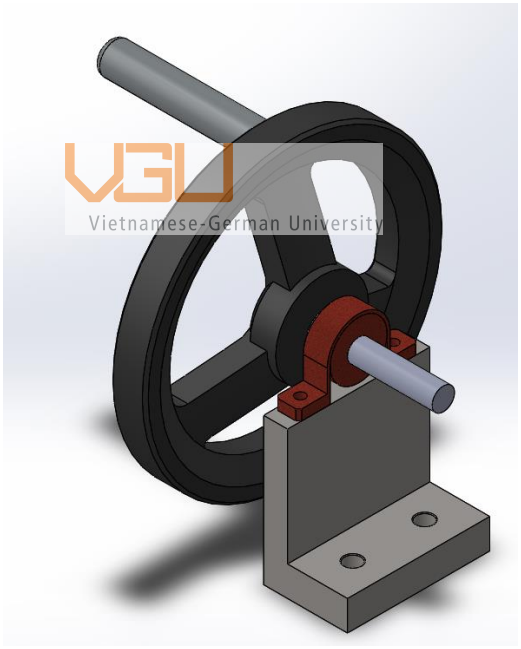

Figure 5.25: The crank mechanism

Two M10 holes are then added to the base of testing model to attach the crank mechanism. As a result, the second version of testing model is:

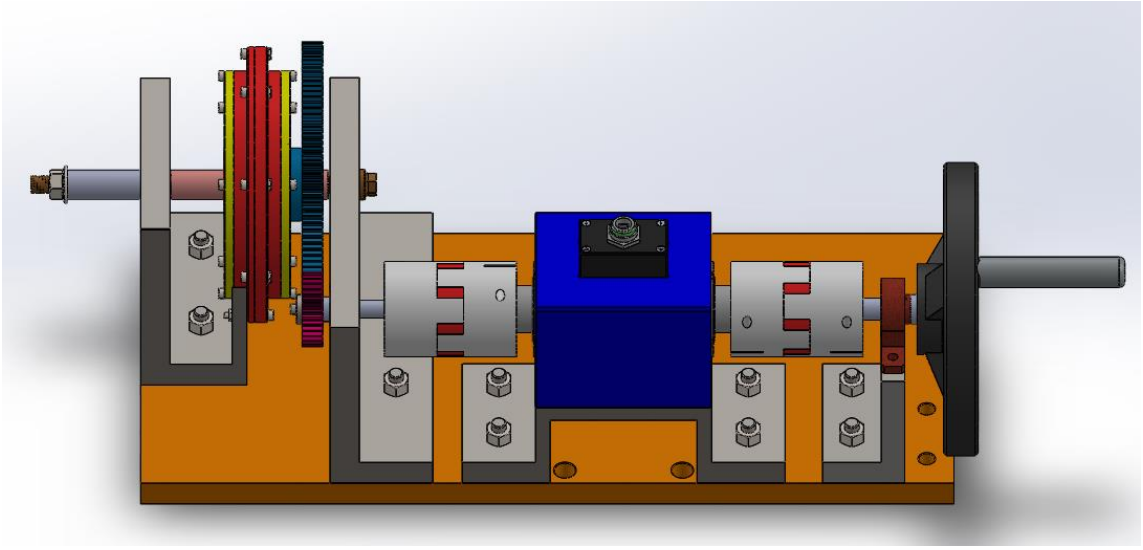

Figure 5.26: Second version of testing model

5.3. 2D drawings of testing model's components

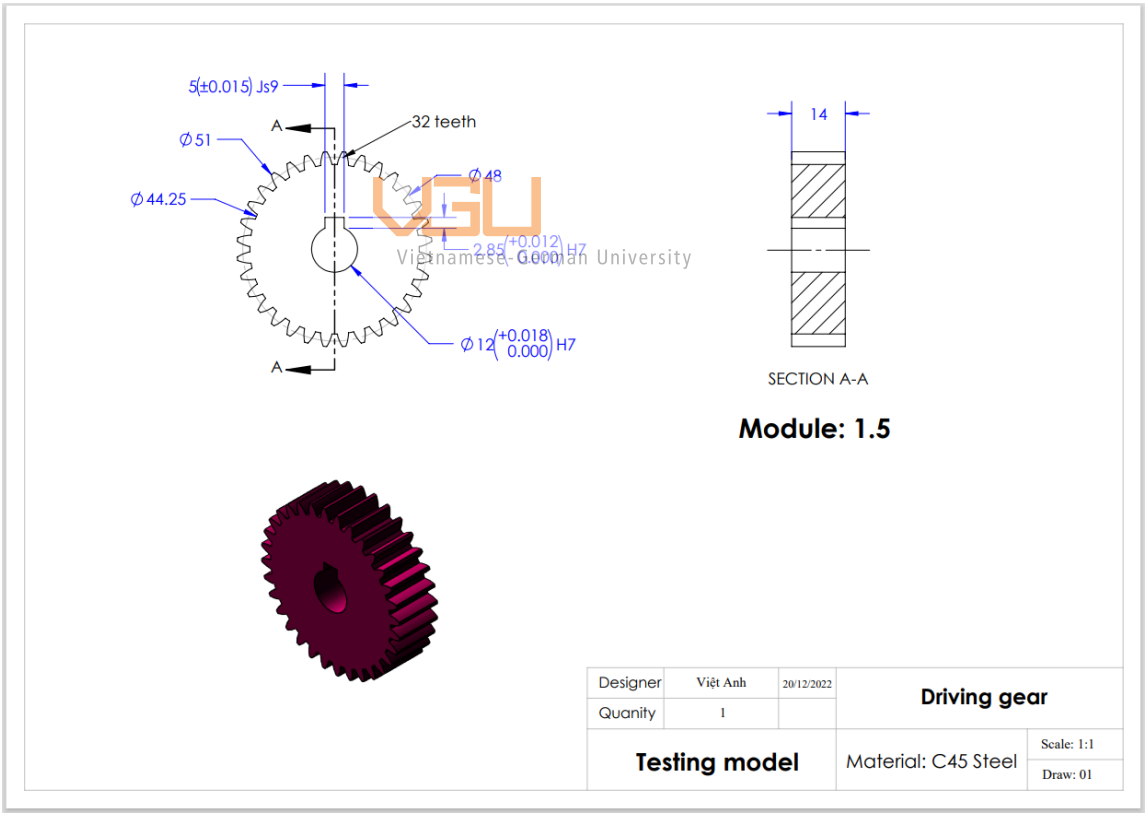

Figure 5.27: 2D drawing of driving gear

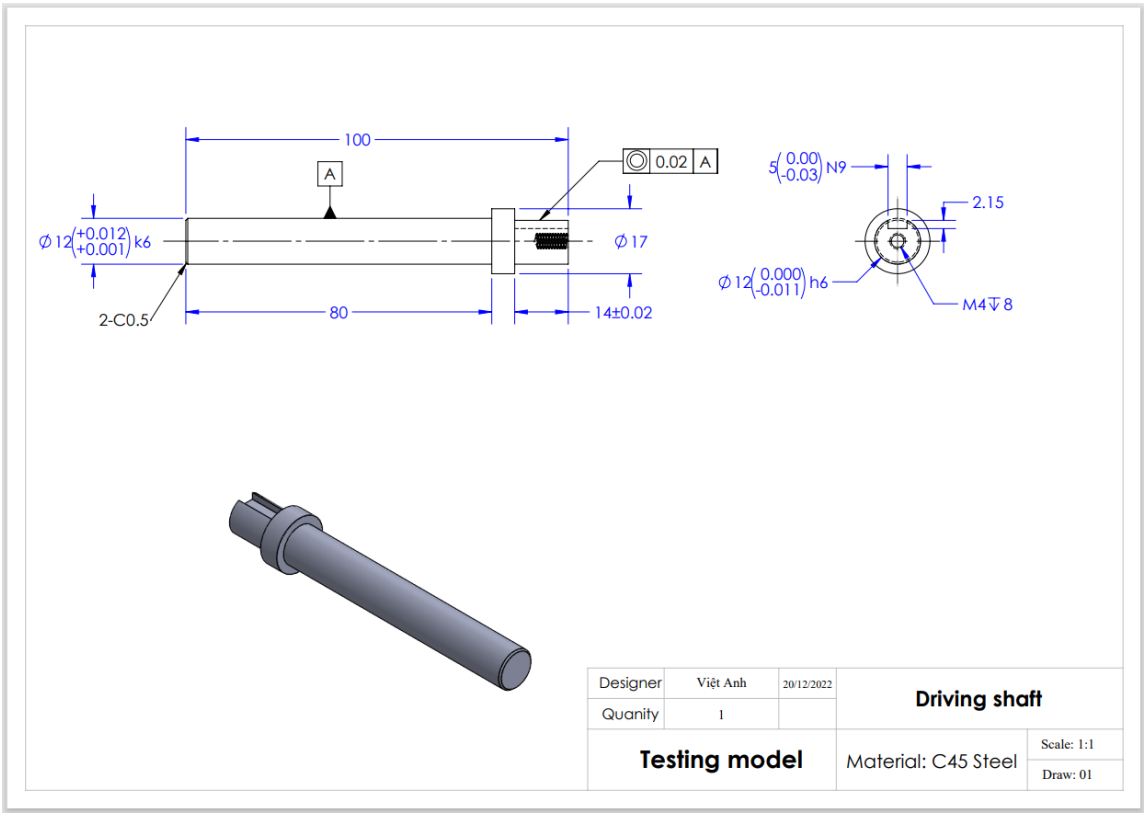

Figure 5.28: 2D drawing of driving shaft

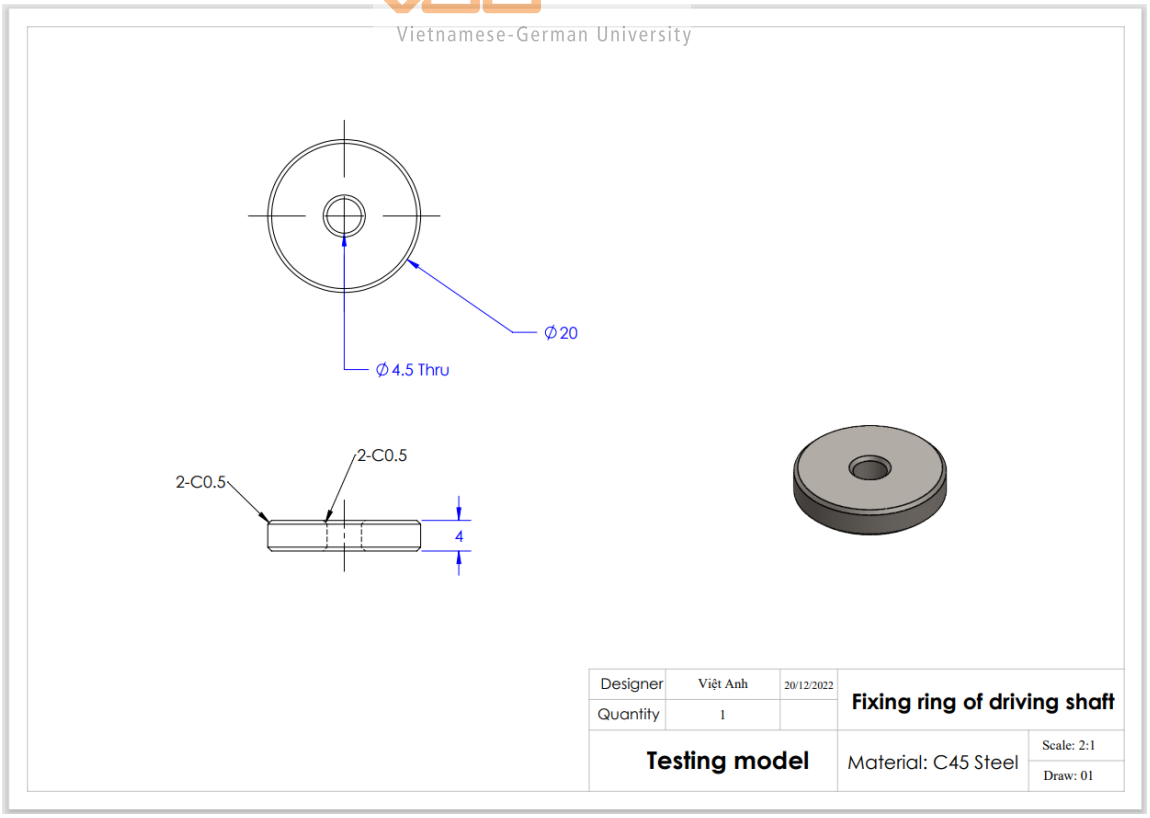

Figure 5.29: 2D drawing of fixing ring for driving shaft

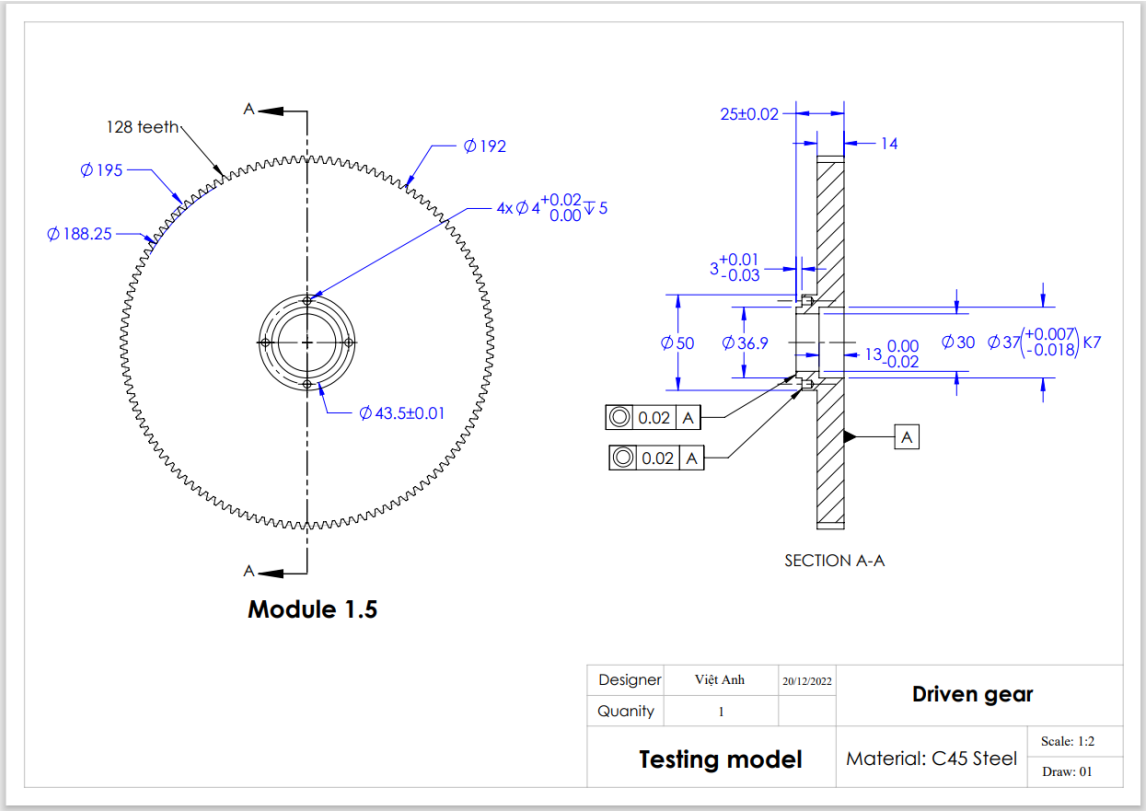

Figure 5.30: 2D drawing of driven gear

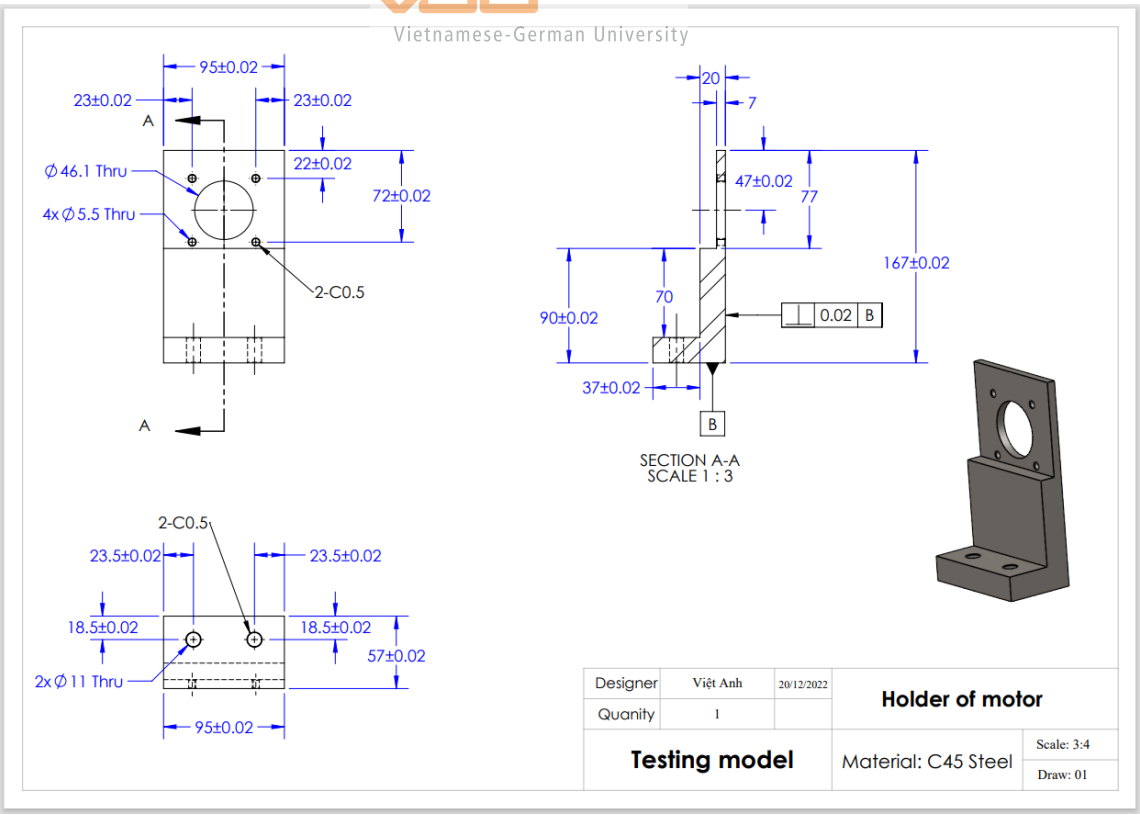

Figure 5.31: 2D drawing of holder of motor

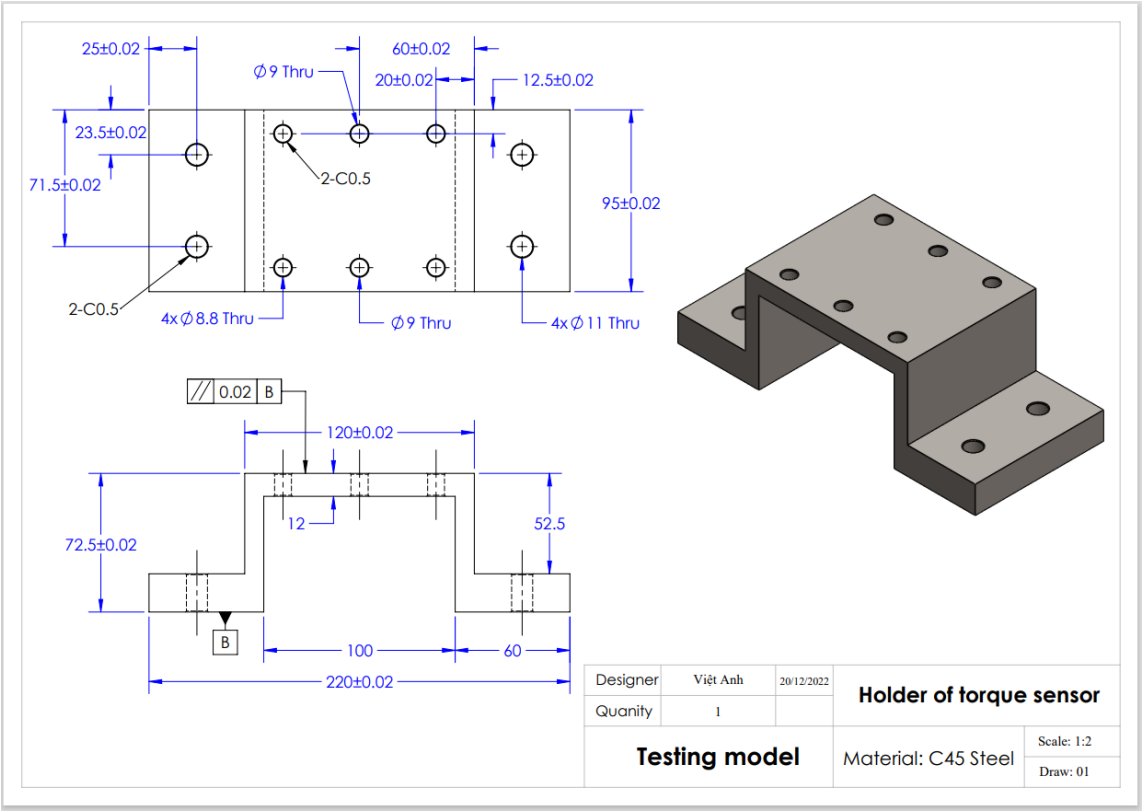

Figure 5.32: 2D drawing of holder of torque sensor

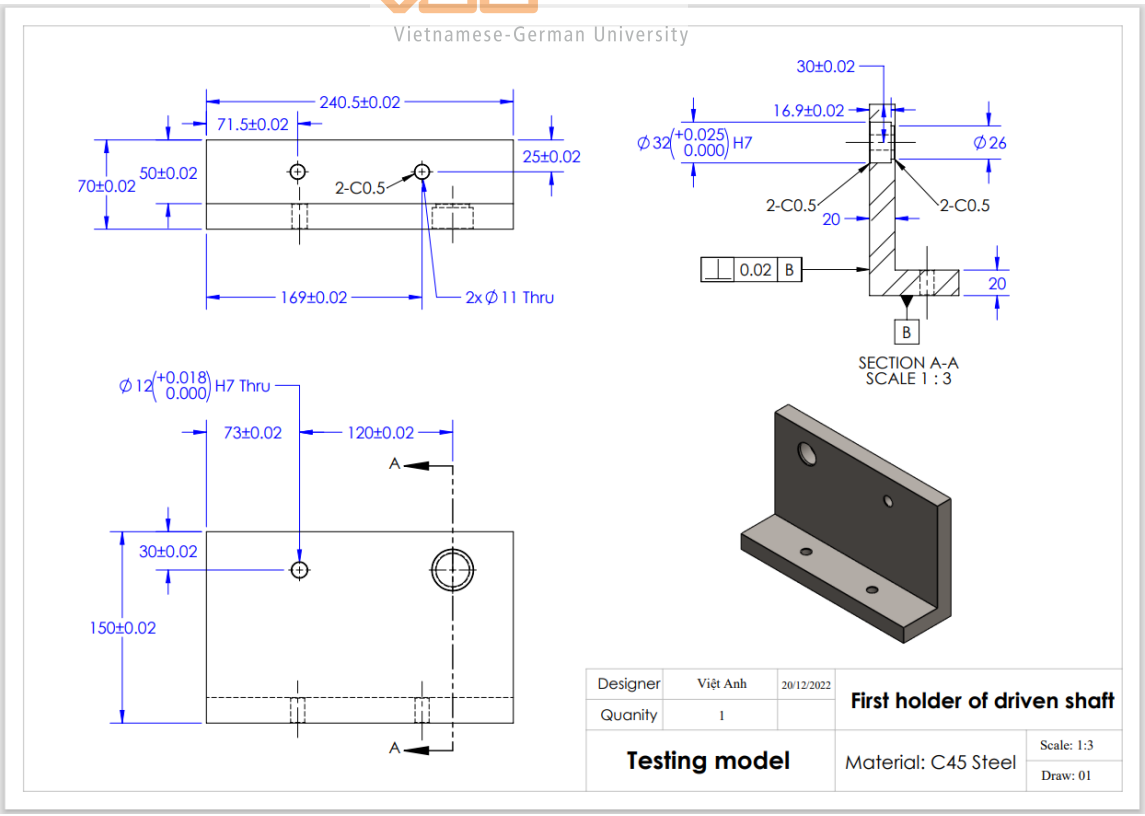

Figure 5.33: 2D drawing of first holder of driven shaft

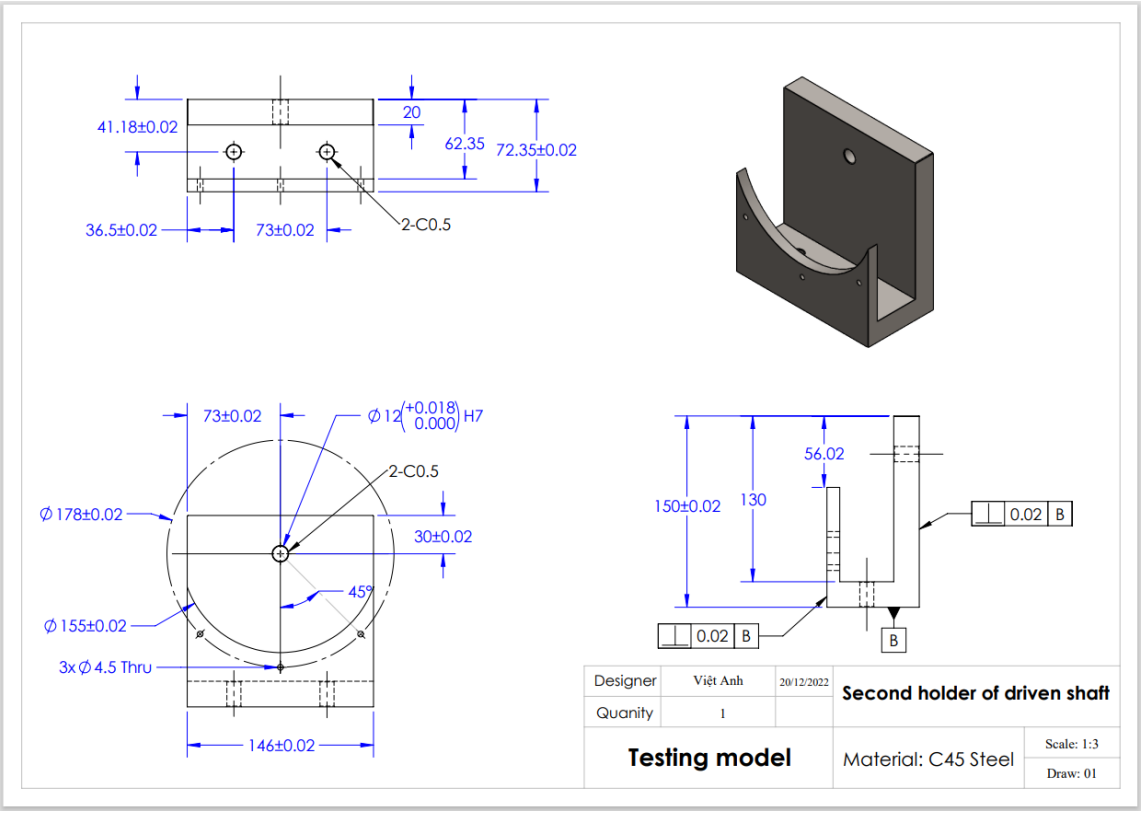

Figure 5.34: 2D drawing of second holder of driven shaft

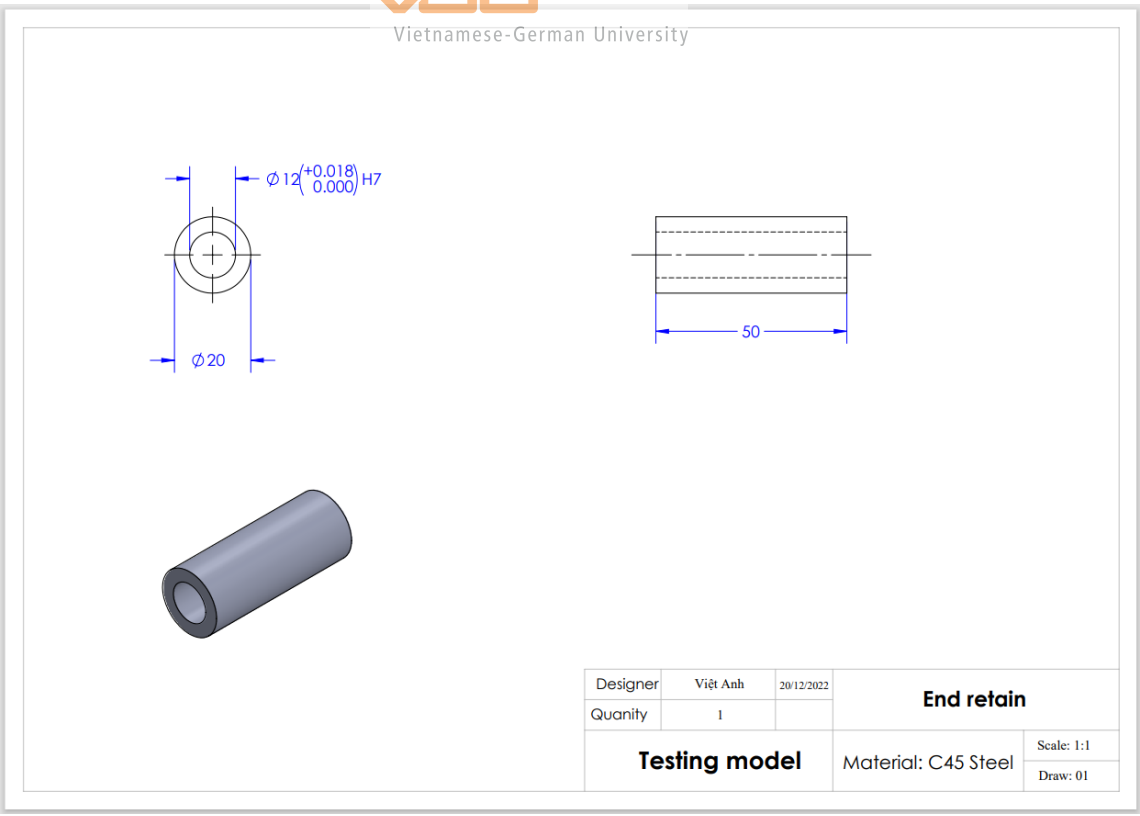

Figure 5.35: 2D drawing of end retaining ring

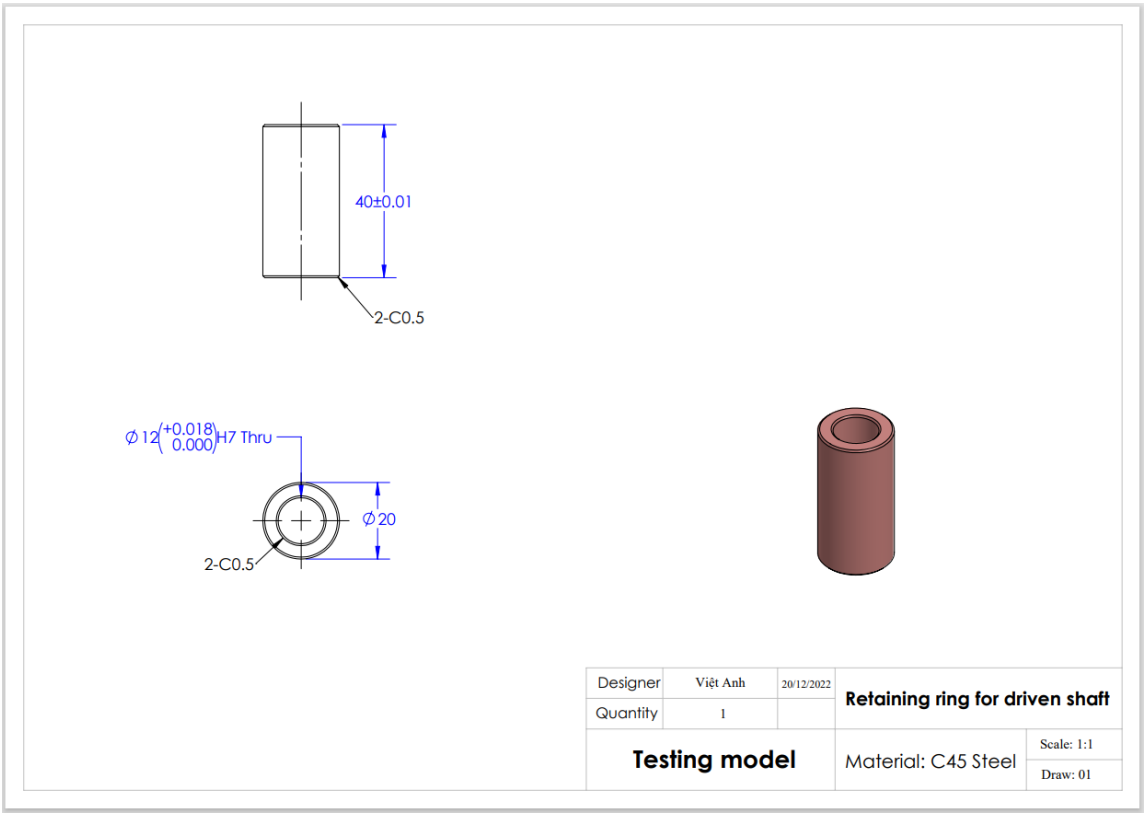

Figure 5.36: 2D drawing of retaining ring 1

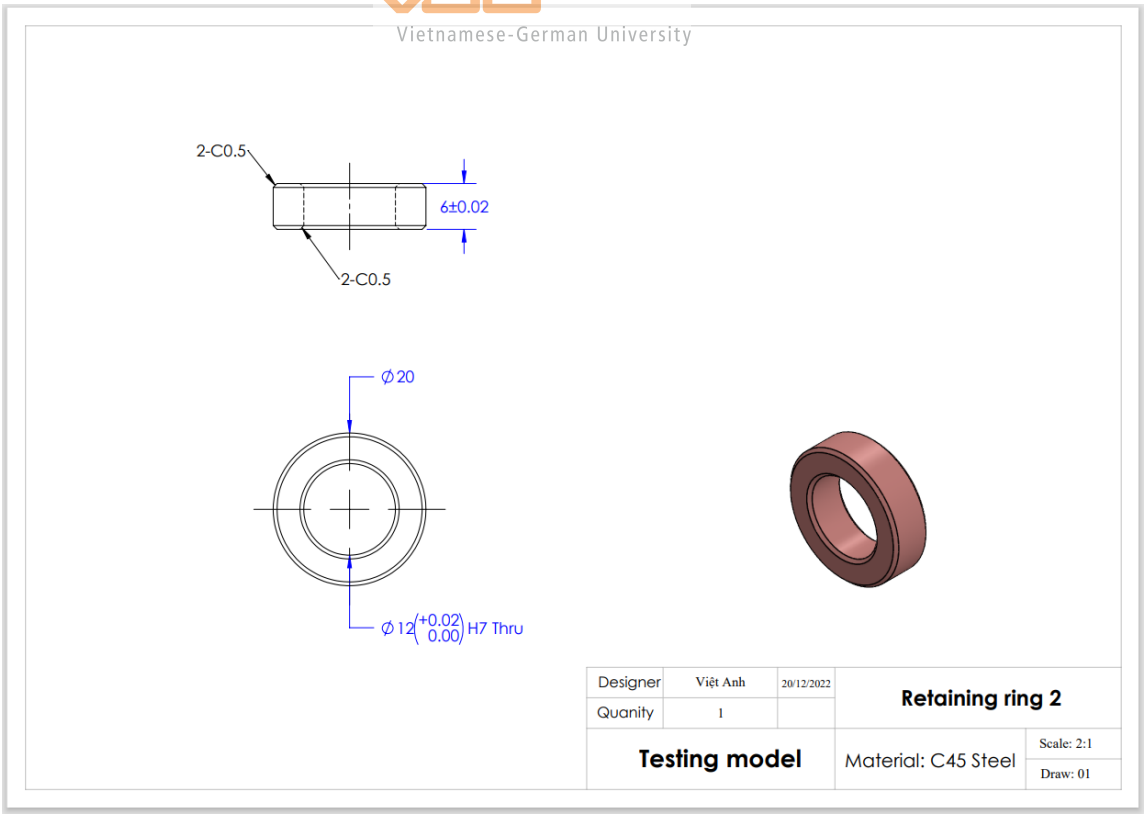

Figure 5.37: 2D drawing of retaining ring 2

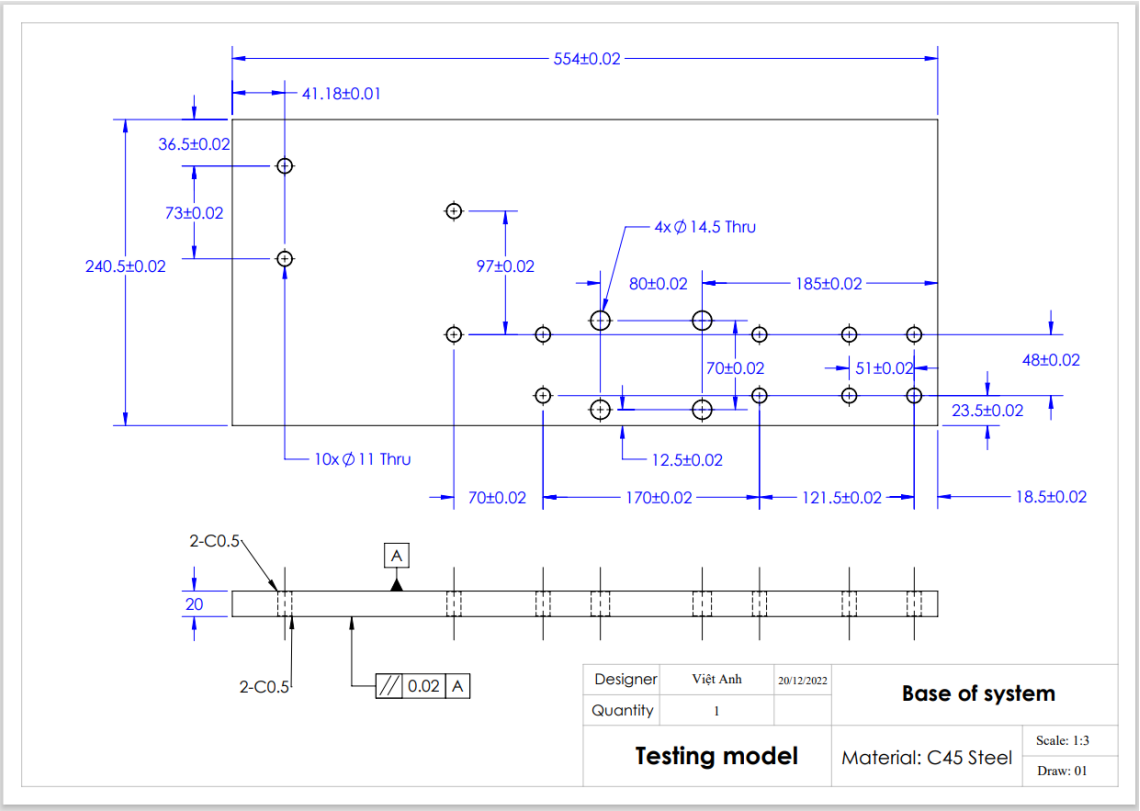

Figure 5.38: 2D drawing of the base

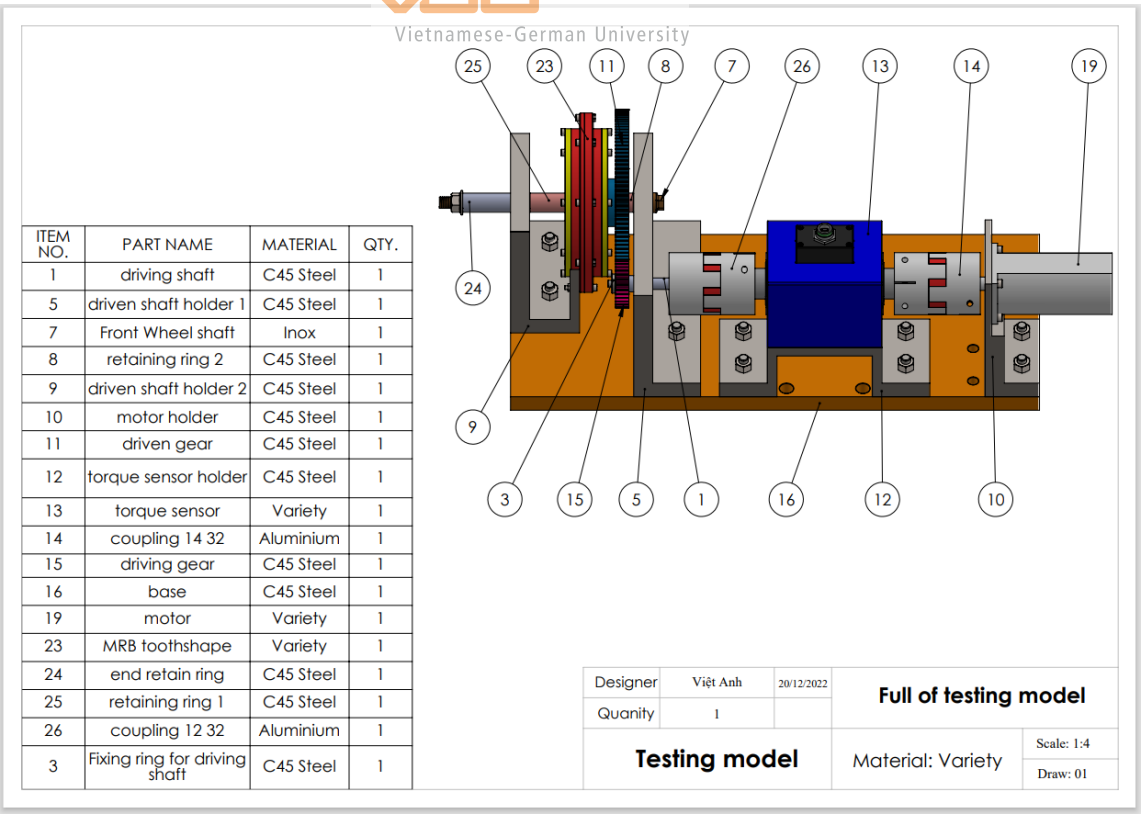

ITEM NO.	PART NAME	MATERIAL	QTY.
1	driving shaft	C45 Steel	1
5	driven shaft holder 1	C45 Steel	1
7	Front Wheel shaft	Inox	1
8	retaining ring 2	C45 Steel	1
9	driven shaft holder 2	C45 Steel	1
10	motor holder	C45 Steel	1
11	driven gear	C45 Steel	1
12	torque sensor holder	C45 Steel	1
13	torque sensor	Variety	1
14	coupling 14 32	Aluminium	1
15	driving gear	C45 Steel	1
16	base	C45 Steel	1
19	motor	Variety	1
23	MRB toothshape	Variety	1
24	end retain ring	C45 Steel	1
25	retaining ring 1	C45 Steel	1
26	coupling 12 32	Aluminium	1
3	Fixing ring for driving shaft	C45 Steel	1

Figure 5.39: Assembly of testing model

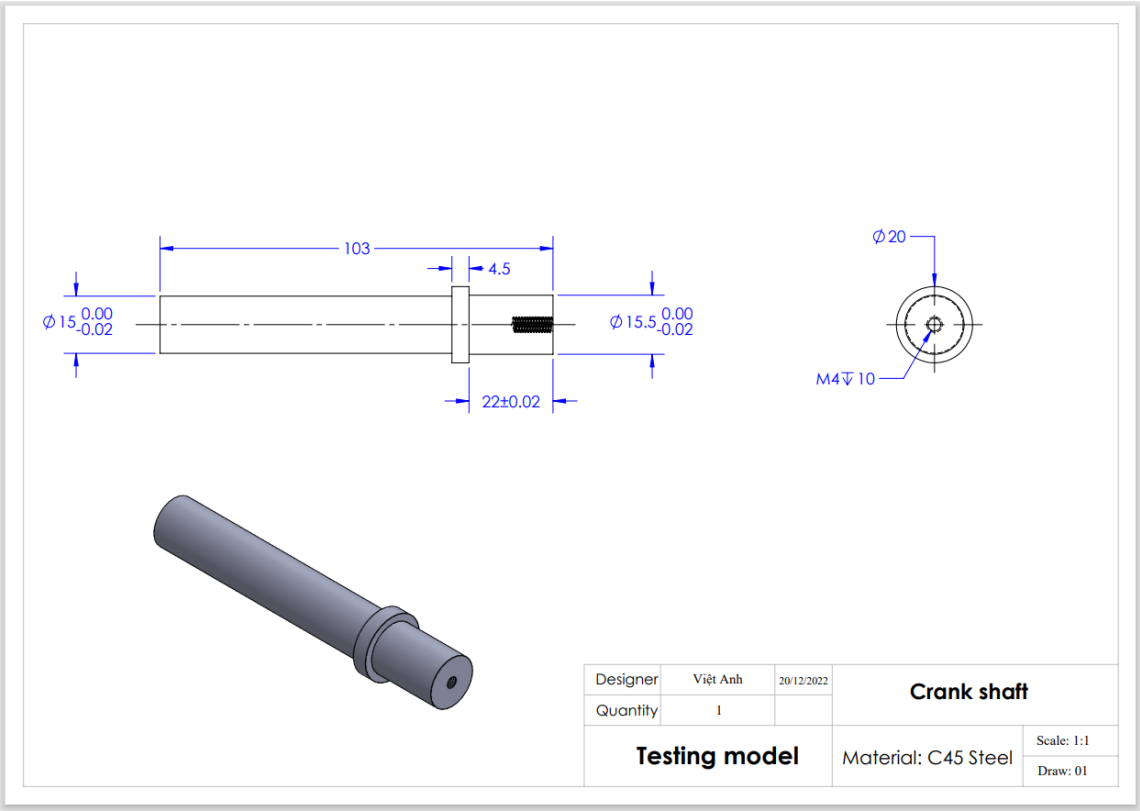

Figure 5.40: 2D drawing of the crank shaft

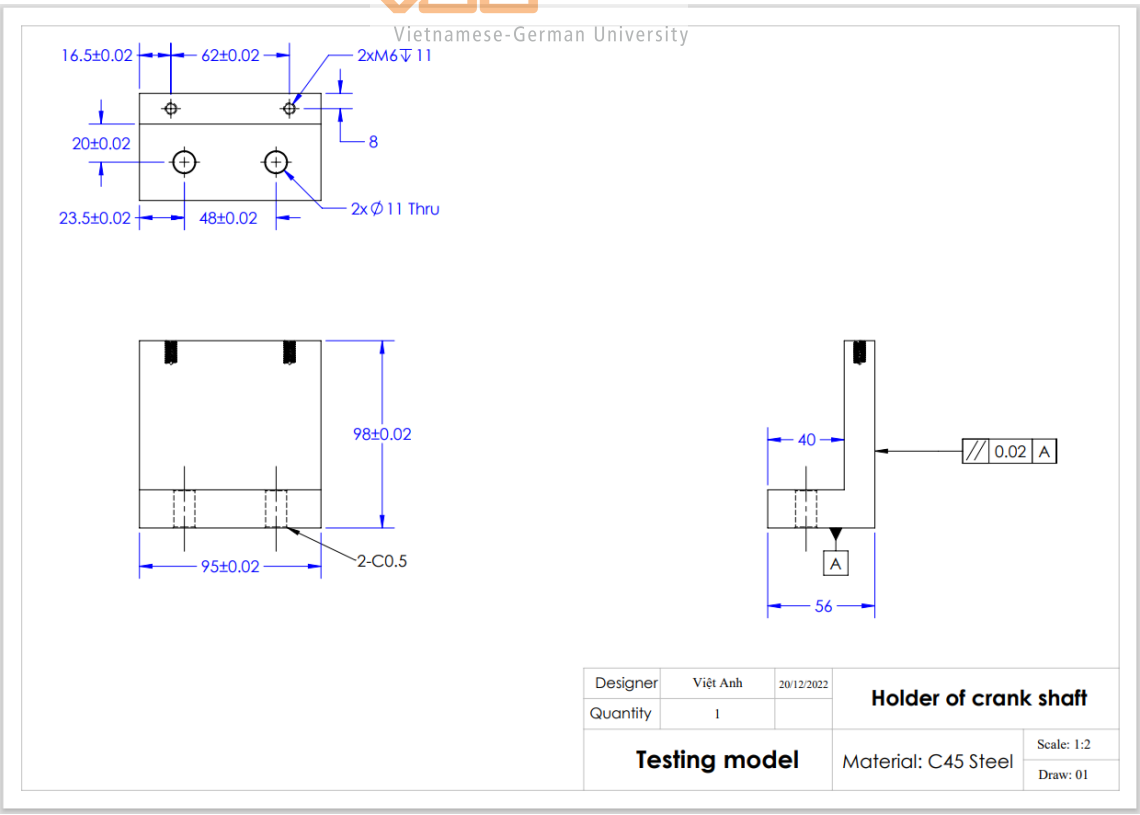

Figure 5.41: 2D drawing of the holder of crank shaft

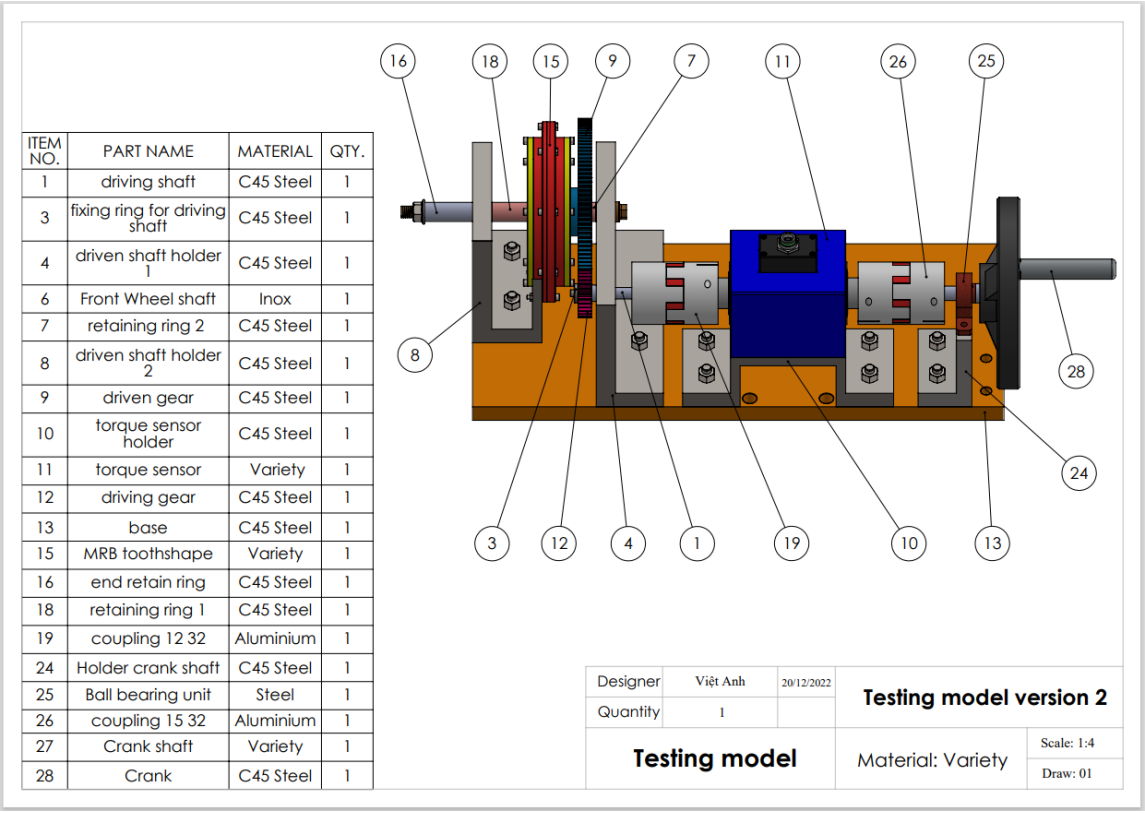

ITEM NO.	PART NAME	MATERIAL	QTY.
1	driving shaft	C45 Steel	1
3	fixing ring for driving shaft	C45 Steel	1
4	driven shaft holder 1	C45 Steel	1
6	Front Wheel shaft	Inox	1
7	retaining ring 2	C45 Steel	1
8	driven shaft holder 2	C45 Steel	1
9	driven gear	C45 Steel	1
10	torque sensor holder	C45 Steel	1
11	torque sensor	Variety	1
12	driving gear	C45 Steel	1
13	base	C45 Steel	1
15	MRB toothshape	Variety	1
16	end retain ring	C45 Steel	1
18	retaining ring 1	C45 Steel	1
19	coupling 12 32	Aluminium	1
24	Holder crank shaft	C45 Steel	1
25	Ball bearing unit	Steel	1
26	coupling 15 32	Aluminium	1
27	Crank shaft	Variety	1
28	Crank	C45 Steel	1

Figure 5.42: Assembly of testing model version 2

Chapter 6: Fabrication of the MRB

6.1. Manufacturing process

All parts of the tooth-shaped MR brake are fabricated by CNC turning and CNC milling machine in order to achieve the desire tolerance and the coils are wrapped by copper wire. Bearings and slip seals are also installed

Figure 6.1: All parts of the tooth-shaped MR brake

6.1.1. MRB shaft and tooth-shaped disc

After manufacturing, the sandpaper is used to remove all the chips which remain on the products. This step will help the assembly process be accuracy and easier. The tooth-shaped disc and MRB are then connected to each other.

Figure 6.2: Assembly of tooth-shaped disc and MRB shaft

Two bearings are also attached on the MRB shaft and the whole mechanism is put on the front wheel shaft of the electric scooter. Thus, the result is they are perfectly fitting.

Figure 6.3: Mechanism of MRB shaft and tooth-shaped disc attached on front wheel shaft of electric scooter

6.1.2. Inner housing, outer housing and coils

In order to make the coils, a plastic mold is created by 3D printing machine. This mold not only help the coil have a desire number of turn, but also guarantee for the coil to be able to put in the inner housing. The inner diameter of the mold is lower limit while the outer diameter is the upper limit of the coil.

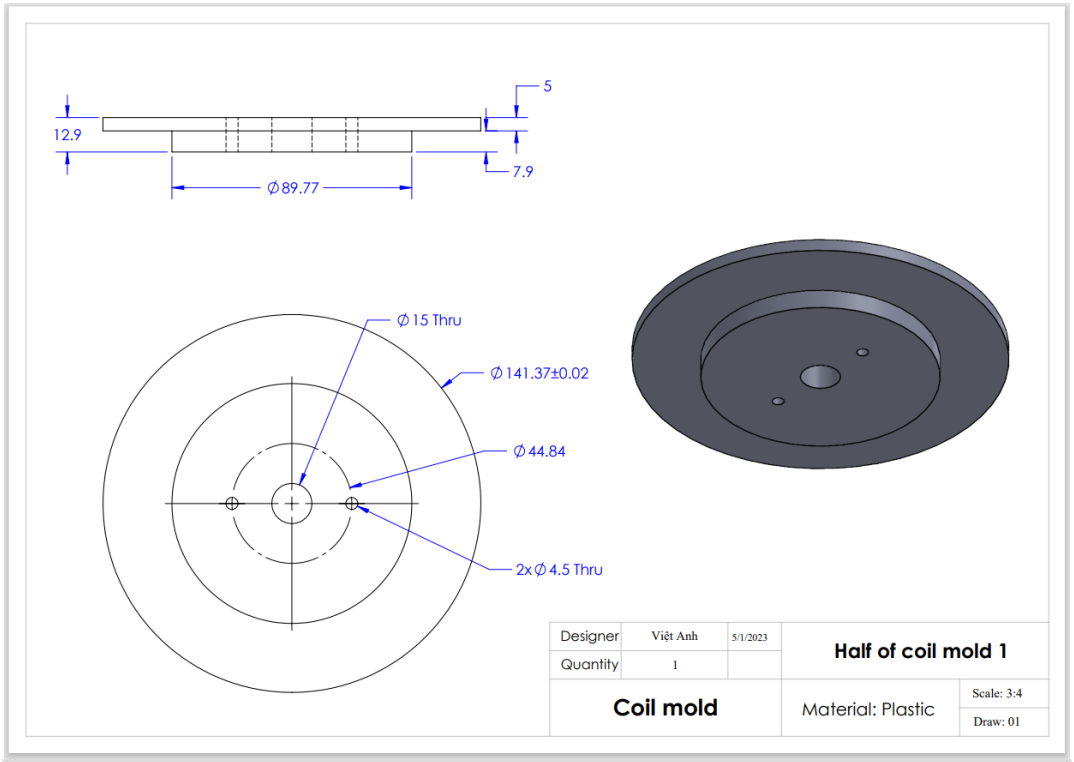

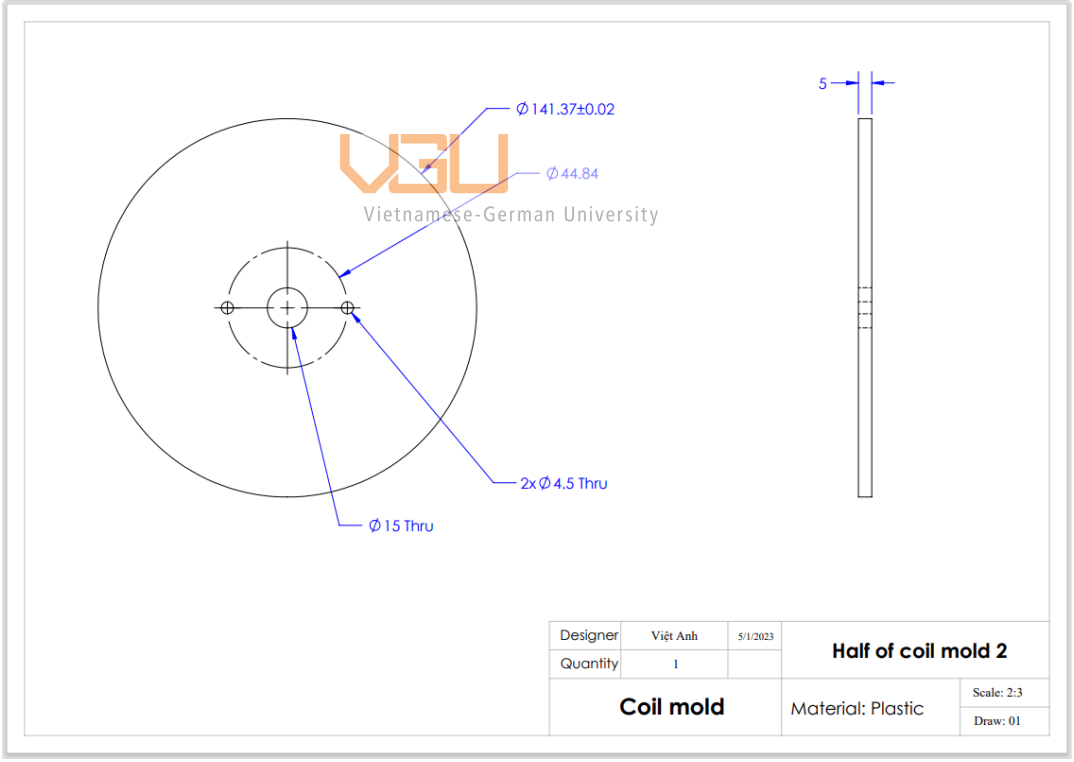

Figure 6.4: 2D drawing of coil mold

There is one note when it comes to wrapping copper wire which is the inner diameter of coil will shrink around 1 – 2 mm when it is taken off the mold. This makes the coil could not be installed in the inner housing of MRB. Thus, a thin tape layer is then made to cover the inner diameter of the coil mold before wrapping copper wire.

Figure 6.5: Wrapping copper wire on the coil mold

After wrapping, the coil only achieves 700/806 turns (87%), this is because of the tape layer's thickness and the inefficient method of wrapping copper wire. However, due to the limit of time for this project, this coil is kept for the MRB prototype and the method of wire wrapping will be improved in the future to reach the necessary number of turns. The coil is then covered by a thin layer of rubber - electrical tape. This ensures the electrical current do not transfer through the housing of the MR brake.

Figure 6.6: Coil of the MRB

The outer housing then seals the coil inside the inner housing. The voltmeter is used to check if there is any electric that leaks out when the electric source is supplied.

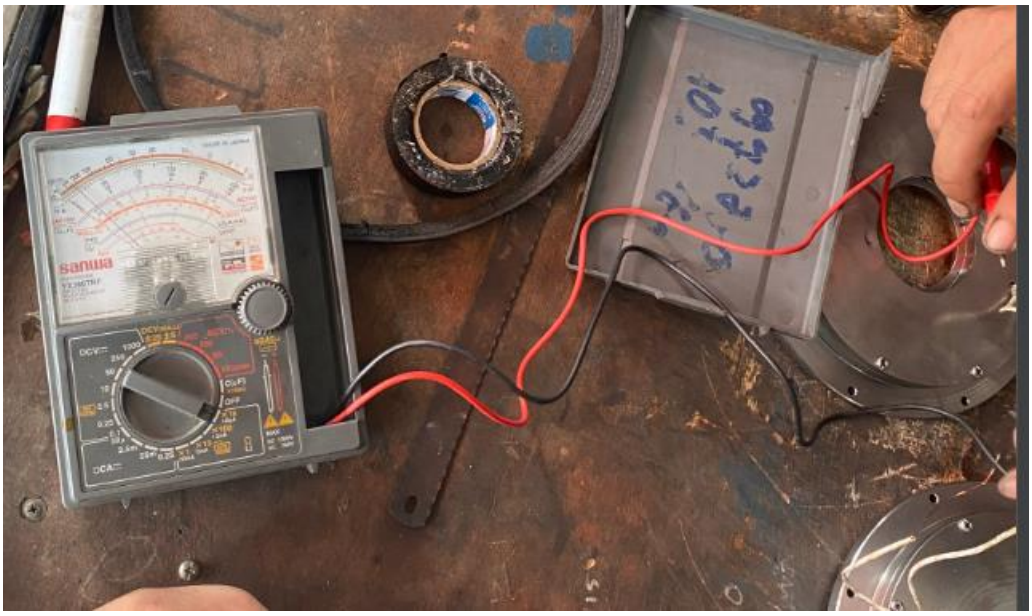

Figure 6.7: Testing by voltmeter

As a figure show, there is just little electrical current in the housing when the electric is applied which can be accepted. The next step is installing O-ring in the housing.

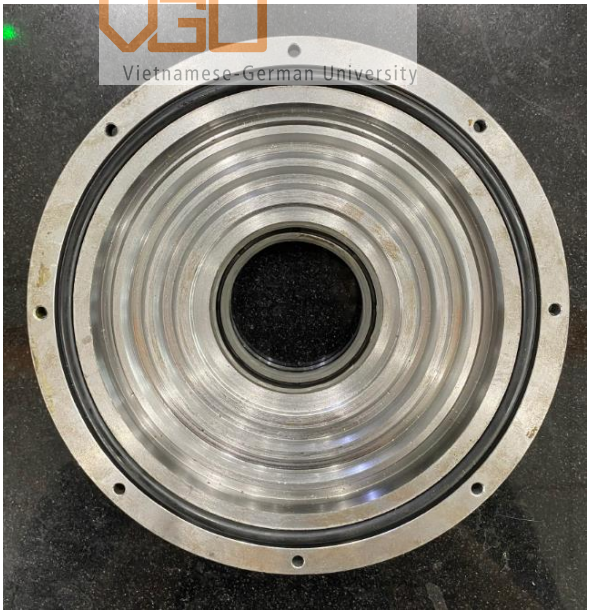

Figure 6.8: O-ring installing

6.1.3. Final prototype

Finally, all parts of the tooth-shaped MRB are assembled together.

Figure 6.9: Prototype of tooth-shaped magneto-rheological brake

The mass of the prototype is 6.6 Kg which is little larger than theorical result (6.16 Kg) in table 3.12. This is due to the additional mass of bearings, seals, screws and bolts.

6.2. Discussion

When it comes to comparison with traditional brake in electric scooter, the mass of designed MRB is much larger than traditional disc brake's mass (1.1 Kg). Despite this disadvantage, the MR brake supplies the smart control which can be applied later in the future. Furthermore, the mass of MRB could be reduced by some innovations for the housings.

Since the number of turns for the copper coil is a lot, 806 turns, wrapping copper wire is a very challenge work. For that reason, 0.5 mm copper wire could be replaced by 1 mm diameter copper wire which will reduce the number of turns for the coil. The smaller number of turns, the more neglection of human factor.

For inner housing, the tolerance at the place where attached the slip seal needs to be re-considered since the connection between slip seal and inner housing is too tight when assembling. This will lead to difficulty in the rotation of the MRB shaft and disc of the tooth-shaped MRB.

Chapter 7: Conclusion and future work

7.1. Conclusion

The thesis project has completed the optimal design, application and manufacturing of the magneto – rheological brake for the chosen electric scooter model. Furthermore, the experiment for testing the perform of MRB is also designed. However, due to the limitation of time, only the prototype of the MRB for electric scooter is produced. The prototype fits perfectly with the front wheel shaft of the electric scooter which proves it could be attached on it. On the other hand, there are some problems of the MRB's prototype that need to be optimized before further testing. Firstly, the mass of the MRB is large when it comes to comparison with traditional brakes. This is because of material of the brake and the limitation of the space on electric scooter. If the thickness of the MRB could be increased, the radius of the brake would be decreased which lead to reducing in the mass of the brake since the radius term is squared in the formular for mass calculating. Secondly, there are lots of gaps between the wire copper and the thickness of electric tape is large which are a result of ineffective procedure in wrapping. This makes the number of turns of the coil be less than the design. Thirdly, the tolerance at the slip seal connection needs to be re – considered for the ability of rotation of MRB shaft and disc. Finally, the housings and discs are being rusty over time so the method for maintenance is necessary.

Thus, there are some innovations that can be conducted in the manufacturing process of the MRB in order to achieve the perfect prototype of the tooth-shaped MR brake:

- Re – wrapping the copper wires for the coil slowly in order to arrange the wire effectively
- Using the bigger copper wire to reduce the number of turns for the coils.
- Using specialized oil to prevent the MRB from rusting
- Remove some unnecessary material of the MRB in order to reduce the mass
- Re – calculated the tolerance at the place installing slip seal of the inner housing.

7.2. Future work

The experiment for testing the performance of the tooth-shaped MR brake will be executed as its conceptual design in this thesis after adjusting the prototype. In case a required braking torque is achieved after testing, the MRB will be attached on the electric scooter for further study before completely application.

Bibliography

[1] Fortune Business Insights. 2022. Electric Scooter Market. Available from: https://www.fortunebusinessinsights.com/electric-scooter-market-102056

[2] E.J. Park, D.Stoikov. Luz, A. Sulerman. 2008. Multidisciplinary design optimization of an automotive magnetorheological brake design. *Mechatronics, 16 (2006), pp. 405-416 Elsevier*

[3] K. Karakoc, EJ. Park, A. Sulerman. 2008. Design consideration for an automotive magnetorheological brake. *Mechatronics (2008) Elsevier.*

[4] Quoc-Hung Nguyen & Seung-Bok Choi. 2012. Optimal Design Methodology of Magnetorheological Fluid Based Mechanisms. *Smart Actuation and Sensing Systems*.

[5] Zubieta M, Eceolaza S, Elejabarrieta M J and Bou-Ali M M. 2009. Magnetorheological fluids: characterization and modeling of magnetization. *Smart Mater. Struct. 18*

[6] thegioixechaydien. 2019. Available from: https://thegioixechaydien.com.vn/xe-may-dien-hkbike-xmen-plus2.html

[7] Q H Nguyen & S B Choi. 2012. Optimal design of a novel hybrid MR brake for motorcycles considering axial and radial magnetic flux.

[8] Van Bien Nguyen, Le Dai Hiep, Quoc Hung Nguyen, Quy Duyen Do, Huu Minh Hieu Do, Seung-bok Choi. 2021. Design and Experimental Evaluation a novel magneto-rheological brake with tooth shaped rotor. *Smart Materials and structures.*

[9] Nguyen Van Bien, Diep Bao Tri, Vu Van Bo, Le Dai Hiep, Do Quy Duyen, Nguyen Quoc Hung. 2021. Development of a compact size magneto-rheological brake featuring I-shaped rotor.

[11] Quoc Hung Nguyen, Van Bien Nguyen, Hiep Dai Le, Do Qui Duyen, Weihua Li, Nguyen Xuan Hung. 2021. Development of a novel magnetorheological brake with zigzag magnetic flux path. *Smart Materials and Structure.*

[12] Avaraham Shitzer. 2006. Wind-chill-equivalent-temperatures: Regarding the impact due to the variability of the environmental convective heat transfer coefficient. *International Journal of Biometeorology 50(4): 224-32.* Available from: https://www.researchgate.net/publication/7373482_Wind-chill-equivalent_temperatures_Regarding_the_impact_due_to_the_variability_of_the_environmental_convective_heat_transfer_coefficient

[13] Subash Acharya & Hemantha Kumar. 2019. Investigation of magnetorheological brake with rotor of combined magnetic and non-magnetic materials. *SN Applied Sciences*

[14] Zahurin Samad & Maher Yahya Salloom. 2011. Simulation and design optimization of magneto rheological control valve. *International Journal of Mechanical and Materials Engineering.*

[15] SKF. 2022. Available from: https://www.skf.com/group

[16] Lemming. 2022. Available from: https://lemming.shop/o-ring-155x5-nbr90-48001102?fbclid=IwAR1TLzd4ruQ58WvDOyg1HBnI3F-E6JAHt9g6lWfXRDusxhPgJbmHc9VVKuk

[17] Lorenz Messtechnik gmbh. 2022. Available from: https://www.lorenz-messtechnik.de/pdfdatbl/m/080883i_dr-3000_en.pdf

[18] Dai Hoa Phu. 2022. Available from: https://daihoaphu.vn/san-pham/khop-noi-truc-duri-djc?fbclid=IwAR22E60RNLnWIml-SnfVt0heWGLsfYOrxlxHRiXvucAiTom9Ebb59jTk7Bg

Appendix

The ANSYS APDL code for optimal design of the tooth-shaped MR Brake:

```
! FOR NON UNIFORM TEETH
/COM,  Magnetic-Nodal
/COM,  Magnetic-Edge
!*
/PREP7
!Element defination
ET,1,PLANE13
KEYOPT,1,3,1
!Material defination
MAT,1,
MPREAD,'C45steel','SI_MPL','D:\COD
E ANSYS',LIB !Use material file
!*
MAT,2,
MPREAD,'C45steel','SI_MPL','D:\COD
E ANSYS',LIB
!*
MPTEMP,,,,,,,,
MPTEMP,1,0
MPDATA,MURX,3,,1
!***********
MPTEMP,,,,,,,,
MPTEMP,1,0
MPDATA,MURX,4,,1
!******************
MAT,5,
MPREAD,'MRF132','SI_MPL','D:\CO
DE ANSYS',LIB
!MPREAD,'MRF140','SI_MPL','D:\CO
DE ANSYS',LIB
!*
RATIO_C=0.81 ! efficient ratio
RATIO_m=1.0
nmesh=6 !Basic mesh size
!Geometric dimension
pi=3.1416
dc=0.000511   ! wire diameter
res=0.01726e-6 ! resistivity
Ac=pi*dc*dc/4   !cross-section area of
coil
rrc=res/Ac
b=4e-3 !disc width
tw=1.0e-3 !Thin wall
to=4e-4 !outer housing thickness
R=55e-3 ! MRB radius
wc1=0.0040187! Coil thickness
hh=5e-3 !tooth height
d=0.8e-3 ! horizontal MRF gap size
L=45e-3 ! MRB thickness
th=L/2-(b/2+d+hh+tw+wc1)      ! side
housing thickness
do=0.9e-3 ! vertical MRF gap size
th1=tw+wc1+th   ! Housing total side
thickness
hb1=2.5e-3
L1=sqrt(hb1*hb1+hh*hh)
th2=b/2+hh+d+th1 ! Half length
hb2=0.003
angle=pi/2-ASIN(hb1/L1)
SinA=sin(angle)
CosA=cos(angle)
dd=(do*SinA-d*CosA)/SinA
```

```
d1=do*SinA ! inclined MRF gap size
hb3=hb2-2*dd ! uniform teeth
hb4=3e-3
lpk=8e-3
Rs=6e-3 ! shaft radius
Ri=R-
(to+do+hb4+5*hb1+2*hb3+2*hb2+lpk)
R1=Ri+lpk
R2=R1+hb1
R3=R2+hb2
R4=R3+hb1
R5=R4+hb3
*SET,R6,R5+hb1
*SET,R7,R6+hb2
*SET,R8,R7+hb1
*SET,R9,R8+hb3
*SET,R10,R9+hb1
*SET,Rd,R10+hb4
*SET,Ro,Rd+do
*SET,hc1,Ro-R2
*SET,nhc1,hc1/dc  ! Number of height
coil
*SET,Scoil1,hc1*wc1
nturn1=(Scoil1/Ac)*RATIO_C
Rc1=rrc*nturn1*2*3.1416*(R2+0.5*hc
1)  ! Resistance
I=2.5 ! current
*SET,JJ1,nturn1*I/Scoil1  ! Current
density
PP1=I*I*Rc1 ! Power consumption of
one coil
PP=2*(PP1)  ! Total power
!Key point create
K,1,Ri,b/2,,
k,2,ri,-b/2,,
k,3,ri,b/2+d,,
k,4,ri,-(b/2+d),,
k,5,ri,b/2+hh+d+tw,,
k,6,ri,-(b/2+hh+d+tw),,
k,7,ri,b/2+hh+d+tw+wc1,,
k,8,ri,-(b/2+hh+d+tw+wc1),,
k,9,ri,b/2+hh+d+tw+wc1+th,,
k,10,ri,-(b/2+hh+d+tw+wc1+th),,
K,21,R1+dd,b/2,,
k,22,r1+dd,-b/2,,
k,23,r1,b/2+d,,
k,24,r1,-(b/2+d),,
k,25,ri,b/2+hh+d,,
k,26,ri,-(b/2+hh+d),,
k,31,r2+dd,b/2+hh,,
k,32,r2+dd,-(b/2+hh),,
k,33,r2,b/2+hh+d,,
k,34,r2,-(b/2+hh+d),,
k,35,r2,b/2+hh+d+tw,,
k,36,r2,-(b/2+hh+d+tw),,
k,37,r2,b/2+hh+d+tw+wc1,,
k,38,r2,-(b/2+hh+d+tw+wc1),,
k,39,r2,b/2+hh+d+tw+wc1+th,,
k,40,r2,-(b/2+hh+d+tw+wc1+th),,
k,41,r3-dd,b/2+hh,,
k,42,r3-dd,-(b/2+hh),,
k,43,r3,b/2+hh+d,,
k,44,r3,-(b/2+hh+d),,
k,45,r3,b/2+hh+d+tw,,
k,46,r3,-(b/2+hh+d+tw),,
k,47,r3,b/2+hh+d+tw+wc1,,
k,48,r3,-(b/2+hh+d+tw+wc1),,
k,49,r3,b/2+hh+d+tw+wc1+th,,
```

k,50,r3,-(b/2+hh+d+tw+wc1+th),,

K,51,r4-dd,b/2,,

k,52,r4-dd,-b/2,,

k,53,r4,b/2+d,,

k,54,r4,-(b/2+d),,

K,55,r5+dd,b/2,,

k,56,r5+dd,-b/2,,

k,57,r5,b/2+d,,

k,58,r5,-(b/2+d),,

k,59,r6+dd,b/2+hh,,

k,60,r6+dd,-(b/2+hh),,

k,61,r6,b/2+hh+d,,

k,62,r6,-(b/2+hh+d),,

k,63,r6,b/2+hh+d+tw,,

k,64,r6,-(b/2+hh+d+tw),,

k,65,r6,b/2+hh+d+tw+wc1,,

k,66,r6,-(b/2+hh+d+tw+wc1),,

k,67,r6,b/2+hh+d+tw+wc1+th,,

k,68,r6,-(b/2+hh+d+tw+wc1+th),,

k,359,r7-dd,b/2+hh,,

k,360,r7-dd,-(b/2+hh),,

k,361,r7,b/2+hh+d,,

k,362,r7,-(b/2+hh+d),,

k,363,r7,b/2+hh+d+tw,,

k,364,r7,-(b/2+hh+d+tw),,

k,365,r7,b/2+hh+d+tw+wc1,,

k,366,r7,-(b/2+hh+d+tw+wc1),,

k,367,r7,b/2+hh+d+tw+wc1+th,,

k,368,r7,-(b/2+hh+d+tw+wc1+th),,

K,455,r8-dd,b/2,,

k,456,r8-dd,-b/2,,

k,457,r8,b/2+d,,

k,458,r8,-(b/2+d),,

K,555,r9+dd,b/2,,

k,556,r9+dd,-b/2,,

k,557,r9,b/2+d,,

k,558,r9,-(b/2+d),,

k,659,r10+dd,b/2+hh,,

k,660,r10+dd,-(b/2+hh),,

k,661,r10,b/2+hh+d,,

k,662,r10,-(b/2+hh+d),,

k,663,r10,b/2+hh+d+tw,,

k,664,r10,-(b/2+hh+d+tw),,

k,665,r10,b/2+hh+d+tw+wc1,,

k,666,r10,-(b/2+hh+d+tw+wc1),,

k,667,r10,b/2+hh+d+tw+wc1+th,,

k,668,r10,-(b/2+hh+d+tw+wc1+th),,

k,79,rd,b/2+hh,,

k,80,rd,-(b/2+hh),,

k,101,rd,b/2,,

k,102,rd,-(b/2),,

k,81,ro,b/2,,

k,82,ro,-(b/2),,

k,83,ro,b/2+hh+d,,

k,84,ro,-(b/2+hh+d),,

k,85,ro,b/2+hh+d+tw,,

k,86,ro,-(b/2+hh+d+tw),,

k,87,ro,b/2+hh+d+tw+wc1,,

k,88,ro,-(b/2+hh+d+tw+wc1),,

k,89,ro,b/2+hh+d+th+wc1+tw,,

k,90,ro,-(b/2+hh+d+th+wc1+tw),,

k,91,r,b/2,,

k,92,r,-(b/2),,

k,93,r,b/2+hh+d,,

k,94,r,-(b/2+hh+d),,

k,95,r,b/2+hh+d+tw,,

k,96,r,-(b/2+hh+d+tw),,

k,97,r,b/2+hh+d+tw+wc1,,

```
k,98,r,-(b/2+hh+d+tw+wc1),,
k,99,r,b/2+hh+d+th+tw+wc1,,
k,100,r,-(b/2+hh+d+th+tw+wc1),,
!*
!Line create
LSTR,    10,    40
LSTR,    40,    50
LSTR,    50,    68
LSTR,    68,   368
LSTR,   368,   668
LSTR,   668,    90
LSTR,    90,   100
LSTR,   100,    98
LSTR,    98,    88
LSTR,    88,    90
LSTR,    88,   666
LSTR,   666,   668
LSTR,   666,   366
LSTR,   366,   368
LSTR,   366,    66
LSTR,    66,    68
LSTR,    66,    48
LSTR,    48,    50
LSTR,    48,    38
LSTR,    38,    40
LSTR,    38,     8
LSTR,     8,    10
LSTR,     8,     6
LSTR,     6,    36
LSTR,    36,    38
LSTR,    36,    46
LSTR,    46,    48
LSTR,    46,    64
LSTR,    64,    66
LSTR,    64,   364
LSTR,   364,   366
LSTR,   364,   664
LSTR,   664,   666
LSTR,   664,    86
LSTR,    86,    88
LSTR,    86,    96
LSTR,    96,    98
LSTR,    96,    94
LSTR,    94,    84
LSTR,    84,    86
LSTR,    84,   662
LSTR,   662,   664
LSTR,   662,   362
LSTR,   362,   364
LSTR,   362,    62
LSTR,    62,    64
LSTR,    62,    44
LSTR,    44,    46
LSTR,    44,    34
LSTR,    34,    36
LSTR,    34,    26
LSTR,    26,     6
LSTR,    26,     4
LSTR,     4,    24
LSTR,    24,    34
LSTR,     9,    39
LSTR,     9,     7
LSTR,     7,    37
LSTR,    37,    39
LSTR,    39,    49
LSTR,    49,    47
LSTR,    47,    37
LSTR,    47,    65
```

LSTR, 65, 67
LSTR, 67, 49
LSTR, 67, 367
LSTR, 367, 365
LSTR, 365, 65
LSTR, 365, 665
LSTR, 665, 667
LSTR, 667, 367
LSTR, 667, 89
LSTR, 89, 87
LSTR, 87, 665
LSTR, 87, 97
LSTR, 97, 99
LSTR, 99, 89
LSTR, 7, 5
LSTR, 5, 35
LSTR, 35, 37
LSTR, 35, 45
LSTR, 45, 47
LSTR, 45, 63
LSTR, 63, 65
LSTR, 63, 363
LSTR, 363, 365
LSTR, 363, 663
LSTR, 663, 665
LSTR, 663, 85
LSTR, 85, 87
LSTR, 85, 95
LSTR, 95, 97
LSTR, 5, 25
LSTR, 25, 33
LSTR, 33, 35
LSTR, 33, 43
LSTR, 43, 45
LSTR, 43, 61
LSTR, 61, 63
LSTR, 61, 361
LSTR, 361, 363
LSTR, 361, 661
LSTR, 661, 663
LSTR, 661, 83
LSTR, 83, 85
LSTR, 83, 93
LSTR, 93, 95
LSTR, 2, 1
LSTR, 1, 21
LSTR, 21, 31
LSTR, 31, 41
LSTR, 41, 51
LSTR, 51, 55
LSTR, 55, 59
LSTR, 59, 359
LSTR, 359, 455
LSTR, 455, 555
LSTR, 555, 659
LSTR, 659, 79
LSTR, 79, 101
LSTR, 101, 102
LSTR, 102, 80
LSTR, 80, 660
LSTR, 660, 556
LSTR, 556, 456
LSTR, 456, 360
LSTR, 360, 60
LSTR, 60, 56
LSTR, 56, 52
LSTR, 52, 42
LSTR, 42, 32

```
LSTR,    32,    22
LSTR,    22,    2
LSTR,    2,     4
LSTR,    22,    24
LSTR,    22,    21
LSTR,    21,    51
LSTR,    51,    52
LSTR,    52,    22
LSTR,    32,    34
LSTR,    44,    42
LSTR,    54,    52
LSTR,    54,    44
LSTR,    54,    58
LSTR,    58,    56
LSTR,    58,    62
LSTR,    62,    60
LSTR,    362,   360
LSTR,    56,    456
LSTR,    56,    55
LSTR,    456,   455
LSTR,    455,   55
LSTR,    456,   458
LSTR,    458,   362
LSTR,    458,   558
LSTR,    558,   556
LSTR,    558,   662
LSTR,    662,   660
LSTR,    80,    84
LSTR,    84,    82
LSTR,    82,    102
LSTR,    82,    81
LSTR,    81,    101
LSTR,    81,    83
LSTR,    83,    79
LSTR,    659,   661
LSTR,    661,   557
LSTR,    557,   555
LSTR,    557,   457
LSTR,    457,   455
LSTR,    457,   361
LSTR,    361,   359
LSTR,    59,    61
LSTR,    61,    57
LSTR,    57,    55
LSTR,    57,    53
LSTR,    53,    51
LSTR,    53,    43
LSTR,    41,    43
LSTR,    31,    33
LSTR,    33,    23
LSTR,    21,    23
LSTR,    23,    3
LSTR,    3,     1
LSTR,    3,     25
LSTR,    94,    92
LSTR,    92,    82
LSTR,    92,    91
LSTR,    91,    81
LSTR,    91,    93
LSTR,    555,   556
LSTR,    556,   102
LSTR,    555,   101
!Area create
FLST,2,4,4
FITEM,2,22
FITEM,2,21
FITEM,2,20
FITEM,2,1
```

AL,P51X
FLST,2,4,4
FITEM,2,20
FITEM,2,19
FITEM,2,18
FITEM,2,2
AL,P51X
FLST,2,4,4
FITEM,2,18
FITEM,2,17
FITEM,2,16
FITEM,2,3
AL,P51X
FLST,2,4,4
FITEM,2,16
FITEM,2,15
FITEM,2,14
FITEM,2,4
AL,P51X
FLST,2,4,4
FITEM,2,14
FITEM,2,13
FITEM,2,12
FITEM,2,5
AL,P51X
FLST,2,4,4
FITEM,2,12
FITEM,2,11
FITEM,2,6
FITEM,2,10
AL,P51X
FLST,2,4,4
FITEM,2,10
FITEM,2,9
FITEM,2,8
FITEM,2,7
AL,P51X
FLST,2,4,4
FITEM,2,23
FITEM,2,24
FITEM,2,25
FITEM,2,21
AL,P51X
FLST,2,4,4
FITEM,2,25
FITEM,2,26
FITEM,2,27
FITEM,2,19
AL,P51X
FLST,2,4,4
FITEM,2,27
FITEM,2,28
FITEM,2,29
FITEM,2,17
AL,P51X
FLST,2,4,4
FITEM,2,29
FITEM,2,30
FITEM,2,31
FITEM,2,15
AL,P51X
FLST,2,4,4
FITEM,2,31
FITEM,2,32
FITEM,2,33
FITEM,2,13
AL,P51X
FLST,2,4,4

FITEM,2,33
FITEM,2,34
FITEM,2,35
FITEM,2,11
AL,P51X
FLST,2,4,4
FITEM,2,35
FITEM,2,36
FITEM,2,37
FITEM,2,9
AL,P51X
FLST,2,4,4
FITEM,2,52
FITEM,2,51
FITEM,2,50
FITEM,2,24
AL,P51X
FLST,2,4,4
FITEM,2,50
FITEM,2,49
FITEM,2,48
FITEM,2,26
AL,P51X
FLST,2,4,4
FITEM,2,48
FITEM,2,47
FITEM,2,46
FITEM,2,28
AL,P51X
FLST,2,4,4
FITEM,2,46
FITEM,2,45
FITEM,2,44
FITEM,2,30
AL,P51X
FLST,2,4,4
FITEM,2,44
FITEM,2,43
FITEM,2,42
FITEM,2,32
AL,P51X
FLST,2,4,4
FITEM,2,42
FITEM,2,41
FITEM,2,40
FITEM,2,34
AL,P51X
FLST,2,4,4
FITEM,2,40
FITEM,2,39
FITEM,2,38
FITEM,2,36
AL,P51X
FLST,2,4,4
FITEM,2,53
FITEM,2,54
FITEM,2,55
FITEM,2,51
AL,P51X
FLST,2,4,4
FITEM,2,55
FITEM,2,132
FITEM,2,135
FITEM,2,140
AL,P51X
FLST,2,4,4
FITEM,2,133
FITEM,2,135

FITEM,2,54
FITEM,2,134
AL,P51X
FLST,2,4,4
FITEM,2,139
FITEM,2,130
FITEM,2,131
FITEM,2,132
AL,P51X
FLST,2,4,4
FITEM,2,131
FITEM,2,141
FITEM,2,49
FITEM,2,140
AL,P51X
FLST,2,4,4
FITEM,2,130
FITEM,2,142
FITEM,2,143
FITEM,2,141
AL,P51X
FLST,2,4,4
FITEM,2,129
FITEM,2,145
FITEM,2,144
FITEM,2,142
AL,P51X
FLST,2,4,4
FITEM,2,146
FITEM,2,144
FITEM,2,143
FITEM,2,47
AL,P51X
FLST,2,4,4
FITEM,2,128
FITEM,2,145
FITEM,2,146
FITEM,2,147
AL,P51X
FLST,2,4,4
FITEM,2,149
FITEM,2,126
FITEM,2,127
FITEM,2,128
AL,P51X
FLST,2,4,4
FITEM,2,147
FITEM,2,127
FITEM,2,148
FITEM,2,45
AL,P51X
FLST,2,4,4
FITEM,2,126
FITEM,2,153
FITEM,2,154
FITEM,2,148
AL,P51X
FLST,2,4,4
FITEM,2,125
FITEM,2,156
FITEM,2,155
FITEM,2,153
AL,P51X
FLST,2,4,4
FITEM,2,124
FITEM,2,158
FITEM,2,157
FITEM,2,156

AL,P51X
FLST,2,4,4
FITEM,2,154
FITEM,2,155
FITEM,2,157
FITEM,2,43
AL,P51X
FLST,2,4,4
FITEM,2,192
FITEM,2,122
FITEM,2,123
FITEM,2,124
AL,P51X
FLST,2,4,4
FITEM,2,123
FITEM,2,159
FITEM,2,41
FITEM,2,158
AL,P51X
FLST,2,4,4
FITEM,2,122
FITEM,2,161
FITEM,2,160
FITEM,2,159
AL,P51X
FLST,2,4,4
FITEM,2,160
FITEM,2,187
FITEM,2,186
FITEM,2,39
AL,P51X
FLST,2,4,4
FITEM,2,162
FITEM,2,189
FITEM,2,187
FITEM,2,188
AL,P51X
FLST,2,4,4
FITEM,2,121
FITEM,2,163
FITEM,2,162
FITEM,2,161
AL,P51X
FLST,2,4,4
FITEM,2,192
FITEM,2,121
FITEM,2,193
FITEM,2,191
AL,P51X
FLST,2,4,4
FITEM,2,117
FITEM,2,191
FITEM,2,125
FITEM,2,151
AL,P51X
FLST,2,4,4
FITEM,2,152
FITEM,2,151
FITEM,2,149
FITEM,2,150
AL,P51X
FLST,2,4,4
FITEM,2,113
FITEM,2,150
FITEM,2,129
FITEM,2,138
AL,P51X
FLST,2,4,4

FITEM,2,137
FITEM,2,138
FITEM,2,139
FITEM,2,136
AL,P51X
FLST,2,4,4
FITEM,2,109
FITEM,2,136
FITEM,2,133
FITEM,2,108
AL,P51X
FLST,2,4,4
FITEM,2,184
FITEM,2,183
FITEM,2,182
FITEM,2,109
AL,P51X
FLST,2,4,4
FITEM,2,181
FITEM,2,180
FITEM,2,110
FITEM,2,182
AL,P51X
FLST,2,4,4
FITEM,2,111
FITEM,2,179
FITEM,2,96
FITEM,2,180
AL,P51X
FLST,2,4,4
FITEM,2,112
FITEM,2,178
FITEM,2,179
FITEM,2,177
AL,P51X
FLST,2,4,4
FITEM,2,177
FITEM,2,176
FITEM,2,175
FITEM,2,113
AL,P51X
FLST,2,4,4
FITEM,2,174
FITEM,2,173
FITEM,2,114
FITEM,2,175
AL,P51X
FLST,2,4,4
FITEM,2,100
FITEM,2,172
FITEM,2,115
FITEM,2,173
AL,P51X
FLST,2,4,4
FITEM,2,171
FITEM,2,172
FITEM,2,116
FITEM,2,170
AL,P51X
FLST,2,4,4
FITEM,2,169
FITEM,2,168
FITEM,2,117
FITEM,2,170
AL,P51X
FLST,2,4,4
FITEM,2,118
FITEM,2,166

FITEM,2,167
FITEM,2,168
AL,P51X
FLST,2,4,4
FITEM,2,104
FITEM,2,165
FITEM,2,119
FITEM,2,166
AL,P51X
FLST,2,4,4
FITEM,2,120
FITEM,2,165
FITEM,2,164
FITEM,2,163
AL,P51X
FLST,2,4,4
FITEM,2,118
FITEM,2,119
FITEM,2,120
FITEM,2,193
AL,P51X
FLST,2,4,4
FITEM,2,152
FITEM,2,114
FITEM,2,115
FITEM,2,116
AL,P51X
FLST,2,4,4
FITEM,2,110
FITEM,2,111
FITEM,2,112
FITEM,2,137
AL,P51X
FLST,2,4,4

FITEM,2,94
FITEM,2,181
FITEM,2,183
FITEM,2,185
AL,P51X
FLST,2,4,4
FITEM,2,98
FITEM,2,174
FITEM,2,176
FITEM,2,178
AL,P51X
FLST,2,4,4
FITEM,2,102
FITEM,2,167
FITEM,2,171
FITEM,2,169
AL,P51X
FLST,2,4,4
FITEM,2,106
FITEM,2,190
FITEM,2,189
FITEM,2,164
AL,P51X
FLST,2,4,4
FITEM,2,93
FITEM,2,79
FITEM,2,95
FITEM,2,94
AL,P51X
FLST,2,4,4
FITEM,2,81
FITEM,2,97
FITEM,2,96
FITEM,2,95

AL,P51X
FLST,2,4,4
FITEM,2,83
FITEM,2,99
FITEM,2,98
FITEM,2,97
AL,P51X
FLST,2,4,4
FITEM,2,85
FITEM,2,101
FITEM,2,100
FITEM,2,99
AL,P51X
FLST,2,4,4
FITEM,2,87
FITEM,2,103
FITEM,2,102
FITEM,2,101
AL,P51X
FLST,2,4,4
FITEM,2,89
FITEM,2,105
FITEM,2,104
FITEM,2,103
AL,P51X
FLST,2,4,4
FITEM,2,91
FITEM,2,107
FITEM,2,106
FITEM,2,105
AL,P51X
FLST,2,4,4
FITEM,2,75
FITEM,2,92
FITEM,2,91
FITEM,2,90
AL,P51X
FLST,2,4,4
FITEM,2,74
FITEM,2,90
FITEM,2,89
FITEM,2,88
AL,P51X
FLST,2,4,4
FITEM,2,69
FITEM,2,88
FITEM,2,87
FITEM,2,86
AL,P51X
FLST,2,4,4
FITEM,2,68
FITEM,2,86
FITEM,2,85
FITEM,2,84
AL,P51X
FLST,2,4,4
FITEM,2,63
FITEM,2,84
FITEM,2,83
FITEM,2,82
AL,P51X
FLST,2,4,4
FITEM,2,80
FITEM,2,82
FITEM,2,62
FITEM,2,81
AL,P51X
FLST,2,4,4

```
FITEM,2,58
FITEM,2,80
FITEM,2,79
FITEM,2,78
AL,P51X
FLST,2,4,4
FITEM,2,56
FITEM,2,59
FITEM,2,58
FITEM,2,57
AL,P51X
FLST,2,4,4
FITEM,2,60
FITEM,2,61
FITEM,2,62
FITEM,2,59
AL,P51X
FLST,2,4,4
FITEM,2,65
FITEM,2,64
FITEM,2,63
FITEM,2,61
AL,P51X
FLST,2,4,4
FITEM,2,66
FITEM,2,67
FITEM,2,68
FITEM,2,64
AL,P51X
FLST,2,4,4
FITEM,2,70
FITEM,2,71
FITEM,2,67
FITEM,2,69
AL,P51X
FLST,2,4,4
FITEM,2,73
FITEM,2,72
FITEM,2,74
FITEM,2,70
AL,P51X
FLST,2,4,4
FITEM,2,77
FITEM,2,76
FITEM,2,75
FITEM,2,73
AL,P51X

! Apply material and meshing
FLST,5,12,5,ORDE,7
FITEM,5,25
FITEM,5,31
FITEM,5,37
FITEM,5,43
FITEM,5,-48
FITEM,5,61
FITEM,5,-63
CM,_Y,AREA
ASEL, , , ,P51X
CM,_Y1,AREA
CMSEL,S,_Y
!*
CMSEL,S,_Y1
AATT,      1, ,   1,      0,
CMSEL,S,_Y
CMDELE,_Y
CMDELE,_Y1
!*
```

```
FLST,5,41,5,ORDE,12
FITEM,5,1
FITEM,5,-8
FITEM,5,14
FITEM,5,-22
FITEM,5,29
FITEM,5,36
FITEM,5,40
FITEM,5,-41
FITEM,5,64
FITEM,5,-75
FITEM,5,81
FITEM,5,-88
CM,_Y,AREA
ASEL, , , ,P51X
CM,_Y1,AREA
CMSEL,S,_Y
!*
CMSEL,S,_Y1
AATT,      2, ,   1,      0,
CMSEL,S,_Y
CMDELE,_Y
CMDELE,_Y1
!*
FLST,5,10,5,ORDE,4
FITEM,5,9
FITEM,5,-13
FITEM,5,76
FITEM,5,-80
CM,_Y,AREA
ASEL, , , ,P51X
CM,_Y1,AREA
CMSEL,S,_Y
!*
CMSEL,S,_Y1
AATT,      3, ,   1,      0,
CMSEL,S,_Y
CMDELE,_Y
CMDELE,_Y1
!*
FLST,5,25,5,ORDE,12
FITEM,5,23
FITEM,5,-24
FITEM,5,26
FITEM,5,-28
FITEM,5,30
FITEM,5,32
FITEM,5,-35
FITEM,5,38
FITEM,5,-39
FITEM,5,42
FITEM,5,49
FITEM,5,-60
CM,_Y,AREA
ASEL, , , ,P51X
CM,_Y1,AREA
CMSEL,S,_Y
!*
CMSEL,S,_Y1
AATT,      5, ,   1,      0,
CMSEL,S,_Y
CMDELE,_Y
CMDELE,_Y1
!*
FLST,5,193,4,ORDE,2
FITEM,5,1
FITEM,5,-193
CM,_Y,LINE
```

```
LSEL, , , ,P51X
CM,_Y1,LINE
CMSEL,,_Y
!*
LESIZE,_Y1, , ,8, , , , ,1
!*
FLST,5,26,4,ORDE,25
FITEM,5,134
FITEM,5,-135
FITEM,5,140
FITEM,5,-142
FITEM,5,145
FITEM,5,147
FITEM,5,-148
FITEM,5,153
FITEM,5,156
FITEM,5,158
FITEM,5,-159
FITEM,5,161
FITEM,5,163
FITEM,5,165
FITEM,5,-166
FITEM,5,168
FITEM,5,170
FITEM,5,172
FITEM,5,-173
FITEM,5,175
FITEM,5,177
FITEM,5,179
FITEM,5,-180
FITEM,5,182
FITEM,5,184
CM,_Y,LINE
LSEL, , , ,P51X
CM,_Y1,LINE
CMSEL,,_Y
!*
LESIZE,_Y1, , ,6, , , , ,1
!*
FLST,5,16,4,ORDE,16
FITEM,5,38
FITEM,5,40
FITEM,5,42
FITEM,5,44
FITEM,5,46
FITEM,5,48
FITEM,5,50
FITEM,5,52
FITEM,5,93
FITEM,5,95
FITEM,5,97
FITEM,5,99
FITEM,5,101
FITEM,5,103
FITEM,5,105
FITEM,5,107
CM,_Y,LINE
LSEL, , , ,P51X
CM,_Y1,LINE
CMSEL,,_Y
!*
LESIZE,_Y1, , ,4, , , , ,1

MSHAPE,0,2D
MSHKEY,0
!*
!*
AMESH,all
```

```
/UI,MESH,OFF
FINISH
/SOL
FLST,2,34,4,ORDE,26
FITEM,2,1
FITEM,2,-8
FITEM,2,22
FITEM,2,-23
FITEM,2,37
FITEM,2,-38
FITEM,2,52
FITEM,2,-53
FITEM,2,56
FITEM,2,-57
FITEM,2,60
FITEM,2,65
FITEM,2,-66
FITEM,2,71
FITEM,2,-72
FITEM,2,76
FITEM,2,-78
FITEM,2,92
FITEM,2,-93
FITEM,2,107
FITEM,2,-108
FITEM,2,134
FITEM,2,184
FITEM,2,-186
FITEM,2,188
FITEM,2,190
DL,P51X, ,ASYM
FLST,2,5,5,ORDE,2
FITEM,2,76
FITEM,2,-80
!*
BFA,P51X,JS, , ,-jj1,0
FLST,2,5,5,ORDE,2
FITEM,2,9
FITEM,2,-13
!*
BFA,P51X,JS, , ,jj1,0
NCNV,0,0,0,0,0,
SOLVE
Finish
/POST1  ! Post processing
!*
/POST1
SET,LAST
! Defined path
PATH,p1,2,30,20,
PPATH,1,0,Ri,b/2+d/2,0,0,
PPATH,2,0,R1,b/2+d/2,0,0,
! Calculate averange magnetic flux
density
PDEF,By1,B,y,AVG
/PBC,PATH, ,0
!*
PCALC,INTG,B1in,By1,S,1,
!*
*GET,B1in,PATH, ,last,B1IN
*SET,B1av,ABS(B1IN)/lpk*RATIO_m
!
!*
PATH,p2,2,30,20,
PPATH,1,0,R1+do/2,b/2+d/2,0,0,
PPATH,2,0,R2+do/2,b/2+d/2+hh,0,0,
!*
PDEF,By,B,sum,AVG
```

```
/PBC,PATH, ,0
!*
PCALC,INTG,B2in,By,S,1,
!*
*GET,B2in,PATH, ,last,B2IN
*SET,B2av,ABS(B2IN)/L1*RATIO_m
!
!*
PATH,p3,2,30,20,
PPATH,1,0,R2,b/2+d/2+hh,0,0,
PPATH,2,0,R3,b/2+d/2+hh,0,0,
!*
PDEF,By3,B,sum,AVG
/PBC,PATH, ,0
!*
PCALC,INTG,B3in,By3,S,1,
!*
*GET,B3in,PATH, ,last,B3IN
*SET,B3av,ABS(B3IN)/(hb2)*RATIO
_m
!
PATH,p4,2,30,20,
PPATH,1,0,R3-do/2,b/2+d/2+hh,0,0,
PPATH,2,0,R4-do/2,b/2+d/2,0,0,
!*
PDEF,By4,B,sum,AVG
/PBC,PATH, ,0
!*
PCALC,INTG,B4in,By4,S,1,
!*
*GET,B4in,PATH, ,last,B4IN
*SET,B4av,ABS(B4IN)/L1*RATIO_m
!
!*
PATH,p5,2,30,20,
PPATH,1,0,R4,b/2+d/2,0,0,
PPATH,2,0,R5,b/2+d/2,0,0,
!*
PDEF,By5,B,sum,AVG
/PBC,PATH, ,0
!*
PCALC,INTG,B5in,By5,S,1,
!*
*GET,B5in,PATH, ,last,B5IN
*SET,B5av,ABS(B5IN)/(hb3)*RATIO
_m
!
PATH,p6,2,30,20,
PPATH,1,0,R5+do/2,b/2+d/2,0,0,
PPATH,2,0,R6+do/2,b/2+hh+d/2,0,0,
!*
PDEF,By6,B,sum,AVG
/PBC,PATH, ,0
!*
PCALC,INTG,B6in,By6,S,1,
!*
*GET,B6in,PATH, ,last,B6IN
*SET,B6av,ABS(B6IN)/L1*RATIO_m
!
!*
PATH,p7,2,30,20,
PPATH,1,0,R6,b/2+d/2+hh,0,0,
PPATH,2,0,R7,b/2+d/2+hh,0,0,
!*
PDEF,By7,B,sum,AVG
/PBC,PATH, ,0
!*
PCALC,INTG,B7in,By7,S,1,
```

```
!*
*GET,B7in,PATH, ,last,B7IN
*SET,B7av,ABS(B7IN)/(hb2)*RATIO
_m
!
PATH,p8,2,30,20,
PPATH,1,0,R7-do/2,b/2+d/2+hh,0,0,
PPATH,2,0,R8-do/2,b/2+d/2,0,0,
!*
PDEF,By8,B,sum,AVG
/PBC,PATH, ,0
!*
PCALC,INTG,B8in,By8,S,1,
!*
*GET,B8in,PATH, ,last,B8IN
*SET,B8av,ABS(B8IN)/L1*RATIO_m
!
!*
PATH,p9,2,30,20,
PPATH,1,0,R8,b/2+d/2,0,0,
PPATH,2,0,R9,b/2+d/2,0,0,
!*
PDEF,By9,B,sum,AVG
/PBC,PATH, ,0
!*
PCALC,INTG,B9in,By9,S,1,
!*
*GET,B9in,PATH, ,last,B9IN
*SET,B9av,ABS(B9IN)/(hb3)*RATIO
_m
!*
PATH,p10,2,30,20,
PPATH,1,0,R9+do/2,b/2+d/2,0,0,
PPATH,2,0,R10+do/2,b/2+d/2+hh,0,0,
!*
PDEF,By,B,sum,AVG
/PBC,PATH, ,0
!*
PCALC,INTG,B10in,By,S,1,
!*
*GET,B10in,PATH, ,last,B10IN
*SET,B10av,ABS(B10IN)/L1*RATIO_
m
!*
PATH,p11,2,30,20,
PPATH,1,0,R10,b/2+hh+d/2,0,0,
PPATH,2,0,Rd,b/2+hh+d/2,0,0,
!*
PDEF,By11,B,sum,AVG
/PBC,PATH, ,0
!*
PCALC,INTG,B11in,By11,S,1,
!*
*GET,B11in,PATH, ,last,B11IN
*SET,B11av,ABS(B11IN)/(hb4)*RATI
O_m
!
!*
PATH,p12,2,30,20,
PPATH,1,0,Ro-do/2,hh+b/2,0,0,
PPATH,2,0,Ro-do/2,0,0,0,
!*
PDEF,Bx,B,x,AVG
/PBC,PATH, ,0
!*
PCALC,INTG,B12in,Bx,S,1,
!*
*GET,B12in,PATH, ,last,B12IN
```

```
*SET,B12av,ABS(B12IN)/(hh+b/2)*R
ATIO_m
!DG fluid properties
ty1=40015-40000*(2*exp(-2.9*B1av)-
exp(-2*2.9*B1av))
nu1=3.9-3.8*(2*exp(-4.5*B1av)-exp(-
2*4.5*B1av))
ty2=40015-40000*(2*exp(-2.9*B2av)-
exp(-2*2.9*B2av))
nu2=3.9-3.8*(2*exp(-4.5*B2av)-exp(-
2*4.5*B2av))
ty3=40015-40000*(2*exp(-2.9*B3av)-
exp(-2*2.9*B3av))
nu3=3.9-3.8*(2*exp(-4.5*B3av)-exp(-
2*4.5*B3av))
ty4=40015-40000*(2*exp(-2.9*B4av)-
exp(-2*2.9*B4av))
nu4=3.9-3.8*(2*exp(-4.5*B4av)-exp(-
2*4.5*B4av))
ty5=40015-40000*(2*exp(-2.9*B5av)-
exp(-2*2.9*B5av))
nu5=3.9-3.8*(2*exp(-4.5*B5av)-exp(-
2*4.5*B5av))
ty6=40015-40000*(2*exp(-2.9*B6av)-
exp(-2*2.9*B6av))
nu6=3.9-3.8*(2*exp(-4.5*B6av)-exp(-
2*4.5*B6av))
ty7=40015-40000*(2*exp(-2.9*B7av)-
exp(-2*2.9*B7av))
nu7=3.9-3.8*(2*exp(-4.5*B7av)-exp(-
2*4.5*B7av))
ty8=40015-40000*(2*exp(-2.9*B8av)-
exp(-2*2.9*B8av))
nu8=3.9-3.8*(2*exp(-4.5*B8av)-exp(-
2*4.5*B8av))
ty9=40015-40000*(2*exp(-2.9*B9av)-
exp(-2*2.9*B9av))
nu9=3.9-3.8*(2*exp(-4.5*B9av)-exp(-
2*4.5*B9av))
ty10=40015-40000*(2*exp(-
2.9*B10av)-exp(-2*2.9*B10av))
nu10=3.9-3.8*(2*exp(-4.5*B10av)-
exp(-2*4.5*B10av))
ty11=40015-40000*(2*exp(-
2.9*B11av)-exp(-2*2.9*B11av))
nu11=3.9-3.8*(2*exp(-4.5*B11av)-
exp(-2*4.5*B11av))
ty12=40015-40000*(2*exp(-
2.9*B12av)-exp(-2*2.9*B12av))
nu12=3.9-3.8*(2*exp(-4.5*B12av)-
exp(-2*4.5*B12av))
*SET,nu0,0.1
*SET,ty0,15
Vo=13.8888 !Speed of eletric scooter
Rw=0.2125 ! Wheel radius
OM=Vo/Rw ! Angular speed
! Torque calculation
*SET,La,b+2*hh
*SET,Tm1,4*pi*ty1*(R1**3-Ri**3)/3
*SET,Tby1,(pi*nu1*R1**4/d)*(1-
(Ri/R1)**4)*OM
*SET,Temp21,1/3*l1*hb1*hb1
*SET,Temp22,R1*R1*L1+R1*l1*hb1
! Cai nayluc cu R1*R1*l la sai
*SET,Tm2,4*pi*ty2*(temp21+temp22)
*SET,Temp23,R1**3*l1+(3/2)*R1**2
*l1*hb1
```

```
*SET,Temp24,R1*l1*hb1**2+(1/4)*l1
*hb1**3
*SET,Tby2,4*pi*nu2*OM/d*(temp23+
temp24)
*SET,Tm3,4*pi*ty3*(R3**3-R2**3)/3
*SET,Tby3,(pi*nu3*R3**4/d)*(1-
(R2/R3)**4)*OM
!!!!!!!!!!!!!!!!!!!!!!!!!!!!!!!!!!!!!!!!!!!!!!!!!
!!!1
*SET,Temp41,1/3*l1*hb1*hb1
*SET,Temp42,R3*R3*L1+R3*l1*hb1
*SET,Tm4,4*pi*ty4*(temp41+temp42)
*SET,Temp43,R3**3*l1+(3/2)*R3**2
*l1*hb1
*SET,Temp44,R3*l1*hb1**2+(1/4)*l1
*hb1**3
*SET,Tby4,4*pi*nu4*OM/d*(temp43+
temp44)
*SET,Tm5,4*pi*ty5*(R5**3-R4**3)/3
*SET,Tby5,(pi*nu5*R5**4/d)*(1-
(R4/R5)**4)*OM
*SET,Temp61,R5*R5*l+R5*l1*hb1
*SET,Temp62,1/3*l1*hb1*hb1
*SET,Temp63,R5**3*l1+(3/2)*R5**2
*l1*hb1
*SETTemp64,R5*l1*hb1**2+(1/4)*l1*
hb1**3
*SET,Tm6,4*pi*ty6*(temp61+temp62)
*SET,Tby6,4*pi*nu6*OM/d*(temp63+
temp64)
*SET,Tm7,4*pi*ty7*(R7**3-R6**3)/3
*SET,Tby7,(pi*nu7*R7**4/d)*(1-
(R6/R7)**4)*OM
!!!!!!!!!!!!!!!!!!!!!!!!!!
*SET,Temp81,1/3*l1*hb1*hb1
*SET,Temp82,R7*R7*L1+R7*l1*hb1
*SET,Tm8,4*pi*ty8*(temp81+temp82)
*SET,Temp83,R7**3*l1+(3/2)*R7**2
*l1*hb1
*SET,Temp84,R7*l1*hb1**2+(1/4)*l1
*hb1**3
*SET,Tby8,4*pi*nu8*OM/d*(temp83+
temp84)
*SET,Tm9,4*pi*ty9*(R9**3-R8**3)/3
*SET,Tby9,(pi*nu9*R9**4/d)*(1-
(R8/R9)**4)*OM
*SET,Temp101,R9*R9*l+R9*l1*hb1
*SET,Temp102,1/3*l1*hb1*hb1
*SET,Temp103,R9**3*l1+(3/2)*R9**
2*l1*hb1
*SET,Temp104,R9*l1*hb1**2+(1/4)*l
1*hb1**3
*SET,Tm10,4*pi*ty10*(temp101+temp
102)
*SET,Tby10,4*pi*nu10*OM/d*(temp1
03+temp104)
*SET,Tm11,4*pi*ty11*(Ro**3-
R10**3)/3
*SET,Tby11,(pi*nu11*Ro**4/d)*(1-
(R10/Ro)**4)*OM
Tby12=2*pi*Ro**2*La*ty12
Tm12=2*pi*Ro**2*La*(nu12*OM*Ro
/do)
*SET,Tm0,4*pi*ty0*(Ro**3-Ri**3)/3
*SET,Tby0,(pi*nu0*Ro**4/d)*(1-
(Ri/Ro)**4)*OM
*SET,Ta0,2*pi*Ro**2*La*(ty0+nu0*
OM*Ro/do)
```

```
*SET,Ta1,2*pi*hh*(R1**2+R3**2+R5**2+R7**2+R9**2)*ty0
*SET,Ta2,2*pi*hh*nu0*OM*(R1**3+R3**3+R5**3+R7**3+R9**3)/do
*SET,Rso,Rs
*SET,Tor,(0.65*(2*Rso*39.37)**2*(OM*30/pi)**(1/3))*0.007061552
*SET,Tb0,(Tm0+Tby0+Ta0+2*(Ta1+Ta2)+2*Tor)
!
Tm=Tm1+Tm2+Tm3+Tm4+Tm5+Tm6
Tm=Tm+Tm7+Tm8+Tm9+Tm10+Tm11+Tm12
Tby=Tby1+Tby2+Tby3+Tby4+Tby5+Tby6
Tby=Tby+Tby7+Tby8+Tby9+Tby10+Tby11+Tby12
Tb=Tm+Tby
```

```
! Mass of MRB
massplus=7800*pi*(R**2)*L
Vcoil=2*pi*((R10)**2-(R2)**2)*(wc1)
Mcoil=Vcoil*8900
Vmrf1=2*pi*((Ro)**2-(Ri)**2)*d+2*pi*Ro*d*La
Vmrf2=2*pi*(R1+R3+R5+R7+R9)*d*hh
Vmrf=Vmrf1+2*Vmrf2
Mmrf=Vmrf*2900
mass=massplus+Mmrf+Mcoil-7800*Vmrf-7800*Vcoil
! Temperature constraint
h=31.25
Ab1=2*(R*R-Ri*Ri)*pi+2*pi*R*L
SV1=(Tb0*OM)/(h*Ab1)
FINISH
```